W-Pos268

VOLUME FLUCTUATIONS IN LIPID BILAYERS: HIGH PRESSURE TIME-RESOLVED FLUORESCENCE STUDIES. ((*Lesley Davenport, #Piotr Targowski and *Jay R. Knutson)) *Department of Chemistry, Brooklyn College of CUNY, NY 11210, #Institute of Physics, Nicolas Copernicus University, ul Grudziadzka 5, 87-100, Torun, Poland, ^LCB, NHLBI, NIH, Bethesda, MD 20892.

We previously examined the effects of applied hydrostatic pressure (0-1.2 kBar) on lipid acyl chain order fluctuations in bilayers of DPPC using the long-lived (τ_w ~ 200 ns) fluorescence anisotropy probe coronene (Biophys. J., Targowski and Davenport, 64:A75). The pretransition *out-of-plane* rotational mobility of coronene was rationalized using either a compartmental or discrete model (heterogeneous lipid environment) and/or a mean-field (Landau) model where a distribution of lipid order parameters are expected.

We have now incorporated the high pressure cell into a time correlated single photon counting fluorometer, driven by a cavity-dumped synchronously pumped dye laser. The global vector analysis program AFIT was modified to include window scrambling and gating factors. Initial studies suggest that the pressure-induced 'freezing' of gated lipid fluctuations proceeds analogously with previously obtained thermal data. Modification of our present distribution (Landau-based) model to include chain-order-volume relationships are in progress. (Supported in part by PSC-CUNY Award, AHA-NYC Affiliate and NSF DMB-9006044).

W-Pos269

FLUORESCENCE PROPERTIES OF NBD-LABELED PHOSPHOLIPIDS IN MEMBRANES ((S. Mazères, V. Schram, S. Fery-Forgues, J.F. Tocanne and A. Lopez)) Labo. Pharmaco. Toxico. Fondament. CNRS, 118, Route de Narbonne, F-31062 Toulouse Cedex, France.

Phospholipids labeled with the 7-nitrobenz-2-oxa-1,3-diazole -4-yl (NBD) group either on their acyl chains or their polar headgroup are widely used for investigating the lateral and transverse distribution and dynamics of lipids in membranes. For a better understanding of the behaviour of these probes, the steady-state and dynamic fluorescence properties of the NBD fluorophore, alone or attached to phospholipids, were studied in solution and in membrane model systems. As a main result, the fluorescence data shows that the fluorescence quantum yield ϕ of the NBD group strongly depends on the polarity of the surrounding medium and also on the nature of the lipid probe itself and of the host lipids. Thus, in solution, the NBD fluorophore displayed ϕ values of 0.03, 0.67 and 0.027 in solvents of low (hexane, $\varepsilon \sim 1.9$), medium (ethyl acetate, $\varepsilon \sim 6$) and high (water, $\varepsilon \sim 80$) polarity respectively (1). When the fluorophore was attached to one of the acyl chain (NBD-PE, NBD-PG, NBD-PC, NBD-PA) or to the polar headgroup (N-NBD-PE) of lipids, ϕ was observed to vary by up to a factor 4 from one lipid probe to the other with the decreasing order NBD-PE > N-NBD-PE > NBD-PG > NBD-PC > NBD-PA, whatever may be the host lipid. For each NBD-labeled lipid probe, ϕ was found to depend on the host lipids with the decreasing order EggPC > PS > EggPA > Egg-PG. The fluorescence lifetimes and quantum yields of the probes indicate that this is the non-radiative constant of de-excitation which is mainly responsible for the observed changes in ϕ. They are also compatible with a localization of the NBD group around the polar headgroup/hydrocarbon interface of the lipid bilayer. These observations should be accounted for when using NBD-labeled lipids for investigating membrane organization.

(1) J. Photochem. Photobiol. A: Chem., (1993) *70*: 229-243

W-Pos270

LYTIC ACTIVITY OF δ-LYSIN FROM STAPHYLOCOCCUS AUREUS IS REFLECTED IN ITS INTERACTION WITH PHOSPHOLIPID MODEL MEMBRANES.
((E. Prenner[1)], A. Hermetter[2)], R. Epand[3)], F. Paltauf[2)], G.Degovics[1)], P. Laggner[1)] and K. Lohner[1)])) [1)]Institute of Biophysics and X-Ray Structure Research, Austrian Academy of Sciences and [2)]Institute of Biochemistry, Techn. University Graz, A-8010 Graz, Austria and [3)]Department of Biochemistry, McMaster University, Hamilton, Ontario, Canada. (Sponsored by A. Kungl)

δ-lysin, a bacterial toxin of 26 amino acids, has lytic effects on eukaryotic cells but no antimicrobial activity. It adopts an amphipathic α-helix, when the peptide is in an aggregate or bound to phospholipid model membranes. Here we report on its interaction with small unilamellar vesicles composed of zwitterionic and negatively charged phospholipids mimicking the main components of above biological membranes. Fluorescence spectroscopy using the single tryptophan at position 15 of the peptide as an intrinsic probe was applied. The analysis of the emission spectra and quenching experiments using the water soluble quencher acrylamide showed that δ-lysin does interact differently with these phospholipid classes.

In the presence of phosphatidylglycerol and phosphatidylserine Trp is exposed to water, whereas vesicles consisting of diacylphosphatidylcholine reveal a rather apolar environment for the fluorescence marker. Experiments performed with choline plasmalogen, the enolether derivative of diacylphosphatidylcholine, indicated a more hydrophilic environment for the peptide's tryptophan in such vesicles as compared to its diacyl analog. The results are consistent with a charge dependant interaction of δ-lysin with the various lipid membranes and demonstrate that headgroup structure and membrane interphase are crucial for the peptide lipid interaction.

W-Pos271

BREWSTER ANGLE MICROSCOPY REVEALS INFORMATION ON THE MICROSCOPIC NATURE OF PHOSPHOLIPID MONOLAYER FILMS.
((K. Lohner[1)], D. Hönig[2)], E. Prenner[1)], D. Spohn[2)] and D. Möbius[2)])) [1)]Institute of Biophysics and X-Ray Structure Research, Austrian Academy of Sciences, A-8010 Graz, Austria and [2)]Max Planck Institut für Biophysikalische Chemie, D-37077 Göttingen, Germany. (Sponsored by E. E. Daniel)

Phospholipid monolayers at the air-water interface provide a simple model for biomembranes. Fluorescent probes have been extensively used to investigate various aspects of the structure, dynamics and molecular organization in such systems. However, the influence of the probe molecules is still controversial. Brewster angle microscopy (BAM) provides information on the microscopic nature of monolayers without requiring any molecular probe. Hence, we applied this novel experimental approach to study monolayer films composed of pure dipalmitoyl-phosphatidylcholine (DPPC) and doped with the side chain-labelled fluorescent probe NBD-PC. Surface pressure and surface potential area isotherms were recorded with the BAM video-images to correlate morphology and monolayer phase state.

Domain size, organization and shape were identical in NBD-PC free and NBD-PC containing monolayer, when the fluorescent probe was used in the low concentration regime, confirming recent results obtained by fluorescence microscopy. However, the domains exhibit a wide variety of shapes depending in detail on the experimental conditions. In particular, using the pure DPPC film we observed structures previously assigned to the addition of the negatively charged cardiolipin. Long-range orientational order within the domains can be observed in certain cases, showing the potential of BAM as a non-perturbing technique for the direct observation of phospholipid monolayers and their ordering phenomena on the micron scale.

W-Pos272

STUDY OF BINARY PHOSPHOLIPID MIXTURE USING SPECTROSCOPIC AND THERMODYNAMIC METHODS((Yan Chen and Enrico Gratton.)) Laboratory for Fluorescence Dynamics, University of Illinois at Urbana -Champaign

Binary lipid mixtures provide a system to study the formation of regular molecular aggregates or microdomains in phospholipid bilayers. The phase behavior of binary phospholipids mixtures is studied by fluorescence generalized polarization (GP) and density measurements. Measurements are carried out with a mixture of dipalmitoyl (DPPC) and 1-palmitoyl-2-oleoyl-phosphatidylcholine (POPC) serving as the model compounds. Fluorescence information is obtained by addition of 2-dimethylamino-6-lauroylnaphthalene (LAURDAN) to the lipid mixtures. The GP spectra of LAURDAN in DPPC and POPC mixtures are measured by systematically varying the ratio of POPC and DPPC at two different temperatures (4°C and 22°C). Surface plots of GP values as a function of emission wavelength and binary mixture ratio are constructed. We have observed the changes in surface curvature at different temperatures and the non-linear behavior of the GP values along the concentration gradient. These observations are discussed in the context of molecular microdomains formed at particular mole ratio of the two phospholipids. The physical properties of these molecular microdomains are also studied with thermodynamic methods. Density measurements yield volumetric information, whereas ultrasonic measurements provide information on the time dependent compressibility and ultrasonic absorption. The nonlinear behavior of density as a function of the molar ratio of the two phospholipids can be explained due to the regular molecular aggregates. The larger volume occupied by the POPC molecule in the DPPC lattice causes a local distortion that give rise to a regular pattern at specific molar ratio of the two phospholipids. It is necessary to achieve an accuracy of one part in 10^5 in both density and ultrasonic measurements for detecting the small changes caused by the formation of regular molecular aggregates. Supported by National Institutes of Health grant RR0315.

W-Pos273

DETERMINATION OF THE DEPTH OF MOLECULES IN MEMBRANES BY NITROXIDE FLUORESCENCE QUENCHING ((Erwin London, Emma Asuncion-Punzalan and Robert Kaiser)) Dept. of Biochemistry and Cell Biology, State University of New York at Stony Brook, Stony Brook NY 11794-5215

Quenching of model membrane bound fluorophores can be used to determine the depth of membrane bound molecules. In previous studies a model was developed that predicts how the decrease in intensity due to quenching will depend on the locations of the quencher and fluorescent molecule in the membrane. Based on this analysis, a method (parallax analysis) was developed in which the amounts of quenching induced by two phospholipids containing the nitroxide group fixed at different membrane depths is substituted into a simple algebraic equation to calculate fluorophore depth. We have now extended the theoretical analysis of quenching to the effect of nitroxides on fluorescence lifetimes. It can be shown that even **for a static quenching process, a significant decrease in fluorescence lifetime is expected.** Furthermore, the decrease in lifetime, unlike that in fluorescence intensity, will be only weakly dependent on the difference between the depth of fluorophore and quencher. Our previous studies have also shown the calculated fluorophore depth is sensitive to the exact concentration of nitroxide-label present. A new, simpler method to calibrate the nitroxide content of lipids by fluorescence has been developed. It involves preparation of anthroyloxy fatty acid containing vesicles in which the nitroxide label content is varied.

W-Pos274

WHERE DO POLAR GROUPS LOCATE IN MEMBRANES?: LOCATION OF FLUOROPHORES IN MEMBRANES BY PARALLAX ANALYSIS OF FLUORESCENCE QUENCHING ((Emma Asuncion-Punzalan, Erwin London, Robert Kaiser)) Dept. of Biochemistry and Cell Biology, State University of New York at Stony Brook, Stony Brook, NY 11794-5215

The depth of fluorophores in model membranes can be determined in angstroms by a method known as the parallax analysis. This method involves the measurement of the degree of fluorescence quenching by phospholipids with spin label quenchers located at two different depths in the bilayer. The degree of fluorescence quenching is dependent on the distance between the fluorophore and the quencher. Fluorophores are quenched more efficiently when they are closer than when they are farther from the quencher. The ratio of the fluorescence intensities obtained in the presence of a shallow and a deep quencher is substituted into a simple equation that allows calculation of fluorophore depth. The parallax analysis was applied to a series of diphenylhexatriene and 9-substituted anthryl derivatives in order to determine the chemical and structural factors that control the depth of molecules in membranes. These studies show that polar functional groups are anchored at the membrane surface. Anchoring by uncharged -COOH and -OH groups is at a shallower depth than anchoring by uncharged -NH_2 groups. In addition, it is found that the depth increases as the number of carbon atoms between the fluorescent group and the polar functional group increases. It was also found that the depth can be dependent on the pH. For example, positively charged amino groups appear to be shallower than their uncharged forms.

W-Pos275

TIME-RESOLVED FLUORESCENCE ANISOTROPY MEASUREMENTS OF TAURODEOXYCHOLATE / FLUORESCENT-LABELED LYSOLIPID AGGREGATES. **((L.J. DELONG AND J.W. NICHOLS)) Emory University School of Medicine, Atlanta, GA 30322. (Spon. by L. DeLong)**

Previous work from this laboratory (Shoemaker & Nichols, *Biochem.*, 29:5837, 1990.) demonstrated that sub-micellar concentrations of the environment sensitive lysolipid, *N*-(7-nitrobenz-2-oxa-1,3-diazol-4-yl)-monomyristoylphospohethanolamine (*N*-NBD-MPE) reached maximum fluorescence yield upon the addition of taurodeoxycholate (TDC) at concentrations well below its critical micelle concentration (CMC) of 2.5mM. These data indicated the formation of small molecular aggregates (SMAs) of the two amphiphiles at concentrations below their respective CMCs. To investigate the size of these SMAs, fluorescence lifetime and differential polarization techniques were performed for a fixed submicellar concentration of *N*-NBD-MPE (2μM) in the presence of varied amounts of TDC both below and above its CMC. Two discrete lifetimes were resolved for the *N*-NBD-MPE molecules both of which initially increase and then plateau at levels above the CMC for TDC. Based on these lifetimes, at TDC concentrations of 1mM and above, two distinct rotational correlation times (ϕ) were established through polarization measurements. The shorter of the two is ascribed to local probe motions, while the longer of the two is in a time range expected for global motions of the SMA (3-6.5ns). At 0.5mM TDC only the shorter ϕ was observed. From the longer ϕ, molecular volume and hydrodynamic radii were calculated. The radius calculated for the SMAs varies from ~15Å at 1mM to ~18Å at 5mM TDC. These data support the conclusions that monomeric lysolipids in solution seed the aggregation of numerous TDC molecules (aggregation number = 11 at 1mM TDC) to form a TDC micelle with a lysolipid core at concentrations below which they self aggregate. Since the SMAs have been shown to coexist and interact with bilayer vesicles (Shoemaker and Nichols, *Biochem.*, 31:3414, 1992) we hypothesize that they may form and serve as shuttle carriers to facilitate the absorption of more hydrophobic amphiphiles in the intestine.

W-Pos276

THE EFFECT OF LIPOPOLYSACCHARIDE (LPS) ON THE FLUORESCENCE ANISOTROPY OF *TRANS*-PARINARIC ACID IN MODEL MEMBRANES - POSSIBLE IMPLICATIONS FOR THE BIOLOGICAL ACTIVITIES OF LPS ((Bernard D. Hummel, Luc R. Bérubé, and Rawle I. Hollingsworth)) Michigan State University, Department of Biochemistry, East Lansing, Michigan 48824

Lipopolysaccharides (LPS, endotoxin) are located on the outer membrane of gram-negative bacteria and induce a wide range of biological responses in mammals including fever, hypotension, induction of cytokines and shock. LPS consists of a hydrophilic polysaccharide region (core, o-antigen) and a lipid region (lipid A). The lipid A anchors LPS to the membrane and is responsible for its biological activities. Due to its unique structure, LPS is capable of forming very tight aggregates. The aggregate size of LPS has been shown to determine its biological activity ("Handbook of Endotoxin", Vol. 1, 1984, pp. 46-58, Elsevier Science Publishers B. V.). Recently, Brandenburg et al. have shown that the phase behavior of LPS is correlated to its biological activity (*Eur. J. Biochem.* (1993) 218:555-563). The supermolecular structure is, therefore critical for the biological activities of LPS. Since LPS can intercalate into host cellular membranes, it may cause large perturbations to the normal membrane dynamics of these cells. These disturbances may be responsible for the broad range of biological activities induced by LPS. The goal of this research is to determine the affect of LPS (*Salmonella typhimurium*) on the dynamics of model membranes (DPPC). To this end, the anisotropy of a fluorescent probe, *trans*-parinaric acid (tPnA), was measured as a function of temperature in DPPC vesicles with and without LPS. tPnA was used since it preferentially partitions into regions of solid lipid phases. Below the lamellar liquid crystalline phase transition, the anisotropy of LPS/DPPC vesicles was significantly larger than vesicles without LPS. The most striking difference is a 3°C ± 1°C increase in the transition temperature of LPS/DPPC vesicles as detected by fluorescence anisotropy. These findings suggest that LPS does induce large changes in membrane dynamics and/or organization.

W-Pos277

WATER CONCENTRATION INCREASES IN PHOSPHOLIPID BILAYERS AFTER OXIDATIVE DAMAGE PRODUCED BY IONIZING RADIATION. ((T. Parasassi, A.M. Giusti, G. Ravagnan, O. Sapora* and E. Gratton**)) Istituto di Medicina Sperimentale, CNR, Roma; *Istituto Superiore di Sanita', Roma, Italy; **Laboratory for Fluorescence Dynamics, Dept. of Physics, Univ. of Illinois at U-C, Urbana, Il 61801.

The two membrane fluorescent probes 2-dimethylamino-6-lauroyl-naphthalene (LAURDAN) and 2-dimethylamino-6-propionyl-naphthalene (PRODAN) have been used to study the molecular basis of the modifications observed in membrane properties treated with ionizing radiations. Hydroperoxide residues are formed in unsaturated lipids. Their presence decreases the hydrophobic interactions between adjacent acyl chains and favour the penetration of water molecules. The increased polarity of the bilayer has been verified using LAURDAN and PRODAN. The two probes display a spectral sensitivity to the polarity of their environment, showing a red shift of both excitation and emission spectra with the increase of the polarity of their environment. Due to their chemical differences, the two probes are anchored in the membrane with different strengths. After oxidative damage and penetration of water molecules, LAURDAN is driven deeper in the bilayer by its lauric acid tail, and its emission is blue shifted. Instead, PRODAN is both partitioned and fluorescent in the presence of water, so that after oxidative damage have been produced its emission spectrum is red shifted. (Supported by CNR and by NIH grant RR03155)

W-Pos278

FLUORESCENCE STUDIES OF THE INTERACTION OF A MUTANT FORM OF CYTOCHROME B5 WITH POPE/POPS MIXED-LIPID VESICLES ((Harold M. Goldston, Jr., A.W. Steggles*, and Peter W. Holloway)) Dept. of Biochemistry, Univ. of Virginia Sch. Med., Charlottesville, VA. *Dept. of Biochemistry, Northeastern Ohio Univ. Coll. Med., Rootstown, OH. (Spon. by W.R. Pearson)

Cytochrome b_5 is an amphipathic integral membrane protein which binds readily to most natural and artificial membrane bilayers through its nonpolar C-terminal domain. The hydrophilic N-terminal domain possesses a net negative charge. It has been previously shown that b_5 does not bind to phosphatidylserine-containing vesicles and it is likely that this is due to charge repulsions. Our present work examines the interaction of a mutant form of cytochrome b_5, in which both Trp-108 and Trp-112 have been replaced by leucines, with mixed-lipid vesicles containing POPE and POPS. Through the use of calorimetric and fluorescence studies, it is seen that in a POPE:POPS (1:1) system at temperatures and buffer conditions under which the two lipids in the system are well-mixed, there is no appreciable binding of cytochrome b_5 to the vesicles. Upon temperature-induced phase separation of the two lipids, however, cytochrome b_5 is able to bind to the mixed-lipid vesicles promoting further de-mixing in the system. This study further explores the effect of ionic strength on this binding phenomenon as well as the kinetics of the binding reaction. Supported by a Grant-in-Aid from the American Heart Association, Virginia Affiliate, Inc.

W-Pos279

EPIFLUORESCENCE MICROSCOPY OF VESICLE ADSORBED MONOLAYERS OF SOME PULMONARY SURFACTANT COMPONENTS. ((K.Nag, J.Perez-Gil and K.M.W.Keough.)) Biochemistry, Memorial University of Newfoundland, St.John's, Canada A1B 3X9 & Bioquimica Y Biologia Molecular, Universidad Complutense, Madrid-28040, Spain.

Pulmonary surfactant (PS) is responsible for alveolar stability and prevents collapse at low lung volume. PS can rapidly adsorb at an air-water interface where as its component phospholipids (PPL) dipalmitoyl phosphatidylcholine (DPPC) and phosphatidylglycerol (PG) adsorb more slowly. Epifluorescence microscopy of vesicle adsorbed monolayers of porcine PS lipid extract (PSL), DPPC, DPPC:dipalmitoyl PG (DPPG) [DPPC:DPPG 7:3 mol/mol], and their mixtures with 3 wt% of protein SP-C fluorescently labelled with fluorescein (F-SP-C) were made. Vesicles (0.06 mg/ml) were injected under an clean air-saline (pH 6.9, 5 mM Calcium) interface and surface fluorescence observed either from low amounts of lipid probe Rhodamine-PE incorporated in the PPL and PSL vesicles or from F-SP-C. DPPC vesicles adsorbed to form surface films showing domains consistent with liquid expanded (LE) and liquid condensed (LC) phase after 30 minutes of adsorption. DPPC:DPPG vesicles adsorbed less rapidly than DPPC. F-SP-C increased the rate of adsorption of DPPC, DPPC:DPPG. F-SP-C occupied the LE domain of the PPL monolayers. The PPL-protein monolayers had similar amounts of LC domains at a similar surface pressure. PS lipid extract vesicles adsorbed faster than any of its components. The LC domains of PS monolayer were different in shape and size compared to any of the components. (Supported by MRC Canada and CIRIT Spain.)

W-Pos280

THE EFFECT OF CYTOCHALASIN D ON THE MECHANICAL PROPERTIES AND MORPHOLOGY OF PASSIVE HUMAN NEUTROPHILS. ((Anne S. Lee, H. Ping Ting-Beall and Robert M. Hochmuth)) Department of Mechanical Engineering and Materials Science, Duke University, Durham, NC 27708-0300.

The actin-rich cortex plays a major role in neutrophil chemotaxis and phagocytosis. In passive neutrophils, 50% of the actin molecules are in the F (filamentous) form, and it is the shifting of equilibrium with its monomeric G (globular) form that controls cell motility and phagocytosis. Cytochalasins have been shown to inhibit cell phagocytosis and ruffling. Using purified actin, it has been demonstrated that cytochalasins cap the barbed ends of actin filaments to prevent polymerization or cause a net depolymerization of filaments. Recent studies with intact cells, however, reveal that the most potent cytochalasin, cytochalasin D (CD) actually increases F-actin content suggesting that CD disrupts the actin network so as to increase the number of actin filament ends for further actin polymerization. In order to assess the site of action of CD on neutrophils, we studied the effects of CD on the mechanical properties and morphology of passive neutrophils with 1, 2, 10, and 20 μM CD. In this study the neutrophil is modeled as a simple Newtonian liquid drop with a constant cortical tension and cytoplasmic viscosity. At 1 and 2 μM CD, the cells remained spherical after 30 min. incubation. However, in the presence of 10 and 20 μM CD, cells were severely deformed and "blebby" as shown by light and scanning electron microscopy. After 1 and 2 μM CD treatment the cells showed a decrease of 19% and 49%, respectively, in cortical tension when measured by static micropipet aspiration experiments. At high concentrations, i.e., 10 and 20 μM, CD disrupted the F-actin network at the cortex so that the cortical tension, if at all present, was not large enough to retain the sphericity of the cells. Similarly, the cytoplasmic viscosities of 1 and 2 μM CD treated cells were also decreased, but only by 17% and 24%, respectively, indicating that the specific action of CD is on the cortical region of the neutrophils. Our results are consistent with the conclusions of Tsai et al. (Biophys. J., 66:2166, 1994) that the actin filaments play a major role in maintaining the cortical tension of passive neutrophils.
This work is supported by NIH Grant #HL23728.

W-Pos281

THE ORIGIN OF THE UNUSUAL POTENCY OF PHOSPHATIDYLETHANOL TO PROMOTE NONBILAYER STRUCTURES IN MODEL MEMBRANES ((Y.-C. Lee*, N. Janes, Y. O. Zheng, G. Moehren, E. Rubin and T.F. Taraschi)) Department of Anatomy, Pathology and Cell Biology, Thomas Jefferson University, Philadelphia, PA 19107.

The membrane destabilizing properties of phosphatidylethanol (PtdEth) may play a role in alcohol-induced cell injury. In order to investigate the unusual potency of PtdEth to promote the formation of a non-bilayer, hexagonal (H_{II}) phase in a liposomal matrix, dilute concentrations (5 mole%) of DOPtdAlc of varying chain length (C_1-C_8) were incorporated into liposomes of 1-palmitoyl-2-oleoyl-phosphatidylethanolamine (POPE) and the effect on the $L_\alpha \rightarrow H_{II}$ transition (T_H) was studied by ^{31}P NMR. The ability of PtdAlc to promote the H_{II} phase is shown to correlate with alcohol chain length, depressing T_H by 1.7 degrees with each additional carbon chain. These results indicate that increasing the headgroup volume of PtdAlc stabilizes the H_{II} state. This conflicts with predicted results employing the shape concept and headgroup volume approach to lipid structure. To test the hypothesis that the hydrophobic effect drives the alkyl headgroup on PtdAlc into the bilayer interior, a series of 1,2-dioleoyl/3-substituted triacylglycerides (0.2-1 mole%) in a liposomal matrix of POPE were examined. Triacylglycerides were also found to strongly stabilize the H_{II} phase, suggesting that the violation is due to a consequence of progressive insertion of the hydrophobic alkyl headgroup of PtdAlc into the membrane interior. Increases in hydrocarbon volume generated by this effect lead to an increase in the packing parameter and promote the formation of nonbilayer structures. Supported by PHS AA07215, AA07463, AA07186, AA00088. 1. Lee et al. *Biophys.J.* 65, 1429-1432(1993).

W-Pos282

LOCAL ENVIRONMENT OF TWO STRUCTURALLY DISTINCT SPIN-LABELED AFFINITY PROBES OF HUMAN ERYTHROCYTE BAND 3 ((D.J. Scothorn, E.J. Hustedt, C.E. Cobb and A.H. Beth)) Dept. of Molecular Physiology and Biophysics, Vanderbilt University, Nashville, TN 37232.

The structure and spatial arrangement of the integral membrane domain of the anion exchange protein of the erythrocyte membrane, band 3, has been studied extensively with regards to mechanisms of anion exchange, and as a model system for other membrane transport proteins. We have developed a number of spin-labeled affinity probes of band 3 for EPR spectroscopic studies of its structure and dynamics. SL-H_2-DADS-maleimide is a spin-labeled stilbenedisulfonate derivative, and BSSDP (bis-[sulfo-N-succinimidyl]-doxyl-pimelate) is a homo-bifunctional agent which forms intra-molecular cross-links on the band 3 monomer. Two complementary techniques have now been used to determine the accessibility of the nitroxide moieties of these labels to various local environments. CW power saturation EPR spectroscopy has been used to determine the collision frequency of these nitroxides with a number of paramagnetic spin exchange agents: molecular oxygen (soluble in water and lipid phases) [the effects of molecular oxygen on the ST-EPR spectra of SL-H_2-DADS-maleimide labeled band 3 are addressed in a poster by Hustedt, *et al.*], chromium oxalate (charged, water soluble), chromium maltolate (uncharged, water soluble [kindly provided by G. Eaton]), and copper-KTSM$_2$ (nonpolar, lipid soluble). The local environments of these nitroxides has also been investigated by determining the accessibility of these spin labels to environment specific reducing agents, using sodium ascorbate (charged, water soluble), β-mercaptoethanol (uncharged, soluble in water and lipid phases) and 1,2-diphenylhydrazine (nonpolar, lipid soluble). From these studies, it has been determined that the nitroxide moiety of SL-H_2-DADS-maleimide is buried in a protein cleft accessible to oxygen but not to other probes, whereas that of BSSDP is highly exposed to the extracellular aqueous environment. Neither spin label is exposed to the intracellular space. Supported by NIH Grants R01 HL34737 and RR04075.

W-Pos283

SATURATION TRANSFER EPR STUDIES OF THE ROTATIONAL DIFFUSION OF BAND 3 IN THE HUMAN ERYTHROCYTE MEMBRANE ((E.J. Hustedt, D.J. Scothorn, C.E. Cobb and A.H. Beth)) Dept. of Molecular Physiology and Biophysics, Vanderbilt University, Nashville, TN 37232.

The band 3 affinity spin-label SL-H_2-DADS-maleimide is proving to be a useful probe of the rotational dynamics of band 3 in the erythrocyte membrane. Previously it has been shown that X-band (≈9.5 GHz) ST-EPR spectra of [^{15}N,D_{13}]-SL-H_2-DADS-maleimide labeled band 3 in intact erythrocytes can be fit assuming a single population of band 3 undergoing uniaxial rotational diffusion about an axis coincident with the membrane normal and at a rate consistent with a band 3 dimer. The global analysis of ST-EPR spectra obtained at three different Zeeman modulation frequencies in terms of a single characteristic rotation time suggests that only a small fraction of band 3, if any, exists in lower mobility states. This result contrasts with time-resolved optical data which are typically interpreted in terms of multiple species of band 3 with different rotational properties. Our goal is to develop a single model of band 3 rotational dynamics which will simultaneously explain the ST-EPR and optical data. Towards this end, we are examining the effects of Zeeman modulation, microwave frequency, oxygen concentration, and other factors on the ST-EPR spectra of [^{15}N,D_{13}]-SL-H_2-DADS-maleimide labeled band 3. As reported in the accompanying poster (Scothorn *et al.*), oxygen has a strong effect on the microwave saturation properties of [^{15}N,D_{13}]-SL-H_2-DADS-maleimide. Oxygen also has a major effect on the ST-EPR spectra of [^{15}N,D_{13}]-SL-H_2-DADS-maleimide labeled band 3 in ghost membranes. Currently, investigations are underway to determine whether this effect is purely a result of an oxygen-induced change in the electron spin-lattice relaxation time, T_{1e}, or if oxygen may have some effect on band 3 rotational dynamics. In addition, ST-EPR have been collected at Q-band (≈34GHz) and are currently being analyzed. The increased influence of the g-tensor anisotropy at Q-band should help to better define the orientation of the nitroxide with respect to the diffusion axis. *Supported by NIH Grants R01 HL34737, T32 DK07186, and P01 CA43720.*

W-Pos284

BAND 3 MODEL FOR REMOVAL OF SENESCENT RBC ((L. Kantor and H. Mizukami)) Biological Sciences, Division of Regulatory Biology and Biophysics, Wayne State University, Detroit, MI 48202

There are several proposals relating an anion transport protein, Band 3 to removal of senescent rbc. One by Low *et al* (1985) suggests that as rbc age, Band 3 molecules cluster leading to bivalent binding of autologous Ab, resulting in rbc removal. Another by Kay (1985) proposes that cleavage of Band 3 takes place in old rbc, forcing a part of it to the surface. A presence of an immunologically foreign fragment on the cell surface, renders such a cell as non-self, resulting in binding of autologous Ab and eventual removal by macrophages follows. Our research will demonstrate that the two proposals are not contradictory but are complementary. We present a new mechanism of senescent rbc removal beginning with clustering of Band 3 molecules in the middle aged cells. The clustering causes conformational changes within Band 3 thus, exposing the previously hidden proteolytic site. This leads to cleavage of Band 3 and dymamic interactions force a part of it to the surface. Consequently, such a cell is recognized as foreign by autologous Ab, and is eventually removed from circulation. These events are supported by agarose and SDS-PAGE gels of age separated rbc. The old cells show a decrease in Band 3, yet show an increase in high MW clusters (HMWC) and various break down products. Immunoblots with mAb to Band 3 indicate that HMWC and the observed breakdown products are indeed Band 3 protein. Further support for our proposal comes from immunofluorescent analysis of age separated rbc using FITC crosslinked mAb to Band 3. It reveals that young rbc have scattered Band 3, producing uniformly weak fluorescent signal. Whereas middle aged and old cells, due to HMWC, produce an irregularly clustered regions with stronger fluorescent intensity.

W-Pos285

AUTOAGGREGATION OF *BIFIDOBACTERIUM* IN RELATION TO ITS SURFACE PROPERTIES

((Perez, P.F.*, De Antoni, G.L.*, Minnaard, J.*, Añón, M.C.* and Disalvo, E.A#.))
***CIDCA, U.N. La Plata, and #FFyB, U. de Buenos Aires , Argentina.**

***Bifidobacterium* plays an important physiological role by adhering to intestinal epithelia. For this reason it is of interest to know its surface properties. A consequence of the surface features is the autoaggregating ability of the strains. In the present work this property was studied in correlation to the hydrophobic index and the surface potential for different strains of *Bifidobacterium*. The first was determined by means of its partition in xylene and the second employing methylene blue as a surface potential probe.**

The autoaggregating strains have an hydrophobic index higher than 90% while it is negligible in the non autoaggregating ones. In addition, the autoaggregating bacteria show a high adsorption of methylene blue. When these are treated with trypsine both the aggregation and the methylene blue decreases drastically. However, the hydrophobic index remains unchanged. The possibility that the autoaggregation is related to protein residues in the cell surface is discussed.

W-Pos286

CHOLESTEROL DISTRIBUTION IN BOVINE ROD OUTER SEGMENT DISK MEMBRANES. ((Arlene D. Albert and Zofia Paw)) Departments of Biochemistry and Ophthalmology, University at Buffalo, Buffalo, NY 14214.

The asymmetric distribution of phospholipids and cholesterol between the two monolayers of biological membranes is likely to play an important role in the normal functioning of membranes. Therefore this distribution of lipids has been the subject of numerous studies. In the rod outer segment disk membrane it has been reported that the phospholipids are asymmetrically distributed with PE and PS favoring the outer monolayer while PC favors the inner monolayer. Cholesterol is present in the disk membranes of rod outer segments at approximately 10 mole percent. Based on thermal properties, it has been suggested that cholesterol is primarily located in the inner monolayer. In this study the cholesterol distribution between the inner and outer monolayers of the disk membrane was investigated. Disk membrane cholesterol was converted to cholestenone using cholesterol oxidase in the presence and in the absence of the detergent taurodeoxycholate. Cholestenone was extracted by the heptane and its concentration determined spectrophotometrically. Studies using 5, 10 and 30 units of cholesterol oxidase per μmole membrane cholesterol indicated that the oxidation reaction was not first order. This data suggested that there at least two populations of cholesterol in the disk membrane which can be oxidized by the enzyme and can be interpreted as inner and outer monolayer cholesterol. Furthermore, approximately 25% of the cholesterol is not readily oxidized even after several hours. Similar results were obtained under bleached and non-bleached conditions. Also treatment of the disks with Sepharose Con A to remove any inside out membranes had no effect. (NEI EY03328)

W-Pos287

THE WORK OF FORMING LIPID CYLINDERS (TETHERS) FROM THE MEMBRANES OF RED BLOOD CELLS. ((R.E. Waugh and W.C. Hwang)) Dept. Biophysics, University of Rochester, School of Medicine and Dentistry, Rochester, NY 14642.

The physical integrity of the cell membrane depends on maintaining proper association between the membrane bilayer and the underlying membrane skeleton. The mechanical formation of membrane strands (tethers) from the cell surface provides a way to measure the work required to separate bilayer from the membrane. (The distribution of membrane components after tether formation and the solubility of tethers in detergent indicate that tethers consist primarily of a bilayer membrane lacking both a membrane skeleton and associated integral proteins.) The reversible work of separation was measured by measuring the force of tether formation under quasi-steady conditions. A red cell was held in the tip of a micropipette and withdrawn from an adherent bead attached to the tip of a calibrated microcantilever. The deflection of the cantilever provided a measure of the tethering force, and the displacement of the cell projection in the pipette was used to calculate the tether radius. The work of separation involves two main components: the energy it takes to bend the membrane bilayer into the high curvature in the tether, and the work of separating the bilayer from the cell surface. Our measurements indicate a bending elastic modulus of the membrane of ~ 1.9 x 10^{-19} J and a reversible work of separation of ~ 0.25 mJ/m^2.

W-Pos288

TETHER FORMATION FROM A NERVE GROWTH CONE WITH THE LASER OPTICAL TWEEZERS: EXPERIMENT AND THEORY. ((J. Dai, J. Y. Shao†, R.M. Hochmuth† and M.P. Sheetz)) Department of Cell Biology and †Mechanical Engineering and Materials Science, Duke University, Durham, NC 27710 (Spon. by M.P. Sheetz)

Mechanical tether formation is an effective method to investigate the mechanical properties of cell membranes, including surface viscosity and membrane tension. We have used the laser optical tweezers to form tethers from nerve growth cones by exerting known forces on latex beads attached to chick dorsal root ganglion (DRG) growth cones. With nanometer-level analysis of the displacement of the bead in the laser trap, the instantaneous force of the tether can be measured. A force (F_0) of ~7 pN was required to form a tether and hold it at a constant length. A theoretical model is proposed that describes tether formation from the growth cone. The bending stiffness of the membrane tether is taken into account using a thermodynamic approach. From the derived relationship between the force required to form a tether and the tether growth rate, a value for the surface viscosity of the growth cone membrane can be calculated. Moreover, the change in the tether force with time when the tether is stopped, is predicted. From this theory, the tether forming force at zero velocity is ~8 pN which approximates the experimental value. The growth cone membrane surface viscosity calculated using this model is ~0.48 x 10^{-4} dyn·s/cm. Finally, for a static tether, a relation between the tether forming force, the bending rigidity and the in-plane membrane tension is discussed. We conclude that the laser trap is useful for dynamic measurements of tether formation on cells with complex surface structure and the theoretical model successfully describes the dynamic tether formation process from nerve growth cones.

W-Pos289

MECHANISMS FOR IMMOBILIZATION OF A GPI-LINKED PROTEIN USING SINGLE PARTICLE TRACKING ANALYSIS. ((E.D. Sheets*, G.M. Lee†, and K. Jacobson†)) Departments of Chemistry* and Cell Biology and Anatomy†, University of North Carolina, Chapel Hill, NC 27599-7090.

Recent studies have found conflicting results regarding the diffusion of lipid-linked proteins in the plasma membrane. We have used single particle tracking (SPT) to analyze, with nanometer-level precision, the mobility of the glycosyl-phosphatidylinositol (GPI) anchored protein, Thy-1. Using video-enhanced microscopy and 40-nm diameter colloidal gold conjugated to the monoclonal antibody T24/3.7, the lateral mobility of Thy-1 was followed on C3H 10T 1/2 fibroblasts. Earlier fluorescence photobleaching recovery (FPR) work has shown that Thy-1 has a diffusion coefficient (D) ≈ 4 x 10^{-9} cm^2/sec and an immobile fraction of ~50% [Ishihara et al., (1987) *PNAS* 84:1290]. Using SPT analysis with a 6.7 sec observation time, we have obtained a mean D ≈ 6 x 10^{-10} cm^2/sec for the rapidly moving fraction (~55%) and a mean D ≈ 6 x 10^{-11} cm^2/sec for the slower freely diffusing fraction (~17%). Because both FPR and SPT indicate ~50% of the molecules are either immobile or hindered in some fashion, a more detailed analysis was done to determine possible causes, such as extremely slow diffusion, corralled diffusion, or localization within caveolae. Preliminary data indicate that ~14% of the particles are corralled and ~14% are immobile. When observed for longer times (66-100 sec), the mobile fraction of Thy-1 diffuses up to 10 μm; in-depth analysis of this behavior will also lend insight into mechanisms restricting diffusion. This work was supported by NIH grant GM 41402.

W-Pos290

LYTIC AND IONPERMEABILITY INCREASING ACTIONS OF MELITTIN ON RED BLOOD CELL MEMBRANES

(K.Blaskó[1], L.V.Schagina[2]) [1]Inst. Biophys., Semmelweis Univ. Med., Budapest, Hungary, [2]Inst. Cytology Russian Academy of Sciences, St. Petersburg, Russia

Melittin is the major protein component of the European bee venom. The peptide being amphipatic is easily soluble in aqueous media but also associates strongly with phospholipid bilayers. Melittin has a drastic lytic effect on cell membrane. Numerous studies have been done to learn the nature of this lytic effect but the mechanism is still unclear and the results are rather inconsistent. One of the proposed mechanisms is that melittin produces lysis of human red cells by a colloid osmotic mechanism (Tosteson et al. J. Membrane Biol. 87, 35-44, 1985).

Data are presented here give evidences that the lytic effect and the ionpermeability increasing effect of melittin on red blood cell membrane are not connected processes. The hemolysis and the ionpermeability of melittin treated RBC-s have been measured simultaneously on cells having different membrane potentials. The permeability of melittin treated cells to ^{22}Na, has been found to depend on the membrane potential. But the extent of hemolysis caused by melittin at a given concentration remains the same when the membrane potential is diminished to zero.

W-Pos291

TRACER CATION FLUXES THROUGH MELITTIN TREATED RED BLOOD CELL MEMBRANES

(L.V.Schagina[1], K.Blaskó[2]) [1]Inst. Cytology, Russian Academy of Sciences, St. Petersburg, Russia, [2]Inst. Biophys. Semmelweis Univ. Med., Budapest, Hungary

Melittin, the main protein component of bee venom has been used as a model of the ion conducting protein channels in biological membranes. It consists of 26 amino acids, has 6 positive charges and amphyphylic structure. The channel properties have been studied by measuring the ^{22}Na and ^{86}Rb fluxes through melittin treated red blood cell (RBC) membranes. Melittin produces potential dependent pores in RBC membranes which are equally permeable to ^{22}Na and ^{86}Rb. The kinetics of these tracer fluxes indicate a fast inactivation (τ<2 min) of melittin formed pores. On the other hand melittin inhibits the ouabain sensitive ^{86}Rb uptake. The extent of inhibition depends on the peptide concentration, and it is completed at a melittin concentration of 3.10^6 molecules/cell. The inhibition may be a result of a direct interaction between melittin and Na/K ATPase enzyme or indirect one, due to the melittin altered lipid organisation in the boundary of the enzyme.

W-Pos292

HUMAN *ATP1AL1* GENE ENCODES A POTASSIUM-DEPENDENT, OUABAIN-SENSITIVE ATPase. ((N. Modyanov¶‡, A. Grishin†§, V. Sverdlov¶§, P. Mathews‡ and K. Geering‡)) ¶Dept. Pharmacol., Med. Col. of Ohio, Toledo, OH 43699; ‡Inst. of Pharmacol., Univ. of Lausanne, Switzerland; §Shemyakin and Ovchinnikov Inst., Moscow, Russia; †Dept. of Cell. and Mol. Physiol., Yale Univ. School of Medicine, New Haven

The cDNA for *ATP1AL1* - the fifth member of human the Na,K-/H,K-ATPase gene family - was cloned and sequenced. The deduced primary *ATP1AL1* translation product is 1039 amino acids in length and has Mr of 114,543. The encoded protein (Atp1al1) has all structural features common to known catalytic subunits of ion-transporting P-type ATPases and is equally distant (63-64 % of identity) from the Na,K-ATPase isoforms and the gastric H,K-ATPase.

The Atp1al1 has been expressed in *Xenopus laevis* oocytes in combination with β-subunit of rabbit gastric H,K-ATPase by cRNA injection. Analysis of the functional properties of the $\alpha\beta$ complex, studied by $^{86}Rb^+$ uptake, demonstrated that Atp1al1 is a new type of the human K^+-dependent ATPase (apparent $K_{1/2}$ for K^+ about 375 μM). The ATPase mediated inward K^+-transport was inhibited by ouabain (K_i about 13 μM) and was found to be sensitive to high concentration of Sch 28080. The ATPase activity resulted in alkalinization of the intracellular milieu of oocytes that provides evidence for outward H^+-transport. The data obtained suggest that the Atp1al1 is, most likely, the catalytic subunit of the human non-gastric H,K-ATPase.

W-Pos293

SLOW ACTIVATION OF Na/K PUMP ON FIRST APPLICATION OF ATP IN GIANT CARDIAC PATCHES: COMPARISON TO Na/Ca EXCHANGE. ((D.W. Hilgemann)) Dept. of Physiol., UTSW Med. Ctr., Dallas, TX, 75235.

In giant membrane patches from guinea pig myocytes, sodium pump current ($I_{Na,K}$) activates very slowly when cytoplasmic ATP is applied for the first time ($\tau = 18$s at 1 mM ATP; $K_d = 7.3$ mM; 35°C). During slow activation, $I_{Na,K}$ turns off and on immediately when ATP is removed and reapplied ($K_d \approx 90$ μM). Stimulation of Na/Ca exchange current ($I_{Na,Ca}$) by ATP is kinetically similar, but evidently involves different mechanisms: 1) When ATP is removed, the effect on $I_{Na,Ca}$ reverses; $I_{Na,K}$ reactivates fully within solution switch times when ATP is reapplied after >20 min. 2) Nonhydrolyzable AMP-PNP has no activating effect on $I_{Na,Ca}$; preapplication of 4 mM AMP-PNP preactivates $I_{Na,K}$, such that subsequently applied ATP is immediately effective. The possible involvement of an ATP/AMP-PNP-activated phospholipase A_2 (Hazen & Gross, JBC, 266, 14526, 1992) in slow activation of $I_{Na,K}$ is being tested: 1) Patch pretreatment with PLA_2 (*T. flavoviridis*) preactivates $I_{Na,K}$ ($P<0.001$). 2) With more variability, cell pretreatment with 4 μM arachidonic acid (AA) also preactivates $I_{Na,K}$ ($P<0.05$). Suppression of slow activation by PLA_2 inhibitors, e.g manoilide (2 μM), is not statistically demonstrated ($P \approx 0.05$). Stimulation of $I_{Na,Ca}$ by ATP evidently involves two other mechanisms: 1) The effect decays in two phases upon removal of ATP ($\tau_1 \approx 15$ s; $\tau_2 > 5$ min). 2) The fast decay is reversibly blocked by 2 mM AMP-PNP, 1 mM ATP-gS, 0.5 mM fluoride, or 4 mM PO_4, but not by VO_4. 3) Slow activation of $I_{Na,Ca}$ by ATP, but not of $I_{Na,K}$, can be blocked by 20 μM extracellular hepta-lysine ($P<0.01$).

W-Pos294

ELECTROGENIC PROPERTIES OF THE NA^+- TRANSPORT PATHWAY IN THE NA,K-ATPASE DETERMINED BY CHARGE-PULSE EXPERIMENTS. ((I. Wuddel and H.-J. Apell)) Dept. of Biology, University of Konstanz, D-78434 Konstanz, Germany.

Na,K-ATPase - containing membrane fragments were adsorbed to planar lipid bilayers. Charge transport through the ion pumps was initiated by the release of ATP from caged ATP by a charge-pulse technique. Charge movements could be detected as voltage changes by the principle of capacitive coupling. The observed charge transfer indicated electrogenic reaction steps, which could be characterized by dielectric coefficients. They are a measure of the amount of charge and dielectric distance over which the charge is moved within the protein perpendicular to the plane of the membrane. The reaction sequence $(Na_3)E_1\text{-}P \rightarrow \ldots \rightarrow P\text{-}E_2$ is the major electrogenic event in the whole pump cycle. It could be resolved kinetically into 4 steps with their corresponding rate constants and dielectric coefficients (T = 20°C):

The conformational transition, $(Na_3)E_1\text{-}P \rightarrow P\text{-}E_2(Na_3)$, was rate limiting in the whole sequence (25 s^{-1}) and turned out to be only weakly electrogenic (≤ 0.1). Na^+ release to the extracellular side occurred in three steps. Following characteristic quantities were found:

reaction step	forward rate	equilibrium constant	dielectric constant
$P\text{-}E_2(Na_3) \rightarrow P\text{-}E_2(Na_2)$	1400 s^{-1}	0.1 M	0.65
$P\text{-}E_2(Na_2) \rightarrow P\text{-}E_2(Na)$	700 s^{-1}	1.5 M	0.1-0.2
$P\text{-}E_2(Na) \rightarrow P\text{-}E_2$	4000 s^{-1}	0.09 M	0.1-0.2

These results are in agreement with previously published and less detailed analyses on giant cardiac membrane patches by Hilgemann (Science 263 (1994) 1429-1432) and fluorescence studies with RH 421 - labeled membranes by Heyse *et al.* (J. Gen. Physiol. 104 (1994) 197-240).

W-Pos295

TISSUE-SPECIFIC VERSUS ISOFORM-SPECIFIC DIFFERENCES IN CATION ACTIVATION KINETICS OF THE NA,K-ATPASE. ((A.G. Thérien[1], W.J. Ball[2], R. Blostein[1])) [1]McGill University, Montreal, Canada and [2]University of Cincinnati, Cincinnati, USA.

With the three α isoforms of the Na,K-ATPase expressed in the same cell line (HeLa), cation activation kinetics indicated that the order of apparent affinities for Na^+ is $\alpha1 \approx \alpha2 > \alpha3$ and that for K^+ is $\alpha3 > \alpha2 \approx \alpha1$[1]. Similar results were obtained in transport studies using rat kidney microsome ($\alpha1$)- and axolemma (mainly $\alpha3$)-fused dog erythrocytes[2]. At face value, these results were difficult to reconcile with those of Shyjan *et al.*[3] who used membranes from rat pineal gland ($\alpha3$), kidney ($\alpha1$) and brain ($\alpha1$, $\alpha2$ & $\alpha3$); in that study, the order of affinities for Na^+ were pineal>brain>kidney. We have confirmed the Na^+-activation profiles described previously[1,2]. In addition, studies of Na^+-activation of $\alpha1$ from different tissues [rat $\alpha1$-transfected HeLa cells, kidney and axolemma (with low [ouabain] to inhibit $\alpha2$ and $\alpha3$)], show that the order of apparent affinities of $\alpha1$ for Na^+ is axolemma>HeLa>kidney. These differences are accounted for, at least partly, by tissue-specific differences in sensitivity of $\alpha1$ to inhibition by K^+ at low [Na^+]. The order of apparent affinity for K^+ is kidney $\alpha1$>axolemma $\alpha3(\alpha2)$>axolemma $\alpha1$. The tissue-specific order of apparent affinities of $\alpha3$ for Na^+ is pineal>axolemma>HeLa. Taken together, these studies indicate that the same isoform may behave differently in different tissues, which partly explains the dichotomy reported previously[1,2]. It remains to be determined whether and to what extent tissue-specific behavior of the same catalytic isoform is due to a distinct membrane environment or to association with various β's, e.g. human $\beta1$ in HeLa cells versus rat $\beta1$ in other tissues, and associations of $\beta1$ with $\alpha3$ in axolemma and of $\beta2$ with $\alpha3$ in pineal gland. Supported by the MRC (Canada), NIH and AHA.

[1] Jewell & Lingrel, J. Biol. Chem., **266**:16925-16930 (1991).
[2] Munzer *et al.*, J. Biol. Chem., **269**:16668-16676 (1994).
[3] Shyjan *et al.*, Proc. Natl. Acad. Sci. USA, **87**:1178-1182 (1990).

W-Pos296

WITHDRAWN.

W-Pos297

ELECTROGENIC LI^+: LI^+ EXCHANGE MEDIATED BY THE SARCOLEMMAL NA^+-K^+ PUMP. ((Paul D. Hemsworth, Helge H. Rasmussen.)) Royal North Shore Hospital, Sydney, NSW, Australia.

Extracellular Li^+ can substitute for K^+ at extracellular sites of the Na^+-K^+ pump. However, despite strong similarities in physico-chemical characteristics between Na^+ and Li^+ it has been difficult to demonstrate a similar ability of Li^+ to substitute for Na^+ at intracellular sites. We have used the whole-cell patch-clamp technique to examine if Li^+ can substitute for Na^+. We voltage-clamped single rabbit ventricular myocytes at 0 mV with wide-tipped patch-pipettes containing (in mM): 160 Li^+, 0 K^+ and 0 Na^+. Tyrode's solution containing 140 Na^+, 5.6 K^+ and 2 Ba^{2+} was superfused. Ouabain (50 μM) induced a shift in holding current, normalised for membrane capacitance, of 0.48 $\pm$ 0.05 pA/pF (n=7, $\pm$ SE). No ouabain induced shift in holding current occurred when 4 cells were superfused with K^+-free Na^+-Tyrode's solution. When we replaced all Na^+ and K^+ in the superfusate with 146 Li^+ and when pipette solutions contained 160 mM Li^+ ouabain induced a shift in holding current of 0.53 $\pm$ 0.03 pA/pF (n=6). The voltage-dependence of this current shift was similar in appearance to the voltage-dependence reported for Na^+-K^+ pump current of cardiac myocytes when the pump operates in the normal Na^+: K^+ exchange mode. No ouabain induced shift in holding current occurred in 4 cells superfused with Li^+-Tyrode's solution when Li^+ in the pipette filling solution was replaced with tetramethylammonium. In summary: 1) Li^+ can substitute for K^+ at extracellular Na^+-K^+ pump sites in cardiac myocytes. 2) Li^+ can substitute for Na^+ at intracellular sites. 3) The Na^+-K^+ pump can mediate electrogenic Li^+: Li^+ exchange. We conclude that, as for extracellular transport sites of the Na^+-K^+ pump, the specificity of intracellular sites for the physiologically transported ions is not absolute

W-Pos298

PHOSPHORYLATION OF ALPHA-SUBUNIT OF Na,K-ATPase FROM DUCK SALT GLAND AND DOG KIDNEY BY PROTEIN KINASE A AND C CHANGES KINETIC PROPERTIES OF THE ENZYME. ((O.D. Lopina, A.M. Rubtsov, I.B. Mollakova, S.P. Petukhov, A.V. Chibalin and A.V. Nickashin)) Dept. Biochemistry, Moscow State University, 119899 Moscow, Russia, and Institute of Experimental Cardiology, RCRC, 121552 Moscow, Russia. (Spon. by W. Rouslin)

Phosphorylation of highly purified preparations of Na,K-ATPase from duck salt gland and dog kidney by protein kinase A results in incorporation of phosphate into the alpha-subunits with a stoichiometry of 1.8 and 0.8 mole/mole, respectively. Phosphorylation of the enzyme from both sources results in nearly identical changes in kinetic behavior: i) the shape of velocity/[ATP] curve is altered from a biphasic to a hyperbolic curve; ii) $K_{0.5}$ for Na^+ is increased from 5±0.5 to 12±1.5 mM (n=3); and iii) the enzyme sensitivity to ouabain appears to increase. Phosphorylation of duck salt gland enzyme by protein kinase C with a stoichiometry of 1.3 mole/mole affects the same parameters in a similar way. Since phosphorylation of only a single site on the dog kidney enzyme serves to alter the kinetics, the data suggest that only one of two putative phosphorylation sites in the Na,K-ATPase molecule is involved in these functional effects. (Supported by ISF Grant ME5000 to ODL).

W-Pos299

A cAMP-DEPENDENT PKA PATHWAY MEDIATES THE INHIBITORY EFFECT OF β-STIMULATION ON NA/K PUMP CURRENT IN GUINEA PIG VENTRICULAR MYOCYTES. ((J. Gao, I.S. Cohen, R.T. Mathias & G.J. Baldo)) Dept. of Physiology & Biophysics, HSC, SUNY at Stony Brook, NY 11794.

The β-agonist isoproterenol (ISO) reduces the Na/K pump current (I_p) via β adrenergic receptors when intracellular calcium ($[Ca^{2+}]_i$) is below 0.15μM (Gao, Mathias, Cohen & Baldo, 1992, *J. Physiol.* 449:689-704). The intracellular signaling pathway was investigated using the whole cell patch clamp technique and 0.015μM $[Ca^{2+}]_i$. The inhibitory effect of ISO was mimicked by application of 0.5mM of the membrane-permeant cAMP analog chlorophenylthio-cAMP; 100μM of the phosphodiesterase inhibitor IBMX; or 50μM of the adenylyl cyclase activator forskolin. Intracellular application of 0.5μM of the synthetic peptide inhibitor (PKI) of protein kinase A (PKA) blocked this effect of ISO. These results suggests the inhibitory effect of ISO on I_p is mediated via phosphorylation induced by a cAMP-dependent PKA pathway. Neither the non-specific protein kinase inhibitor H_7 (100μM) nor the protein phosphatase inhibitor calyculin A (0.5μM) had any effect on I_p in the absence of ISO. In the presence of ISO, however, H_7 increased and calyculin A reduced I_p (1μM and 12nM, respectively). These results indicate a low basal phosphorylation level which makes the effects of H_7 and calyculin A difficult to detect in the absence of an ISO-induced increase in phosphorylation level. Supported by grants HL20558, HL28958 and the AHA.

W-Pos300

β-STIMULATION AND THE I-V RELATIONSHIP OF NA/K PUMP CURRENT IN GUINEA PIG VENTRICULAR MYOCYTES. ((J. Gao, R.T. Mathias, I.S. Cohen, J. Shi & G.J. Baldo)) Dept. of Physiology & Biophysics, HSC, SUNY at Stony Brook, NY 11794.

We used the whole cell patch clamp technique and hyperpolarizing voltage ramps to investigate the effects of the β-agonist isoproterenol (ISO) on the I-V relation of the 1mM DHO-blockable Na/K pump current (I_p). We have shown elsewhere the effects of ISO are mediated through activation of the A kinase. In elevated (1.4μM) $[Ca^{2+}]_i$, ISO shifts the I-V relationship of I_p in the negative direction by 25-40mV without altering the maximum I_p at depolarized potentials. In low (0.015μM) $[Ca^{2+}]_i$, ISO reduces I_p equally at all potentials by 20-30% without inducing any voltage shift in the I-V relation. We used Na^+-free Tyrode to remove the voltage dependence of I_p and re-examined $[Ca^{2+}]_i$ effects on ISO-induced I_p inhibition. Under these conditions, ISO caused a Ca^{2+} concentration-dependent inhibition of I_p with a maximum of 20-30% and a half-maximally effective $[Ca^{2+}]_i$ of 0.144μM. We tested whether calmodulin-dependent kinase II contributes to Ca^{2+} action by adding inhibitor fragment 290-309 to our pipette solution. This did not alter ISO's effects at 1.4μM $[Ca^{2+}]_i$. Thus, we are uncertain of the pathway connecting $[Ca^{2+}]_i$ to the ISO-induced effects on I_p. We conclude, however, at least three events are taking place: *i)* β stimulation via A kinase activation inhibits I_p in the absence of $[Ca^{2+}]_i$; *ii)* increasing $[Ca^{2+}]_i$ reduces and ultimately eliminates the inhibitory effect of β stimulation; and *iii)* elevated $[Ca^{2+}]_i$ in concert with β stimulation and A kinase activation shift the voltage dependence of I_p negative. Supported by grants HL20558, HL28958 and the AHA.

W-Pos301

KINETICS OF POTASSIUM TRANSPORT BY THE Na^+,K^+-ATPASE. ((P. Pratap, A. Palit and J.D. Robinson)) Dept. of Physics and Astronomy, UNCG, Greensboro, NC 27412 and Dept of Pharmacology, SUNY-HSC, Syracuse, NY 13210

Conformational changes for the reaction $E_2(K^+) \rightarrow E_1 \cdot Na^+$ (accelerated by ATP) in a dog kidney Na^+, K^+-ATPase preparation labeled with 5-iodoacetamidofluorescein (IAF) were followed with a stopped-flow fluorimeter in terms of the rate constant (k_{IAF}) of fluorescence change: on rapid mixing of IAF-enzyme+5mM K^+ with 20 mM Na^++varying [ATP] at 20°C, fluorescence increased: k_{IAF} increased with ATP from 0.6 s^{-1} at 0 ATP to 36 s^{-1} at 5 mM ATP. These data were fitted with the equation: $k=k_{max} \cdot [ATP]/(K^{ATP}_{1/2}+[ATP])$, to give $K^{ATP}_{1/2}$=700 μM, and k_{max}=53 s^{-1}. As a function of temperature from 5 to 25°C, k_{max} increased sigmoidally from 1 to 63 s^{-1} (with an 8X increase in the range from 15 to 25°C), and $K^{ATP}_{1/2}$ increased from 80 to 700 μM. These results indicate that K^+ deocclusion is the rate-limiting step.

Kinetics of the reverse reaction were examined on the same preparation: on rapidly mixing IAF-enzyme plus Na^+ (0, 0.1, or 1 mM) with varying K^+ (0-5 mM), k_{IAF} increased from 0 to 175 s^{-1} with a half-maximal [K^+] of 3 mM when [Na]=0. Addition of Na^+ *or* pretreatment of enzyme with oligomycin shifted $K^K_{1/2}$ to higher values: kinetics of enzyme+0.1 mM Na^++oligomycin were the same as those of enzyme+1 mM Na^+-oligomycin. When temperature was varied from 15 to 25°C, the maximal rate-constant increased 2.6-fold, independent of [K^+]. These data indicate that (i) the rate-limiting step seen by IAF in the two experiments are different, and (ii) oligomycin increases the Na^+-affinity of the E_1 form of the enzyme. [Supported by grants from NIH].

W-Pos302

STRUCTURAL BASIS FOR SPECIES SPECIFICITY IN PHOSPHORYLATION OF Na,K-ATPase BY PROTEIN KINASE C. (M.S. Feschenko and K.J. Sweadner) Neuroscience Center, Massachusetts General Hospital, Charlestown, MA 02129.

Phosphorylation of the α1 subunit of Na,K-ATPase by protein kinase C can be demonstrated *in vitro* using purified components. We have shown that rat α1 can be phosphorylated to a stoichiometry of close to 1 mole per mole, while α1 from dog or pig can be phosphorylated to only 10% of that level. Tests for a contaminating phosphatase in dog and pig Na,K-ATPase preparations were negative. Examination of the sequence differences among these species reveals only 3 places where Ser or Thr residues are present in rat but not in dog or pig α1. Limited proteolysis was used to digest the Na,K-ATPase, and specific antibodies were used to identify the resulting phosphorylated fragments. Proteolytic fingerprinting resulted in a phosphorylated peptide pattern identical to that stained by antibodies against the N-terminus of rat α1. Cleavage by trypsin at the T2 site, Lys^{32}, removed the phosphate, leaving otherwise intact α1. There is no Thr and only two Ser, Ser^{11} and Ser^{18}, in the sequence 1-32, and only Ser^{18} is in a motif for protein kinase C phosphorylation (KKSKKAKK). This serine is missing in both dog and pig α1 (KKKAKK). A low level of phosphorylation was also seen by others near the N-terminus of *Bufo* α1 where there is no serine homologous to Ser^{18}. Phosphorylation at Ser^{11} may thus account for the low level seen in dog and pig α1. We showed that phosphate incorporation into rat α1 was affected by Na,K-ATPase conformation, but no detectable inhibition of maximal ATPase activity was seen.

W-Pos303

NaK-ATPase: PROXIMITY OF THE β-SUBUNIT TO THE C- and N-TERMINAL INTRAMEMBRANE SEGMENTS OF THE α-SUBUNIT. ((N.A. Sarvazyan and A. Askari)) Dept. Pharmacology, Med. Coll. of Ohio, Toledo, OH 43699

Extensive tryptic digestion of renal NaK-ATPase in the presence of Rb^+ removes large portions of the cytoplasmic domains of α. The remaining complex occludes cations, and contains β and several defined peptides consisting largely of the intramembrane segments of α. Since β regulates cation occlusion, we tried to detect β interactions with the α-fragments by solubilizing the above complex with digitonin, and subjecting it to Cu^{2+}-induced cross-linking. We showed before (FASEB J 8, A299, 1994) that one of the two resulting cross-linked products contained β and the 19-kDa C-terminal fragment of α. Extending these studies, we have now identified both products by partial sequencing and reactivity with sequence-specific antibodies. One product is a dimer of 19-kDa C-terminal peptide and the 11-kDa N-terminal peptide of α. The other is a trimer of β, 19-kDa, and 11-kDa peptides. These findings indicate the proximities and interactions of β and the terminal transmembrane segments of α. Supported by NIH grant HL36573.

W-Pos304

CORRELATION BETWEEN THE ACTIVITIES OF MICROSOMAL ATPASES AND IP_3 RECEPTORS FROM EPITHELIAL CELLS OF PORCINE TRACHEA. ((Young-Kee Kim, Hyoung-Jin Cho, and Sung-Shin Park)) Dept. of Agricul. Chem., Chungbuk National University, Cheung-Ju, Chungbuk, 360-763, Korea.

Membrane vesicles were prepared by differential centrifugation from the epithelial cells of porcine trachea. The microsomes appeared to be tight-sealed vesicles since they showed a saturation in $^{45}Ca^{2+}$ uptake experiment. The uptake occurred fast and 80% saturation was obtained within 2 minutes although the complete saturation took more than 10 minutes. Total activity of microsomal ATPases was measured spectrophotometrically by a coupled enzyme assay in the solution containing NADH and 50 μM Ca^{2+}. The steady-state activity was 217±45 (nmoles/min · mg protein) and this was increased to 308±30 by the addition of 4 μM inositol 1,4,5-trisphosphate (IP_3), an agonist of IP_3-sensitive Ca^{2+} release channels (IP_3 receptors). Since the activation of IP_3 receptors increased the activity of ATPases, these results suggest that the concentration gradient of Ca^{2+} across the microsomal membrane builds up rapidly and thus the activity of ATPases (mostly Ca^{2+}-ATPases) is dependent on the amount of Ca^{2+} released by IP_3 receptors. In order to test the dependence of the activity of ATPases on the activity of IP_3 receptors, the activity of ATPases was monitored in various Ca^{2+} concentration using EGTA-Ca^{2+} buffers. The activity appeared biphasic and the maximal activity of 397±36 was obtained in the solution containing 100 nM of free Ca^{2+}. Below or above this concentration, the activity of ATPases was decreased. The addition of IP_3 increased the activity of ATPases in the whole range of Ca^{2+} concentration. These results strongly support the positive correlation of activities between ATPases and IP_3 receptors since the Ca^{2+}-dependent activation and inactivation is one of the important character of IP_3 receptors.

COUPLED TRANSPORTERS

W-Pos305

CPX, A SELECTIVE A_1 ADENOSINE RECEPTOR ANTAGONIST, REGULATES INTRACELLULAR pH IN CYSTIC FIBROSIS CELLS. ((Valeria Casovola, R. James Turner, Colleen Guay-Broder, Kenneth A. Jacobson, Ofer Eidelman and Harvey B. Pollard)) LCBG & LBC, NIDDK; CIPCB, NIDR; NIH, Bethesda, MD, 20892, USA and Università Degli Studi di Bari, Italy.

Na^+/H^+ exchange activity in CFPAC-1 cells carrying the CFTR (ΔF508) mutation is inhibited by 8-cyclopentyl-1-3-dipropylxanthine (CPX), a selective A_1-adenosine receptor antagonist. This down-regulation is much less pronounced in CFPAC-1 cells transfected with wt CFTR. CPX has been reported to activate chloride efflux from cystic fibrosis cells such as pancreatic CFPAC-1 and lung IB3 cells bearing the CFTR(ΔF508) mutation, but has little effect on the same process in cells repaired by transfection with wild type CFTR (Eidelman *et al.*, 1992 *PNAS* 89:5562-5566). The effect of CPX on Na^+/H^+ exchange in CFPAC-1 cells depends on the presence of adenosine, since pretreatment of the cells with adenosine deaminase mimics CPX effect and blunts further inhibition by CPX. Similar effect of CPX was observed in the IB3 cell line. We also show that, by contrast, CPX action on these cells does not lead to alterations in intracellular free $[Ca^{2+}]$. We conclude that CPX affects pH regulation in CFPAC-1 cells, probably by antagonizing the tonic action of endogenous adenosine.

W-Pos306

THE Na^+-H^+ ANTIPORTER IS ELECTRONEUTRAL AND VOLTAGE-INDEPENDENT. ((N. Demaurex, M. Woodside, J. Orlowski and S. Grinstein)) Cell Biology, HSC, Toronto, ON M5G 1X8 and Physiology, McGill University, Montreal, PQ H3G 1Y6 (Spon. by S. Grinstein).

The paradigm that Na^+-H^+ exchange in vertebrates is electroneutral has recently been challenged by measurements of antiport-mediated currents in turtle colon epithelium (*J. Gen. Physiol.* 103:895, 1994). We assessed the electrogenicity of mammalian antiporters using the whole-cell patch-clamp technique while measuring intracellular pH (pH_i) by microfluorimetry. In murine macrophages, which were shown by RT-PCR to express the NHE-1 isoform of the antiporter, activation of Na^+-H^+ exchange induced sizable pH_i changes that were associated with transmembrane currents. The Na^+-dependent, amiloride-sensitive currents were carried by H^+ (equivalents). The activation kinetics, pH-dependence and pharmacology of these H^+ currents were identical to those described earlier for the voltage-gated H^+ conductance of macrophages. It was therefore conceivable that electroneutral Na^+-H^+ exchange was indirectly modulating the activity of a separate conductive pathway. This possibility was tested in CHO cells, which were found to lack the voltage-gated H^+ conductance. Antiport activation in CHO cells was not associated with detectable currents, despite the occurrence of the anticipated pH_i changes. Similar results were obtained in CHO cells transfected with either the NHE-1, NHE-2 or NHE-3 isoforms. Moreover, the rate of antiport-mediated pH_i changes was independent of the holding voltage in all the isoforms. We conclude that the mammalian Na^+-H^+ antiporter is electroneutral and voltage-independent. However, in cells endowed with a pH-sensitive H^+ conductance, activation of Na^+-H^+ exchange can modulate the transmembrane H^+ current. The currents reported in turtle colon might be due to a similar "cross-talk" between the antiporter and a H^+ conductance.

W-Pos307

OSMOTIC RESPONSIVENESS OF THREE ISOFORMS OF THE Na^+/H^+ EXCHANGER ((A. Kapus[1], L. Bianchini[2], J. Pouyssegur[2], J. Orlowski[3] and S. Grinstein[1])) [1]Cell Biology, HSC, Toronto ON M5G1X8, Canada, [2] Centre de Biochimie, CNRS, Nice, France, [3] Dept. Physiology, McGill University, Montreal PQ H3G 1Y6, Canada (Spon. by Y. Marunaka)

The aim of the present study was to establish the osmotic responsiveness of three recently cloned isoforms of the mammalian Na^+/H^+ exchanger (NHE-1-3) and to define the structural basis of osmosensitivity. Antiport-deficient fibroblastic cell lines were stably transfected with one of the 3 isoforms or with different truncation mutants of NHE-1. Transport activity was determined isotopically, as amiloride-sensitive $^{22}Na^+$ uptake, as well as fluorimetrically, as Na^+-dependent changes in cytoplasmic pH (pH_i) measured in either single cells or populations of cells loaded with BCECF. Wild type NHE-1 and 2 were stimulated by hypertonicity. Conversely, these isoforms were inhibited by hypotonic media. Stimulation by hyperosmolarity is mediated by an alkaline shift in the pH_i-dependence of the antiport. Deletion of the last 125 carboxy-terminal amino acids of NHE-1 (Δ689) had no effect on osmotic responsiveness. Truncation at position 635 (Δ635) caused basal activation of the antiport and the loss of the osmotic stimulation, suggesting that the central portion of the cytoplasmic tail may exert an autoinhibitory effect. In contrast to NHE-1 and 2, the epithelial isoform NHE-3 is markedly inhibited by hyperosmolarity. The inhibition is rapid, reversible and seems to require the presence of intracellular Cl^-. Osmotic inhibition of NHE-3 is primarily due to an acidic shift in the pH_i dependence of the exchanger. Activation of NHE-1 and 2 by hyperosmolarity is consistent with a role in regulatory volume increase. By contrast, NHE-3, which displays a diametrically opposed behaviour, may instead be involved in the regulation of Na^+ and H^+ transport in epithelia subject to varying osmolarity.

W-Pos308

DOES HUMAN CYTOMEGALOVIRUS (HCMV) INFECTION OF MRC-5 FIBROBLASTS RESULT IN REDUCED NA^+/H^+ EXCHANGER ACTIVITY? **((W.E. Crowe, A.A. Altamirano, J.C. Russell and J.M. Russell.)) Dept. of Physiology, Medical College of Pennsylvania, Philadelphia, PA 19129.**

We have previously reported a difference in the values of resting pH_i and the pH_i response to hyperosmotic solution between HCMV-infected and mock-infected MRC-5 fibroblasts, 72h post exposure (Altamirano et al., Biophys. J. 66: A338, 1994). These differences may reflect an alteration in kinetic properties of the Na^+/H^+ exchanger; therefore we studied the Na^+ dependence of acid extusion using the pH-sensitive dye, BCECF. Experiments were conducted in HEPES buffered solution and in the presence of 100μM H_2DIDS to block any residual activity of HCO_3^- dependent ion transporters. Cells were first incubated in Na^+ free ($NMDG^+$ replacement) until a steady state pH_i was obtained (HCMV: 27±2min, pH_i=7.28±0.02, n=8; Mock: 5.5±0.3min, pH_i=7.04±0.04, n=8). Next, some of the $NMDG^+$ was replaced with Na^+ (i.e. 8, 16, 32, 64 mM) and the rate of pH_i increase (dpH_i/dt) was measured. To obtain specific H^+ fluxes at pH_i=7.3, dpH_i/dt values were corrected for the basal rate of acid loading, multiplied by the buffering power and divided by an index of the cell surface area. The buffering power at pH_i=7.3 was determined using the NH_4^+/NH_3 technique (HCMV: β=10±2, n=3; Mock: β=12±4, n=3). The relative surface area of HCMV-infected cells, estimated from ouabain binding data, is 2.5 fold greater than in mock-infected cells (Altamirano et al., Virol. 199: 151, 1994). Since the density of Na^+ pumps may be reduced in HCMV-infected cells, the relative estimate of surface area may be underestimated. Calculated H^+ fluxes at the different $[Na^+]_o$ were then fitted to the Michaelis-Menten equation and the estimates of K_ms' were 30±6mM and 27±12mM, and V_{max}s' were 2.4±0.2 and 5.1±1.0mM/min/unit area, for HCMV- and mock-infected cells respectively (r^2 = 0.99 and 0.97). These observations suggest that there is no difference in the Na^+ affinity of the Na^+/H^+ exchanger between HCMV- and mock-infected cells. The observed reduction in V_{max} of HCMV-infected cells, may either result from a decrease in the density of transporters and/or reduced turnover rate of individual transporters. Supported by DHHS NS 11946.

W-Pos309

ANGIOTENSIN II STIMULATES THE Na^+/HCO_3^- SYMPORT IN HEART. ((Trudy A. Kohout and Terry B. Rogers)) Dept. of Biological Chemistry, Univ. of Maryland School of Medicine, Baltimore MD 21201

Angiotensin II (AngII) is a cardioactive peptide hormone that alters contractility as well as evokes changes in myocyte growth. While changes in contractility are associated with activation of the phosphoinositide/ protein kinase C pathway, it is less clear what crucial mechanisms underlie long term changes in growth.

Since many mitogens regulate pH in their target cells, the goal of this study was to determine if AngII regulated pH in neonatal rat ventricular myocyes. Changes in intracellular pH, pH_i were monitored in single cells using the fluorescent pH indicator carboxy-SNARF-1. Stimulation with AngII (10 nM) resulted in a rapid receptor-mediated alkalinization of 0.09±0.02 pH units which was blocked by the AT_2-specific antagonist CGP42112A (10 nM). Furthermore, using the NH_4^+ prepulse technique, the AngII-treated myocytes increased the initial rate of recovery from the imposed acid load by 2.71±0.81 fold over control cells. The intracellular alkalinization and transporter activation are HCO_3^--dependent and Cl^--independent suggesting the involvement of the Na^+/HCO_3^- symport. In contrast, the alkalinization induced by phorbol ester activation of PKC is HCO_3^--independent and results from the stimulation of the Na^+/H^+ exchanger as evidenced by its block with amiloride. Although AngII and phorbol esters both alkalinize the cell their mechanisms of action in neonatal rat ventricular myocytes are quite distinct.

W-Pos310

THE Cl/HCO_3 EXCHANGE IN NEONATAL RAT VENTRICULAR CELLS. ((Irina Korichneva, Michel Pucéat, Robert Cassoly* and Guy Vassort)) INSERM U.390, CHU Arnaud de Villeneuve, Montpellier France. *CNRS UMR 9922, Institut Jacques Monod, Paris, France.

The Cl/HCO_3 exchanger is an acidifying anionic exchanger (AE) that regulates pH_i in most cell types including cardiomyocytes. We recently identified in adult rat cardiomyocytes two proteins (80 and 120 kDa) immunologically related to the erythroid band 3 protein, that are likely to mediate the anionic exchange. Herein, we further investigated the expression of these proteins during the development of two days old neonatal rat cardiomyocytes kept in culture for two weeks. In cells cultured for three days, both band 3-like proteins were present as assessed by Western-blotting using an anti-whole band 3 antibody. Using antibodies raised against specific sequences of erythroid AE1 and predicted cardiac AE3, we found that the 80 kDa protein is likely to be a truncated product of the AE1 gene and that the 120 kDa protein is encoded by AE3. Subcellular fractionation of cardiomyocytes showed the presence of the band 3-like proteins in membrane, nuclear and myofibril fractions. Cell immunostaining with the anti-whole band 3 antibody combined with confocal microscopy more specifically revealed a perinuclear distribution of the proteins at early stage of development. The proteins were colocalized with specific markers of the Golgi complex (i.e., WGA, CTR433 antibody). Later on, the proteins were found in the newly organized sarcomeric units between the bands decorated by an anti-myosin antibody. This suggests the presence of the proteins in costameres, areas of attachment of myofibrils to the sarcolemma. We are currently microinjecting the specific anti-AE antibodies in order to determine the respective role of AE1 and AE3 in the function of Cl/HCO_3 exchange in cardiomyocytes.

Ca^{2+}-ATPases

W-Pos311

CHOLESTEROL IS A NATURAL REGULATOR OF THE Ca-ATPase AND Na-Ca EXCHANGER ACTIVITY FROM T-TUBULE MEMBRANES OF SKELETAL MUSCLE. ((Alicia Ortega)) Depto. de Bioquimica, Facultad de Medicina, Universidad Nacional Autonoma de Mexico, 04510.

Lipids and proteins can diffuse rapidly in the plane of some membranes. Thus the high fluidity prompts the question of whether persistent interactions between protein and lipids must occur to support protein functions. Cholesterol a significant component of most plasma membranes, is enriched in t-tubule membranes which are invaginations of the sarcolemma. Thermal analysis and DSC of the Ca-Mg-ATPase and Na-Ca exchanger activities, in native and t-tubule membranes partially depleted of cholesterol were made. The inactivation temperature (T_I) of the Ca-ATPase revels two transitions with T_I at 57 and 49 °C that correspond to the Mg-ATPase and Ca-ATPase/ and ATP dependant Ca-transport respectively, whereas the Na-Ca exchanger T_I is lower for both Na dependent Ca influx and Ca efflux. In membranes with low cholesterol, the thermal inactivation profile changes drastically leading to a less stable protein structure. The DSC profile of the native T-tubule have tree major transitions, in contrast with the membranes with lower cholesterol that shows up six transitions. The correlation of T_I of the Ca-ATPase and Na-Ca exchanger with the T_m of the components of the DSC profile of t-tubule membranes will be discuss.

W-Pos312

QUERCETIN EXERTS A BIPHASIC EFFECT ON CARDIAC SARCOPLASMIC RETICULUM Ca^{2+}ATPase ACTIVITY. ((Edward McKenna, Kathleen E. Coll, Ernest J. Mayer, Elaine K. Mazack, Joanne Antanavage, Richard T. Wiedmann, Jeffrey S. Smith, and Robert G. Johnson, Jr.)) Merck Research Laboratories, West Point, PA 19486

In cardiac sarcoplasmic reticulum SR, low concentrations of quercetin (0.5-10 μM) stimulate Ca^{2+}ATPase activity and $^{45}Ca^{2+}$ uptake, while higher quercetin concentrations inhibit both activities. Other flavonoids (quercetagitin, myricetin, robinetin, fisetin, and apigenin) also produce low-dose stimulation of cardiac SR Ca^{2+}ATPase. Quercetin is an inhibitor of skeletal muscle SR Ca^{2+}ATPase as previously shown [Shoshan and MacLennan 1981, JBC 256,887-892]. Quercetin's stimulatory effect appears to be protein-dependent with its maximal effect occurring at 300 nmole/mg cardiac SR. Quercetin (10 μM) increased the apparent calcium sensitivity of the Ca^{2+}ATPase by about 0.1 pCa units, i.e., it appears to mimic the effect of phospholamban (PLB) phosphorylation. Further, the stimulation requires a phospholamban-regulated Ca^{2+}ATPase: after deoxycholate-solubilization followed by bio-bead treatment, mild trypsinization, or pre-treatment of the cardiac SR with monoclonal anti-PLB antibody, quercetin produces only inhibitory effects. Stimulatory concentrations of quercetin had little or no effect on phosphoenzyme (E_1-P) formation from $\gamma[^{32}P]$-ATP, but inhibited formation at higher concentrations. Phosphoenzyme (E_2-P) formed from $[^{32}P]$-P_i was inhibited at all concentrations. Part of quercetin's inhibitory action results from competitive interaction with the MgATP binding site on the Ca^{2+}ATPase as inhibitory concentrations of quercetin increase the apparent K_m for MgATP. The mechanism of the stimulatory effect is unclear, but the data suggest that quercetin and phospholamban may interact at or near the nucleotide binding domain of Ca^{2+}ATPase to alter conformational transitions that occur during Ca^{2+} transport.

W-Pos313

DIABETIC ALTERATIONS OF PHOSPHOLAMBAN(PLB) AND Ca^{2+}-ATPase EXPRESSION IN RAT CARDIAC SARCOPLASMIC RETICULUM(SR) ((S. Y. PARK, H. W. KIM)) Dept. of Pharmacology, Univ. of Ulsan College of Medicine, Seoul 138-040, Korea

PLB, the inhibitor of cardiac SR Ca^{2+}-ATPase, regulate the Ca^{2+} transport by phosphorylation/ dephosphorylation. In diabetes mellitus, cardiomyopathy has been suggested to be caused by the intracellular Ca^{2+} overload in the myocardium, which is partly due to the defect of calcium transport of the SR. In the present study, the defect of calcium transport was observed in cardiac SR from the chronic diabetic rats. Both the maximal Ca^{2+} uptake rate and the affinity for Ca^{2+} were decreased in the diabetic rat cardiac SR in comparison with the control. We examined whether the decrease of the cardiac SR function in streptozotocin-induced diabetic rat is associated with the level of PLB phosphorylation. Upon SDS-PAGE and autoradiography with γ^{32}P-ATP, the levels of PLB phosphorylation in diabetic rat cardiac SR were increased, compared with that in control cardiac SR. To determine whether the increased PLB phosphorylation level is associated with the increased PLB expression, western blot analysis was performed. The level of Ca^{2+}-ATPase was decreased (77.6±4.7%) in diabetic heart, however, PLB level was increased (122.9± 6.7%). Consequently, the relative PLB/Ca^{2+}-ATPase ratio was 1.6 in diabetic hearts, and these changes correlated with changes in the EC_{50} of the SR Ca^{2+} uptake for Ca^{2+}. Since PLB is the inhibitor of SR Ca^{2+}-ATPase, the increase of PLB and the decrease of Ca^{2+}-ATPase levels in the diabetic state could explain well the functional defect of SR. These results suggest that the impaired cardiac SR function in diabetic rat is a consequence of the decreased SR Ca^{2+}-ATPase level, which is further impaired due to the inhibition by the increased level of PLB.

W-Pos314

H-89, A "SELECTIVE" INHIBITOR OF cAMP-DEPENDENT PROTEIN KINASE INHIBITS CARDIAC & SKELETAL MUSCLE SR-Ca^{2+} PUMPS. ((P. Lahouratate, J. Guibert, J.C. Camelin and I. Bertrand.)) SmithKline Beecham, Lab. Pharm., BP-58, 35762 Saint Grégoire, France. (Spon. by J. Su)

H-89 is a selective inhibitor against cAMP-dependent protein kinase (cAPrK) by competing against ATP (J. Biol. Chem., 265 : 5267-,1990). To determine its usefulness for studying cardiac SR-Ca^{2+} pump regulation by cAPrK, its effects were studied on SR-Ca^{2+} ATPase of canine cardiac (CCM) and rabbit fast skeletal muscles (RFSM) SR-microsomes prepared according to Jones et al. (J. Biol. Chem., 254: 530-, 1979) and to Mitchell et al. (J. Cell Biol., 96: 1008-, 1983). The effect of H-89 on Ca^{2+} ATPase activity (colorimetric determination of Pi) was measured by incubating microsomes (with 2 μM A-23187), in (mM) KCl, 100; $MgCl_2$, 2; MOPS, 50; Na_2ATP, 2 and (pCa 6.2), pH 6.8 at 30°C.
H-89 inhibited specifically SR-Ca^{2+}ATPase activities both in CCM and RFSM with IC_{50} of 8.6 and 7.2 μM, and with n_{Hill} of 0.98 and 1.09, respectively. Analysis at several ATP concentrations (0.2 to 4 mM) showed that H-89 inhibits both ATPases by competing in a non-competitive fashion with ATP (K_i of 14.3 and 6.6 μM in CCM and RFSM, respectively). Because the effect of H-89 is similar on CCM and RFSM (phospholamban is absent in the later one as confirmed by the lack of stimulatory effect of heparin), the inhibition of cardiac Ca^{2+} ATPase activity can therefore be considered a consequence of a direct interaction with the ATPase and not to involve suppression of a cAPrK-mediated phosphorylation of phospholamban. Our results show that a direct effect on SR-Ca^{2+} ATPase plays an important role in the action of H-89.

W-Pos315

REDUCED SERCA EXPRESSION CORRELATES WITH PROLONGATION OF THE SYSTOLIC CA^{2+} TRANSIENT IN HYPERTROPHIED NEONATAL RAT VENTRICULAR MYOCYTES. ((Gina-Lee Toaldo, Colleen A. Hefner, Beth A. Bailey and Steven R. Houser)) Temple University School of Medicine, Phila. PA, 19140.

Changes in the systolic cardiac muscle Ca^{2+} transient during development and hypertrophy are thought to involve changes in the expression of Ca^{2+} regulatory proteins, including the SR Ca^{2+} ATPase (SERCA). We examined the effects of α_1-adrenergic (phenylephrine, PHE, 20 μM) stimulation on systolic Ca^{2+} transients (with Indo-1) and mRNA levels of SERCA and phospholamban (PHL) in cultured neonatal rat ventricular myocytes. Control and PHE treated myocytes were cultured in defined media for 48 hours. Ca^{2+} transients were measured at 35°C in normal Tyrode and total mRNA was isolated using the acid-guanidinium phenol-chloroform method. 48 hours of exposure to PHE induced significant hypertrophy and prolongation of the systolic Ca^{2+} transient (0.31 ± .02 sec. vs. 0.26 ± .01 sec. in controls, 0.5 Hz). Northern blot analysis suggests that mRNA expression of SERCA and PHL are reduced in PHE-treated myocytes. These data support the idea that changes in SR Ca^{2+} transport are responsible for the associated changes in the Ca^{2+} transient.

W-Pos316

OXIDANT-INDUCED CONFORMATIONAL CHANGES OF NUCLEOTIDE AND MEMBRANE-SPANNING DOMAINS OF THE SARCOPLASMIC RETICULUM Ca-ATPase. ((T.E. Jones, D. A. Ferrington, and D.J. Bigelow)) Dept. of Biochemistry, University of Kansas, Lawrence, Kansas 66045.

In view of the observed relationship between oxidative stress in the cell and loss of calcium homeostasis, we have investigated the oxidative sensitivity of the skeletal muscle sarcoplasmic reticulum Ca-ATPase to peroxyl radicals generated in the bulk solvent from thermolysis of 2,2'-azobis (2- amidinopropane) hydrochloride (AAPH). Previously (Viner et al., (1994) *Biophys. J.* 66, a120), we reported oxidant conditions that result in progressive inactivation of the Ca-ATPase accompanied by undefined structural changes characterized by increased sensitivity to tryptic digestion and decreased thermal stability. Using intrinsic tryptophan fluorescence of the Ca-ATPase as a structural probe of membrane-spanning peptides, we observe substantial oxidant-induced decreases in average fluorescence lifetimes correlated with loss of enzyme activity. However, these structural perturbations do not extend to altered solvent accessibility of tryptophan sidechains. On the other hand the nucleotide site probe, fluorescein isothiocyanate (FITC), exhibits only minimal changes in emission properties and solvent accessibility when bound to the oxidized protein, suggesting that the nucleotide site is unmodified by peroxyl radicals.

W-Pos317

CHANGES IN ASSOCIATIONS BETWEEN INDIVIDUAL Ca-ATPase POLYPEPTIDE CHAINS ACCOMPANY REGULATION OF CARDIAC CALCIUM TRANSPORT ((Linda Chen, Kim Brungardt, and Diana Bigelow)) Department of Biochemistry, University of Kansas, Lawrence, KS 66045

We have examined the spatial arrangements of Ca-ATPase polypeptide chains in cardiac compared with skeletal SR membranes. We have utilized fluorescein 5' isothiocyanate (FITC) and iodoacetamido fluorescein (IAF), two site directed fluorescent probes of nucleotide and cytoplasmic regions, respectively. The spectral properties of these fluorophores provide a means to monitor both (1) the proximity between individual Ca-ATPase polypeptide chains and (2) local protein environment. Under conditions that result in the phosphorylation of phospholamban in cardiac SR, we observe changes in fluorophore polarization that indicate a large-scale spatial rearrangement of Ca-ATPase polypeptide chains. These spatial reorientations follow the calcium concentration dependence of Ca-ATPase activation and are accompanied by changes from a monomeric to dimeric functional unit of the enzyme. When skeletal SR is subjected to identical conditions, these effects are not observed. Polarization data indicate more extensive Ca-ATPase protein associations in cardiac than skeletal SR. At the same time, we observed no alterations in local probe environment as monitored by emission decay kinetics, and fluorophore accessibility to solvent.

W-Pos318

LOCALIZATION OF 2,2'-AZOBIS(2-AMIDINOPROPANE) HYDROCHLORIDE (AAPH) - DERIVED PEROXYL RADICALS THAT REACT WITH SR MEMBRANES. ((Arkadi G. Krainev, Linda T. Chen and Diana J. Bigelow)) Dept. of Biochemistry, Univ. of Kansas, Lawrence, KS 66045-2106.

Spin trapping with 5,5-dimethyl-1-pyrroline 1-oxide (DMPO) and its hydrophobic analogue 2,2-dimethyl-4-phenyl-2*H*-imidazole 1-oxide (DMPIO) was used to identify peroxyl radicals ($ROO^{\cdot}$) and monitor $ROO^{\cdot}$ concentration in oxidation reactions initiated by AAPH. We have demonstrated that AAPH-derived $ROO^{\cdot}$s are the only radical species detectable in the aqueous phase. Hyperfine splitting constants were a_N = 14.86, $^{\beta}a_H$ = 14.47, $^{\gamma 1}a_H$ = 0.7, $^{\gamma 2}a_H$ = 0.52 and a_N = 13.46, $^{\beta}a_H$ = 12.53 Gauss for DMPO- and DMPIO-spin adducts, respectively. In the presence of skeletal and cardiac sarcoplasmic reticulum (SR) membranes only a small portion of AAPH-derived radicals was trapped by DMPIO. Spectral characteristics of the DMPIO-spin adduct indicate its location at the lipid-water interface. There was little effect of SR on the rate of formation and steady-state level of the DMPO-spin adduct. The presence of egg phosphatidylcholine liposomes, but not SR proteoliposomes resulted in about two-fold faster disappearance of both DMPO- and DMPIO-spin adducts than in the presence of AAPH alone. However, cardiac SR membranes were shown to be more effective inhibitors of spin adduct formation than membranes of skeletal SR, suggesting differences in the reactivity of their respective membrane proteins. No lipid-derived free radicals were detected in SR membranes employing lipid-soluble N-t-butyl-α-phenylnitrone (PBN) spin trap. SDS-PAGE of SR proteins revealed formation of protein aggregates in the presence of DMPIO and PBN, but not in the presence of DMPO. From these data we suggest that the bulky cytosolic domains of the SR Ca^{2+}-ATPase selectively react with radicals generated in the bulk (aqueous) solvent and thus protect the membrane surface.

W-Pos319

PEROXYNITRITE OXIDIZES PROTEIN CYSTEINE RESIDUES OF SR Ca^{2+}-ATPase. ((Rosa Viner[§], Andreas Hühmer[#], Diana Bigelow[§] and Christian Schöneich[#])) Depts. of [§]Biochemistry and [#]Pharm. Chem., Univ. of Kansas, Lawrence, KS 66045. (Spon. by R.Hersh)

Reactive oxygen species (ROS) are known to play a vital role under conditions of oxidative stress which accompany pathological states such as, e.g., inflammation, hyperoxia, and ischemia/reperfusion. Recently, peroxynitrite ($O=N-O-O^{-}$) has been forwarded as a likely candidate for a highly reactive but nevertheless selective ROS which is formed upon diffusion-controlled reaction of nitric oxide (NO) with superoxide anion ($O_2^{\cdot-}$). An important biological event under conditions of oxidative stress is the loss of Ca^{2+}-homeostasis primarily thought to be caused by oxidative inactivation of Ca^{2+}-regulating and transporting proteins. Therefore, we have characterized the potential inactivation and the molecular products of the reaction of $ONOO^{-}$ with the membrane protein SR Ca^{2+}-ATPase. The reaction with $ONOO^{-}$ primarily causes sulfhydryl oxidation paralleled by the loss of activity but no formation of (i) covalent protein aggregates, (ii) protein fragments, or (iii) lipid peroxidation products of the SR membrane. In addition we find (iv) no significant oxidation of other amino acids (as revealed by amino acid analysis). The oxidized protein is, however, more susceptible to limited tryptic digest. The results will be important for a mechanistic understanding of oxidative stress on the molecular level.

W-Pos320

ORIENTATION AND STRUCTURE OF THE PHOSPHOLAMBAN ION CHANNEL IN PHOSPHOLIPID MEMBRANES. ((I.T. Arkin[‡], M. Rothman[§], C. Ludlam[§], S. Aimoto[¶], D.M. Engelman[¥], K.J. Rothschild[§] and S.O. Smith[¥])) Departments of Cell Biology[‡] and Molecular Biophysics & Biochemistry[¥], Yale University, New Haven, CT. Department of Physics[§], Boston University, Boston, MA. Institute for Protein Research[¶], Osaka University, Osaka 565 Japan.

Phospholamban is a 52 amino acid membrane protein that plays a critical role in the regulation of calcium levels across cardiac SR membranes. The N-terminal 30 residues of the protein are largely hydrophilic and include two sites whose phosphorylation is thought to dissociate an inhibitory complex between phospholamban and the Ca^{2+} ATPase. The C-terminal 22 residues are largely hydrophobic, anchor the protein in the membrane and are responsible for Ca^{2+} selective ion conductance. Specific interactions between the transmembrane domains stabilize a pentameric protein complex. We have obtained CD and attenuated total reflection FTIR (ATR-FTIR) spectra of the full length protein and a 28 residue peptide that includes the transmembrane domain. Both proteins reconstituted into phospholipid membranes are largely α-helical by CD and FTIR. Polarized ATR-FTIR measurements show that both the cytosolic and transmembrane helices have a net orientation perpendicular to the membrane plane, in agreement to that calculated from a model of the transmembrane domain of phospholamban suggested by mutagenesis and molecular modeling. Based on these data we propose a model for the entire protein pentameric complex. The pentameric complex is composed of a left handed coiled-coil of five single long helices (40 ± 3 residues) that extend from the membrane carboxy terminus to the phosphorylation site in the cytosol. The helix bundle forms a perpendicular ion pore that may begin at a distance (ca. 17 - 29 Å) from the membrane surface.

W-Pos321

THE OLIGOMERIC STATE OF WILD TYPE AND MUTANT PHOSPHOLAMBAN IN THE LIPID BILAYER, DETERMINED BY EPR. ((Răzvan L. Cornea, Joseph M. Autry†, John D. Stamm, Larry R. Jones†, and David D. Thomas)) Department of Biochemistry, University of Minnesota Medical School, Minneapolis, MN 55455; and †Indiana University School of Medicine, Indianapolis, IN 46202.

Phospholamban (PLB), a 52-residue peptide integral to cardiac sarcoplasmic reticulum, is the key to β-adrenergic regulation of the cardiac calcium pump. PLB is pentameric in SDS micelles, but is its oligomeric state in this highly denaturing detergent similar to that in a phospholipid bilayer? To find out, we performed lipid EPR experiments on reconstituted wild-type PLB, as well as on mutants that form smaller oligomers or monomers in SDS. The lipid used in reconstitution was di(18:$1^{\Delta 9\text{-}cis}$)PC (DOPC) doped 1:100 with a phospholipid spin label, 14-PCSL, which detects protein contact. EPR spectra of this probe were used to determine the fraction of the total lipid that is in contact with PLB (boundary lipid). The boundary lipid fraction was minimal in wild-type PLB and maximal in a mutant that is monomeric in SDS. The results fit quantitatively to a model in which the oligomeric state is the same in SDS as in the bilayer. In particular, we conclude that wild-type **PLB is pentameric in phospholipid bilayers**, and that the L37A mutant is monomeric.

W-Pos322

STRUCTURE AND DYNAMICS OF SPIN-LABELED PHOSPHOLAMBAN: INSERTION AND PHOSPHORYLATION EFFECTS. ((Răzvan L. Cornea, Yvonne Kobayashi†, Christine Karim, Larry Jones†, and David D. Thomas)) Department of Biochemistry, University of Minnesota Medical School, Minneapolis, MN 55455, and †Krannert Institute for Cardiology, Indiana University School of Medicine, Indianapolis, IN 46202.

Phospholamban's (PLB) insertion in dimyristoyl phosphatidylcholine (DMPC) bilayers, and the dependence of its structure and molecular dynamics upon phosphorylation, were probed using electron paramagnetic resonance (EPR) spectroscopy. Two labels were used, targeting either Lys 3 in the hydrophilic N-terminal part of PLB or Cys 36, 41, and 46 in the hydrophobic C-terminal stretch. The probe on Lys 3 was highly mobile. This mobility was insensitive to the lipid phase transition, but it increased substantially upon phosphorylation of Ser 16 by PKA. In contrast, there was a dramatic lipid phase-dependent mobility shift for the labels located in the hydrophobic region of PLB, where the phosphorylation effect was very slight. These results suggest a model in which the C-terminal domain is inserted in the bilayer, while the N-terminal segment is cytoplasmic and undergoes the major conformational change upon phosphorylation.

W-Pos323

FLUORESCENCE DETECTION OF PHOSPHORYLATION-INDUCED STRUCTURAL CHANGE IN PHOSPHOLAMBAN (PLB)
((Ming Li, Larry R. Jones* and David D. Thomas)), (Spon. by Richard E.Poppele
University of Minnesota Medical School, Minneapolis, MN 55455 and *Indiana University Medical School, Indianapolis, IN 46202

We have used fluorescence to detect the proposed conformational change of PLB upon phosphorylation, in order to study the regulation mechanism of calcium transport in cardiac sarcoplasmic reticulum (SR). In cardiac SR, a small membrane protein, phospholamban (PLB), plays an important role in regulating the Ca pump activity. PLB phosphorylation stimulates the SR Ca pump, and this phosphorylation regulation through phospholamban has been proposed to be the underlying mechanism for beta-adrenergic stimulation in the heart. Even though the regulatory role of PLB in cardiac SR is well established, the mechanism of this phosphorylation-dependent regulation remains to be revealed. In the present study, we have measured the fluorescence of the intrinsic tyrosine (Tyr 6) to detect the proposed conformational change of PLB upon phosphorylation. Phosphorylation of PLB by cyclic AMP-dependent protein kinase increased the tyrosine fluorescence intensity by 62±2%, shifted the emission maximum to a shorter wavelength, and decreased the fluorescence quenching by KI and acrylamide, indicating a **conformational change of PLB upon phosphorylation, with Tyr 6 becoming less exposed to the solvent.**

W-Pos324

MOLECULAR DYNAMICS DURING ACTIVE CALCIUM PUMPING. ((Min Zhao, and David D. Thomas)) Dept. of Biochemistry, University of Minnesota Medical School, Minneapolis, MN 55455.

We have used **time-resolved phosphorescence anisotropy (TPA)** to probe the rotational dynamics of Ca-ATPase in skeletal sarcoplasmic reticulum (SR). Most previous studies on this system have been done with dye attached to Lys-515 of the Ca-ATPase, which inactivates the enzyme by inhibiting the binding of ATP. Therefore, in the present study, the SR Ca-ATPase was specifically labeled at Cys-674 with erythrosin iodoacetamide (ErIA) with 100% retention of the calcium-dependent ATPase activity. TPA was performed at 4°C with 2 μM of SR Ca-ATPase and 10 μM of Ca^{2+}, in the presence of 1 mM of ATP or 1 mM AMPPCP, which is an analog of ATP. AMPPCP is not a substrate of the SR Ca-ATPase, and the TPA experiment can tell us if the effects occur at the binding stage or during the process of active calcium pumping. The TPA results show significant changes in the dynamics upon nucleotide binding. Further studies under way to determine whether these effects are due to changes in protein-protein association or internal conformation of the enzyme.

W-Pos325

A CONTINUOUS SPECTROPHOTOMETRIC ASSAY FOR SIMULTANEOUS MEASUREMENT OF CALCIUM UPTAKE AND ATP HYDROLYSIS IN SARCOPLASMIC RETICULUM. ((Brad S. Karon, Erin R. Nissen, John Voss, and David D. Thomas)) Dept. of Biochemistry, University of Minnesota Medical School, Minneapolis, MN 55455 (Sponsored by Joseph V. Mersol)

A continuous, spectrophotometric assay to simultaneously measure Ca uptake and ATP hydrolysis has been developed in order to assess the function of the Ca-ATPase in skeletal and cardiac sarcoplasmic reticulum (SR) vesicles. The absorbance of Fura Red was measured continuously at 490 nm during assays of oxalate-facilitated or phosphate-facilitated active Ca uptake in skeletal SR. Simultaneous measurement of ATP hydrolysis during phosphate-facilitated Ca uptake was accomplished by measuring the disappearance of NADH at 340 nm, coupled to the hydrolysis of ATP by an enzyme-linked, continuous ATPase assay. This new method, unlike the standard ^{45}Ca-filtration assay, measures Ca uptake in real time and eliminates the need for radioactivity. Moreover, the rate of Ca uptake and ATP hydrolysis can now be measured simultaneously, allowing direct quantitative comparison of the two parameters. We are using this assay to study the effects of protein structural changes and other SR perturbations on the coupling between ATP hydrolysis and Ca uptake.

W-Pos326

ANESTHETICS REVEAL FUNCTIONAL DIFFERENCES BETWEEN THE CARDIAC AND SKELETAL MUSCLE ISOFORMS OF THE CA-ATPASE. ((Brad S. Karon and David D. Thomas)) Dept. of Biochemistry, University of Minnesota Medical School, Minneapolis, MN 55455

We have studied the effects of the volatile anesthetic halothane on Ca-ATPase enzymatic activity, oligomeric state, and conformational equilibrium in cardiac sarcoplasmic reticulum (CSR). We used time-resolved phosphorescence anisotropy to detect Ca-ATPase oligomerization in CSR. Halothane inhibited and aggregated the Ca-ATPase. Halothane inhibition of the Ca-ATPase appears competitive with respect to [Ca], with an apparent K_I in the clinical range of the anesthetic. Halothane stabilized the E2 conformation of the Ca-ATPase with respect to the E1 and E2-P conformations. Phosphorylation of phospholamban (PLB) resulted in greater halothane-induced inhibition, aggregation, and E2 stabilization than observed in the absence of phosphorylation. We have previously observed that halothane activates and dissociates the Ca-ATPase in skeletal SR, with clinical levels of anesthetic having little effect. Because PLB phosphorylation accentuates differences between halothane action on skeletal and CSR, we conclude that halothane inhibition of the Ca-ATPase in CSR is due to a unique interaction of halothane with the cardiac isoform of the Ca-ATPase.

W-Pos327

EFFECTS OF THAPSIGARGIN ON ISOMETRIC TENSION AND FLUO-3 CALCIUM TRANSIENTS OF AMPHIBIAN SKELETAL MUSCLE FIBERS. ((C. Caputo and P.Bolaños)) CBB, IVIC, Caracas, Venezuela.

Thapsigargin (TG) is a specific high-affinity inhibitor of the Sarcoplasmic Reticulum (SR) Ca^{2+} pump. We studied the effects of TG on single skeletal muscle fibers dissected from Leptodactylus insularis and loaded with Fluo-3 AM. TG (2 μM) rapidly (10 s) potentiates twitch tension and slows down its relaxation phase. Most of the relaxation phase from tetani follows a single exponential with a rate constant of about 15.3 sec^{-1} at 21° C; in a tipical fiber, in the presence of TG, two components were observed with rate constants of 3.5 sec^{-1} and 0.23 sec^{-1}. The slowest component accounted for more than 50% of maximal tension. The same features were observed when the external main cation was Na^+ or Li^+, indicating that in the presence of TG, the Na/Ca exchange is not important for relaxation. After few tetani, peak tension was progressively reduced, due to depletion of the SR Ca^{2+} stores. With twitches, the size of Ca^{2+} transients was not increased, but their decay phase presented a clear late slow component which was even more conspicuous and slower with tetani. With TG, the decay phases of tension and Ca^{2+} transients of K-contractures were also much slower, nevertheless the resting values of these parameters could be eventually reached in the high K^+, 0 Na^+ medium. Supported by CEE contract CI1-CT92-0020.

W-Pos328

INHIBITION OF SR CA^{2+}-ATPASE REVEALS THE CONTRIBUTION OF PARVALBUMIN (PA) TO RELAXATION IN FROG SKELETAL MUSCLE. ((Y. Jiang, J. David Johnson and Jack A. Rall)) Depts. of Physiology and Medical Biochemistry, Ohio State University, Columbus, OH 43210.

2,5-di(*tert*-butyl)-1,4-benzohydroquinone (TBQ, 2.5 μM) was used to produce nearly total inhibition of the SR Ca^{2+}-ATPase and to examine its effect on Ca^{2+} transients (using fluo-3 fluorescence) and force in twitches and tetani of fiber bundles from frog skeletal muscle at 10 °C. TBQ prolonged the half-time of the fall of both the Ca^{2+} transient (from 44 ± 9 to 71 ± 18 ms) and force (from 107 ± 25 to 214 ± 14 ms) and increased peak twitch force (2.2 ± 0.4 fold) without increasing the amplitude of the Ca^{2+} signal (n = 6) (Mean ± S.D.). In a long (1.1 s) tetanus where PA is saturated with Ca^{2+}, TBQ caused a near total failure of both relaxation and Ca^{2+} sequestration. In a short tetanus (0.3 s) where PA is predominantly in the Mg·PA form and can contribute to relaxation, TBQ caused the Ca^{2+} transient to fall at a rate of 2.8 ± 0.3 s^{-1} (n = 3) and relaxation to occur at a rate ~ 8 fold slower than control. Thus when the SR Ca^{2+}-ATPase is non-functional, Mg·PA can sequester Ca^{2+} and produce relaxation at a rate which is defined by the rate of Mg^{2+} dissociation from PA (~2 s^{-1} at 10 °C). Support by NIH AR20892 (JAR/JDJ) and DK33727 (JDJ).

W-Pos329

MUTATIONAL AND STRUCTURAL ANALYSIS OF THE Ca2+ BINDING DOMAIN OF THE SARCOPLASMIC RETICULUM ATPase. ((M.E. Kirtley, L. Chen, D. Lewis, C. Sumbilla, E. Di Cera*, and G. Inesi)) Dept. of Biochemistry, Univ. Maryland at Baltimore, and Dept. of Biochemistry, Washington University*, St. Louis.

Clarke et al. (Nature 339, 476, 1989) suggested that six residues originating from four transmembrane helices (H) (H4:Glu309; H5:Glu771; H6:Asn796, Thr799 and Asp800; H8: Glu908) are involved in Ca2+ binding, based on interference by point mutations with Ca2+ inhibition of ATPase phosphorylation by Pi. Molecular modeling of the four clustered helices, however, reveals that the diverging side chain angles of the three residues on H6 prevent their simultaneous participation in Ca2+ complexation. We then repeated the mutational work and found that mutation of Asn796 to Ala interferes with ATP dependent Ca2+ transport, but allows normal levels of ATPase phosphorylation by Pi which is susceptible to Ca2+ inhibition. Glu309 to Gln, Glu771 to Gln, Thr799 to Ala, Asp800 to Asn, and Glu908 to Ala do interfere with Ca2+ inhibition, but Glu908 to Gln does not. Analysis of the structural coordinates using valence maps supports a duplex Ca2+ binding model, with participation of the Glu309, Glu771, and Asp800 carboxyl and carbonyl oxygens, Glu908 carbonyl oxygen and Thr799 hydroxyl. Lys297 provides a gating positive charge at the lumenal end of the Ca2+ binding channel. (NIH supported.)

W-Pos330

THE TIME COURSE OF DEPLETION OF INTRACELLULAR Ca^{2+} STORES FOLLOWING RECEPTOR ACTIVATION OR INHIBITION OF MICROSOMAL Ca^{2+}/ATPase. ((Chris Mathes)) Dept. of Biol. Sci., Hopkins Marine Station, Stanford University, Pacific Grove, CA 93950.

In many cell types measurements have been made of the time taken to refill intracellular Ca^{2+} stores emptied by receptor activated Ca^{2+} release. However, the time course of Ca^{2+} store depletion has not been measured until now. Calcium stores were depleted in N1E-115 neuroblastoma cells by M1 muscarinic activation with carbachol (CBC;1 mM) or by microsomal Ca^{2+}/ATPase inhibition with thapsigargin (THAPS;1 μM). Subsequent to depletion of stores by CBC or THAPS, a voltage independent Ca^{2+} current is activated that refills the depleted Ca^{2+} stores (Mathes & Thompson, *JGP*, 104(1):107-121, 1994). $(Ca^{2+})_i$ was measured with fura-2 imaging. The amount of depletion following muscarinic activation was determined at 30, 45, 60 and 90 seconds. The % depletion was calculated as the inverse of the releasable IP_3-sensitive Ca^{2+} pool, which was determined by applying bradykinin to make additional IP_3 and release Ca^{2+} remaining in the stores. At 30 sec. stores are 63 ± 3% depleted. At 60 sec. Ca^{2+} stores are 77 ± 1% depleted and at this time Ca^{2+} current is activated maximally. Depletion by THAPS was assessed by activating Ca^{2+} release from the remaining pool with CBC at 2, 8, and 15 min. Two min. after THAPS treatment stores are depleted by 25 ± 3% and at 8 minutes by 85 ± 3%. Fifteen min. after addition of THAPS Ca^{2+} stores are depleted maximally at 93 ±1%. For both CBC and THAPS the relationship between depletion of Ca^{2+} stores and activation of Ca^{2+} entry supports the *capacitative* model. [supported by S. H. Thompson, NIH NS14519, and by predoctoral fellowships from the NIMH (MH 10425) and American Foundation for Aging Research to CM]

W-Pos331

^{45}Ca ACCUMULATION IS AFFECTED BY PRE-LOADING RAT BRAIN MICROSOMES. ((K.M. Nutt)) Department of Physiology, Emory University School of Medicine, Atlanta, GA 30322.

Rat brain microsomes were isolated, incubated at 37°C, and pre-loaded in one of two HEPES-buffered solutions (pH 7.4): (A) 0 Ca^{2+} and 0 ATP; (B) 25 μM Ca^{2+} and 3 mM ATP. Uptake for 30, 60, 120, 300, or 900 seconds was initiated by the addition of 25 μM Ca^{2+}, 3 mM ATP, and tracer $^{45}Ca^{2+}$. For all solutions, no calcium chelators were used, and free Ca^{2+} concentrations were verified with electrodes. I found that for both preparations of microsomes $^{45}Ca^{2+}$ accumulation increased with time and reached a plateau. I found significantly different values for both the initial $^{45}Ca^{2+}$ uptake rate (0.027± 0.009 μmol g^{-1} s^{-1} for the unloaded microsomes (A); 0.011±0.004 μmol g^{-1} s^{-1} for the pre-loaded microsomes (B)) as well as the steady state $^{45}Ca^{2+}$ accumulation (1.65±0.29 μmol/g protein for (A); 1.10±0.15 μmol/g protein for (B)). However, I found no significant difference in τ, the time to reach 63% of steady state accumulation: 61.5±17.0 seconds for (A) and 97.9±30.3 seconds for (B). I conclude that altering the state of filling of the ER affects the Ca^{2+} pump rate, but not the Ca^{2+} efflux rate constant. High intravesicular Ca^{2+} may inhibit the ER Ca^{2+}-ATPase, as suggested for the SR Ca^{2+}-ATPase in studies using fragmented SR membranes (Ikemoto, 1974, JBC, Vol. 249, pp. 649-51). Supported by NIH NS-19194.

W-Pos332

DIFFERENCES IN THE INHIBITION OF ERYTHROCYTE Ca^{2+}-ATPase ACTIVITY BY DIFFERENT GROUPS OF GENERAL ANESTHETICS. ((Ioulia Fomitcheva and Danuta Kosk-Kosicka)), Johns Hopkins University, School of Medicine, Department of Anesthesiology, Baltimore, MD 21287.

Our previous studies have revealed that volatile anesthetics (VA) inhibit activity of the plasma membrane Ca^{2+}-ATPase. The inhibition is dose-dependent, reversible, involves hydrophobic interactions, and occurs at clinically relevant concentrations (Anesthesiology 79, 774-780, 1993). The purpose of the present study was to establish whether the inhibitory effects are unique to VA or are also exhibited by other groups of general anesthetics. For the comparison we have selected short chain alcohols (ethanol) and barbiturates (pentobarbital). The study has been performed at 37°C on the enzyme purified from human erythrocytes. We demonstrate that all 3 groups of general anesthetics inhibit the Ca^{2+}-ATPase activity in a dose-dependent manner; however, only VA inhibit at concentrations that have anesthetic effects. The onset of inhibition is fastest for VA (2-5 min as compared to 20-25 min for the others). Based on the effective concentrations of the three investigated agents in the reactions media, VA appear to be the most potent inhibitors. Halothane does not change Ca^{2+} affinity of the Ca^{2+}-ATPase activity. In contrast, pentobarbital and ethanol decrease Ca^{2+} affinity up to 3 times. Our findings indicate differences in the mechanism of inhibition of the Ca^{2+}-ATPase by VA as compared to barbiturates and alcohols. (NIH GM 447130)

W-Pos333

VOLUME EXCLUSION EXPOSES NEW KINETIC CONFIGURATION OF THE PLASMA MEMBRANE Ca^{2+}-ATPase ((D. Kosk-Kosicka[1], I. Fomitcheva[1], V. L. Lew[2], and G. Roszczynska[1])), [1]Johns Hopkins University, School of Medicine, Dep. Anesthesiology, Baltimore, MD 21287, and [2] University of Cambridge, Physiol. Lab., Cambridge CB2 3EG, UK.

We have characterized two active species of the purified plasma membrane Ca^{2+}-ATPase: (1) monomers plus calmodulin and (2) dimers. At enzyme concentrations above 40 nM the configuration of Ca^{2+}-ATPase is that of calmodulin-insensitive dimers. Dilution of the enzyme generates progressively higher proportions of calmodulin-sensitive monomers with lower V_{max} and Ca^{2+} sensitivity than the dimeric enzyme. Whereas the kinetics of the oligomerized pump is consistent with the behavior of the pump in intact cells at physiological and subphysiological $[Ca^{2+}]_i$ levels, monomeric kinetics seems to explain best the calmodulin-sensitive behavior of the pump in ghosts. Radiation inactivation studies performed in other laboratories on ghosts indicated the existence of heterogeneous populations of pumps, including dimers. Thus monomer-dimer configuration changes may occur in native cell membranes. We investigated whether concentration by volume exclusion, obtained by addition of a large molecular weight dextran to a monomeric Ca^{2+}-ATPase would elicit dimer-like behavior. The results reveal an unknown dextran-induced kinetic state of the Ca^{2+}-ATPase, with high V_{max} comparable to that of oligomers but with the low Ca^{2+}-sensitivity of the monomeric enzyme. ([1]AHA 92010190, [1]NIH GM 447130 and [2]The Wellcome Trust).

W-Pos334

Ca^{2+} EFFLUX IS ACTIVATED BY EXTRACELLULAR PROTONS AND INHIBITED BY CADMIUM IN MUSCLE CELLS: EVIDENCE FOR Ca^{2+}/H^+ EXCHANGE *VIA* THE Ca^{2+} PUMP. ((J.DeSantiago, D.Batlle[a], S.Dedhiac[a] & H.Rasgado-Flores)) Dept.Physiol. & Biophys. FUHS/Chicago Med.Sch. N.Chicago, IL 60064 and [a]Dept. Medicine. Northwestern Univ.Med.Sch. Chicago, IL 20742.

In vascular smooth muscle, free cytosolic Ca^{2+} ($[Ca^{2+}]_i$) regulation and exit *via* the plamalemmal Ca^{2+} ATPase appears linked to H^+ entry (JASN 4,509,1993). We reasoned that such a process should be dependent on extracellular pH and sensitive to inhibition by Cd^{2+} (an agent that internally blocks the plasmmalemmal Ca^{2+} pump). Using barnacle muscle cells which can be perfused internally, we tested this hypothesis by assessing for the presence of a ^{45}Ca efflux mechanism that would be activated by extracellular acidification, dependent on ATP and blocked by small concentrations of intracellular Cd^{2+}. The intracellular perfusion fluid contained 1-10 μM $[Ca^{2+}]$, 4 mM ATP-Mg, and an ATP regenerating system. The extracellular solutions were free of Na^+ and Ca^{2+} to prevent unidirectional Ca^{2+} efflux mediated by the Na/Ca exchanger (*via* Na/Ca and Ca/Ca exchange) and contained 0.1 mM verapamil to prevent Ca^{2+} flux through Ca^{2+} channels. Extracellular acidification from pH 7.8 to 7.4 promoted a Ca^{2+} efflux whose magnitude was a function of $[Ca^{2+}]_i$ and reached 15 pmoles/ cm^2 sec at 10 μM $[Ca^{2+}]_i$ whereas extracellular alkalinization inhibited the Ca^{2+} efflux. Either addition of 20 nM intracellular Cd^{2+} or the simultaneous removal of ATP and addition of apyrase (to degrade ATP) abolished the extracellular acidification-induced Ca^{2+} efflux. This indicates the presence of a Ca/H exchange in barnacle muscle cells likely mediated by the plasmalemmal Ca^{2+} ATPase.

W-Pos335

MODULATION OF Ca^{2+} EFFLUX IN *APLYSIA* BAG CELLS BY SECOND MESSENGERS ((E.N. Yamoah and P.J.S. Smith)) MBL, Woods Hole, MA 02543.

Second messengers regulate intracellular Ca^{2+} (Ca^{2+}_i) levels through their regulatory mechanisms on intracellular Ca^{2+} storage and through their modulatory effects on voltage and ligand-gated Ca^{2+} channels. Ca^{2+} homeostasis, an essential component of intracellular signaling, is also maintained by activities of Ca^{2+} ATPase, Na^+-Ca^{2+}-exchanger and intracellular protein buffers. We examined steady state Ca^{2+} efflux through the plasma membrane of *Aplysia* bag cells in culture using the calcium sensitive vibrating probe technique and assessed the extent to which analogs of c-AMP, c-GMP, phorbol ester (TPA), caffeine and IP_3 influence this efflux.

Bag cells were cultured as described by Knox *et al.*, 1992. Recordings were made at low external Ca^{2+} ~ 100 µM. While c-AMP and phorbol ester reduced steady state Ca^{2+} efflux, c-GMP enhanced Ca^{2+} efflux through the plasma membrane. Caffeine and IP_3 had no effect on the steady state Ca^{2+} efflux on the bag cells. We further examined the effects of these second messengers on voltage-gated Ca^{2+} currents under voltage clamp conditions. Whereas cAMP and TPA enhanced the voltage-gated Ca^{2+} current, c-GMP caused a reduction of the current. The results suggest that these second messengers may have a direct modulatory effect on either Ca^{2+}-ATPase or Na^+-Ca^{2+} exchanger. However, indirect action of a second messenger by either raising or reducing Ca^{2+}_i and the enhancement or reduction of the activity of the Ca^{2+}-ATPase or Na^+-Ca^{2+} exchanger may be used to explain the present results.

W-Pos336

ROTATIONAL DYNAMICS OF THE SARCOPLASMIC RETICULUM Ca-ATPase ISOLATED FROM SKELETAL AND CARDIAC MUSCLE. ((Sewite Negash, Shaohui Huang, Gregory W. Hunter, and Thomas C. Squier)) Department of Biochemistry, University of Kansas, Lawrence, KS 66045-2106.

We have used saturation-transfer EPR and frequency-domain phosphorescence anisotropy to measure the rotational dynamics of the Ca-ATPase in rabbit skeletal and porcine cardiac sarcoplasmic reticulum (SR) membranes that were selectively and specifically labeled with either a maleimide spin-label (for EPR) or erythrosin 5-isothiocyanate (Er-ITC; for phosphorescence). The specificity of labeling was assessed by the colocalization of these labels with the Ca-ATPase on SDS-PAGE, and in the case of the skeletal SR Ca-ATPase the sites of Er-ITC labeling have been identified. In agreement with previous results (Birmachu et al., *Biochemistry* 32: 9445), we report that the rotational dynamics of the Ca-ATPase as assessed by ST-EPR in cardiac SR membranes (107 ± 5 µsec) is reduced by about two-fold relative to that observed in the skeletal membranes (57 ± 3 µsec). We observe analogous rotational correlation times associated with overall protein rotational motion using phosphorescence anisotropy, and *we observe little residual anisotropy*. This suggests that the spin-label is selectively measuring the overall protein rotational dynamics under our labeling conditions. Additional measurements, under a range of experimental conditions, will be presented in order to provide additional insight into the physical nature of the observed correlation times.

W-Pos337

ErITC LABELS MULTIPLE SITES WITHIN THE NUCLEOTIDE BINDING POCKET OF THE Ca-ATPASE FROM SKELETAL SARCOPLASMIC RETICULUM. ((Shaohui Huang*, Todd D. Williams+, Thomas C. Squier*)) Department of Biochemistry* and Mass Spectrometer Lab+, University of Kansas, Lawrence, KS 66045-2106.

Erythrosin 5-isothiocyanate (ErITC) has been used to study the rotational dynamics of the Ca-ATPase due to its long excited state lifetime. We find that ErITC reacts specifically with the extramembranous domain of the Ca-ATPase, as indicated by the ability to release the probe from the membrane following exhaustive tryptic digestion, and the correspondence of the fluorescence with the Ca-ATPase band on SDS-PAGE gels. At low labeling stoichiometries (i.e., less than 2 nmol/mg), ErITC has a similar inactivation profile of ATPase activity to that of fluorescein 5-isothiocyanate (FITC), which has previously been shown to selectively label K_{515} in the nucleotide binding cleft. Following exhaustive digestion, the tryptic fragments associated with ErITC on the ATPase were separated using reversed-phase HPLC chromatography. These tryptic fragments are not labeled when the Ca-ATPase is incubated with ATP during labeling, indicating that these sites are associated with the nucleotide binding cleft. Positive FAB mass spectrometry was used to identify these labeling sites. We find five ATP protectable sites derivatized with ErITC, corresponding to K_{141}, K_{365}, R_{476}, R_{560}, and either R_{460} or K_{464}, that account for more then 80% of the ErITC label associated with the Ca-ATPase. No single site accounts for more then 20% of the bound label.

W-Pos338

Phosphatidylethanolamine-Induced Ca-ATPase Functional Changes and Bilayer Physical Properties. ((Gregory Hunter, Thomas Squier)) Dept. of Biochemistry, University of Kansas, Lawrence, KS 66045.

Optimal coupling states of the Ca-ATPase require the presence of non-bilayer forming lipids such as phosphatidylethanolamine (PE) (Navarro, et al., *Biochemistry 23*, 130). We have investigated the physical basis of the sensitivity of the Ca-ATPase from skeletal muscle sarcoplasmic reticulum to changes in the concentration of PE. The Ca-ATPase was purified from endogenous lipids and contaminating proteins using an affinity column, and was asymmetrically reconstituted into vesicles of a defined lipid composition, as described previously (Lévy et al., *Biochim. Biophys. Acta* 1107, 283). The size of the resulting vesicles as characterized by dynamic light scattering was independent of the PE concentration, permitting us to interpret changes in activity in terms of the physical properties of the membrane. We find that increasing concentrations of PE relative to phosphatidylcholine reduces both ATPase and calcium transport activity. Assessments of lipid dynamics using frequency-domain fluorescence spectroscopy indicate that PE does not perturb membrane fluidity. Measurements of protein rotational motion using frequency-domain phosphorescence anisotropy indicate that increasing concentrations of PE increases protein rotational mobility, suggesting that the enhancement of coupling efficiency by PE involves either an induced conformational change or an alteration in the degree of associations between Ca-ATPase polypeptide chains.

W-Pos339

OXIDATION OF VICINAL METHIONINES IN CALMODULIN DISRUPTS THE ASSOCIATION BETWEEN THE AMINO TERMINAL DOMAIN AND THE AUTOINHIBITORY DOMAIN OF THE PLASMA MEMBRANE Ca-ATPase. ((Yihong Yao, Jun Gao, Diana J. Bigelow, and Thomas C. Squier)) Department of Biochemistry, University of Kansas, Lawrence, KS 66045.

Upon selective oxidation of the vicinal methionines in the carboxyl-terminal domain of calmodulin (CaM) using H_2O_2, we find that CaM acts as a noncompetitive inhibitor with respect to the activation of erythrocyte ghost membrane Ca-ATPase by native CaM. In order to investigate the physical mechanism involving the ability of the oxidatively modified CaM to nonproductively bind to the PM-Ca-ATPase, we have used fluorescence resonance energy transfer and anisotropy measurements to compare the structural properties of native and oxidatively modified CaM associated with the autoinhibitory domain of the Ca-ATPase, as previously described (Yao et al., *Biochemistry* 33: 7797). In both cases, immunoblots indicate that CaM binds selectively to the Ca-ATPase. Upon association with the autoinhibitory domain on the Ca-ATPase we observe that CaM adopts a restricted range of conformations that brings the globular domains within closer proximity. In the case of the oxidatively modified CaM the conformational heterogeneity of the bound CaM is much larger. The rotational correlation time (ϕ_2) associated with native CaM/ATPase complex is 260 ns, indicating that CaM binds tightly to the autoinhibitory domain. In contrast, ϕ_2 for the oxidized CaM/ATPase complex is analogous to that observed for CaM in solution (i.e., ϕ_2 ~15 ns for the CaM/ATPase complex and ~10 ns for the uncomplexed CaM), indicating that the amino-terminal domain of the oxidatively modified CaM does not tightly associate with the ATPase.

W-Pos340

STRUCTURE AND DYNAMICS OF CALMODULIN BOUND TO THE AUTOINHIBITORY DOMAIN OF THE PLASMA MEMBRANE Ca-ATPase. ((Yihong Yao and Thomas C. Squier)) Department of Biochemistry, University of Kansas, Lawrence, KS 66045-2106.

We have used fluorescence resonance energy transfer and anisotropy measurements to identify the structural properties of calmodulin (CaM) complexed to the autoinhibitory domain of the erythrocyte ghost plasma membrane (PM) Ca-ATPase, and compare the structural properties of CaM with that observed when CaM is associated with a peptide with an analogous sequence to the autoinhibitory domain. Immunoblots using antibodies specific for both CaM and the PM-Ca-ATPase indicate that CaM selectively associates with the Ca-ATPase. Upon association with the autoinhibitory domain on the Ca-ATPase we observe that CaM adopts a restricted range of conformations that brings the globular domains within closer proximity, which is analogous to that observed in the model peptide. Frequency-domain lifetime and anisotropy measurements indicate that upon association with the autoinhibitory domain of the PM-Ca-ATPase that i) the environment around the pyrene label located at Cys_{27} is analogous to that observed for the peptide, and ii) that the overall rotational dynamics of the complex are much slower (ϕ_2 = 260 ns) than observed when CaM binds peptide (ϕ_2 = 10.9 ns), consistent with the global motion of the autoinhibitory domain. These results suggest that upon CaM complexation, the autoinhibitory domain is released from the binding pocket, and thereby releases the inhibition of the Ca-ATPase.

W-Pos341

IMPAIRMENT OF Ca^{2+}-ATPase ACTIVATION BY NATURALLY OCCURRING MUTANT CALMODULINS. ((D. Kosk-Kosicka*, I. Fomitcheva*, G. Roszczynska*, K-Y. Ling+, C. Kung+)), *Johns Hopkins University, School of Medicine, Department of Anesthesiology, Baltimore, MD 21287 and +University of Wisconsin, Laboratory of Molecular Biology, Madison, WI 53706.

Viable calmodulin (CaM) mutants of *Paramecium* have altered transmembrane currents and easily recognizable eccentricities in their swimming behavior. Their CaMs fall into two classes in accordance with the location of amino acid substitutions: (1) little or no Ca^{2+}-dependent K^+ currents (C-lobe mutants) and (2) little or no Ca^{2+}-dependent Na^+ current (N-lobe mutants). The purpose of the present study was to determine how these naturally occurring mutations affect the function of CaM-dependent plasma membrane Ca^{2+}-ATPase responsible for the maintenance of low intracellular Ca^{2+}. The study was inspired by similarity of the described bipartite separation of CaM functions on the Ca^{2+}-dependent channels and our previous findings with several engineered CaMs which showed that the CaM-dependent activation of the red cell Ca^{2+}-ATPase was significantly more affected by alterations in the C-lobe than in the N-lobe of CaM. In the present study, we have determined, interestingly, that out of seven naturally occurring CaM mutants isolated from *Paramecium* the four C-lobe mutations (no Ca^{2+}-dependent K^+ currents) impair CaM-dependent Ca^{2+}-ATPase activation more than the N-lobe mutations. Both K_{Ca} and K_{CaM} are increased significantly. *AHA 92010190 and +NIH GM22714.

W-Pos342

IMPAIRMENT OF Ca^{2+}-ATPase ACTIVATION BY NATURALLY OCCURRING MUTANT CALMODULINS. ((D. Kosk-Kosicka*, I. Fomitcheva*, G. Roszczynska*, K-Y. Ling+, C. Kung+)), *Johns Hopkins University, School of Medicine, Department of Anesthesiology, Baltimore, MD 21287 and +University of Wisconsin, Laboratory of Molecular Biology, Madison, WI 53706.

Viable calmodulin (CaM) mutants of *Paramecium* have altered transmembrane currents and easily recognizable eccentricities in their swimming behavior. Their CaMs fall into two classes in accordance with the location of amino acid substitutions: (1) little or no Ca^{2+}-dependent K^+ currents (C-lobe mutants) and (2) little or no Ca^{2+}-dependent Na^+ current (N-lobe mutants). The purpose of the present study was to determine how these naturally occurring mutations affect the function of CaM-dependent plasma membrane Ca^{2+}-ATPase responsible for the maintenance of low intracellular Ca^{2+}. The study was inspired by similarity of the described bipartite separation of CaM functions on the Ca^{2+} channels and our previous findings with several engineered CaMs which showed that the CaM-dependent activation of the red cell Ca^{2+}-ATPase was significantly more affected by alterations in the C-lobe than in the N-lobe of CaM. In the present study, we have determined, interestingly, that out of seven naturally occurring CaM mutants isolated from *Paramecium* the four C-lobe mutations (no Ca^{2+}-dependent K^+ currents) impair CaM-dependent Ca^{2+}-ATPase activation more than the N-lobe mutations. Both K_{Ca} and K_{CaM} are increased significantly. *AHA 92010190 and +NIH GM22714.

W-Pos343

MUTATIONAL ANALYSIS OF TRANSMEMBRANE SEQUENCE M8 IN FAST-TWITCH SKELETAL MUSCLE CALCIUM ATPASE. ((William J. Rice and David H. MacLennan)) Banting and Best Department of Medical Research, University of Toronto, Toronto Canada M5G 1L6

The Ca^{2+} ATPase of skeletal muscle sarcoplasmic reticulum (SERCA1) has been extensively analyzed by site-directed mutagenesis. Earlier studies implicated six residues in Ca^{2+} binding. These residues are located in transmembrane segments M4, M5, M6, and M8. Previous mutational analysis of transmembrane domains M4, M5, and M6 revealed that patches of residues were sensitive to mutation. These residues tended to surround the putative Ca^{2+} binding ligands, and several mutations resulted in conformational blocks. These studies have now been extended to M8. Mutation of Ala^{912} to Phe resulted in a ten-fold decrease in apparent Ca^{2+} affinity. Mutation of Val^{905} to Ala or Phe resulted in a three-fold decrease in apparent Ca^{2+} affinity. These two residues are predicted to be located above and below the putative Ca^{2+} binding ligand Glu^{908} in the α-helix. In addition, mutation of Ala^{900} to Phe resulted in an E_1P to E_2P conformational block. Further mutations to residues in M8 are being carried out to clarify the role of M8 in Ca^{2+} transport. (Supported by National Institutes of Health, U.S.A. and the Medical Research Council of Canada.)

W-Pos344

GENERAL ANESTHETICS ALTER Ca^{2+} BINDING TO PLASMA MEMBRANE Ca^{2+}-ATPase. ((Marimar Lopez and Danuta Kosk-Kosicka)), Johns Hopkins University, School of Medicine, Department of Anesthesiology, Baltimore, MD 21287.

The purified plasma membrane Ca^{2+}-ATPase from erythrocytes undergoes a change of intrinsic tryptophan fluorescence upon specific Ca^{2+} binding; the fluorometric Ca^{2+} titration curves are identical to the Ca^{2+} concentration dependence of the Ca^{2+}-ATPase activity (FEBS Lett. 189, 67-71, 1985). In the present study we have used the fluorescence intensity measurements to determine the effect of six compounds representing three different groups of general anesthetics (volatile anesthetics, barbiturates, and short chain alcohols) on Ca^{2+} binding to the enzyme. We have established that all of them abolish the Ca^{2+}-sensitive increase in tryptophan fluorescence in a dose-dependent manner. The decrease correlates well with the inhibition of Ca^{2+}-ATPase activity studied under comparable conditions at 25°C. In addition, we have demonstrated a shift in Ca^{2+} concentration dependence of the fluorescence effect in the presence of alcohols. The shift is comparable to the 2-3-fold decrease in Ca^{2+} affinity observed for the Ca^{2+}-ATPase activity. Our findings suggest that the mechanism of action of general anesthetics on the enzyme is through impairment of Ca^{2+} binding which results in inhibition of the Ca^{2+}-ATPase activity. Supported by NIH GM 447130.

W-Pos345

NEW STRUCTURAL INFORMATION FOR A MODEL OF THE H^+,K^+-ATPASE EMBEDDED IN A LIPID BILAYER. A FOURIER TRANSFORM INFRARED SPECTROSCOPY STUDY. ((V. Raussens; J.M. Ruysschaert and E. Goormaghtigh)) ULB-CP206/2, B-1050 Brussels, Belgium

The H^+,K^+-ATPase from stomach parietal cells is responsible for acid secretion. Structural models of the enzyme have been derived from hydropathy plots. The α-subunit is thought to contain 8 transmembrane α-helices while the β-subunit contains only one. Kinetics of cleavage of extramembraneous protein segments by proteinase K on vesicles with well charaterized orientation of the protein reveal that 37% of the protein is present on the cytoplasmic side of the membrane (instead of 63% according to the current model) and 15% on the opposite side (instead of 22% according to the model). In turn, 48% of the amino acids (instead of 15%) are embedded in the membrane. These results were obtained by dosage of the peptide bonds by infrared spectroscopy since all colorimetric methods tested so far yield unreliable results. Attenuated total reflection Fourier transform infrared spectroscopy indicates that, in agreement with the current model, there are indeed α-helices present in the membrane. Their strong linear dichroism confirms their transmembrane orientation. However, secondary structure of the membrane embedded part of the protein obtained from the analysis of the shape of amide I also indicates the presence of 34% of β-sheet with no defined dichroism. This unexpected membrane component could account, in part, for the additional amino acid residues present in the membrane. Analysis of rate of amide hydrogen/deuterium exchange indicate a packing and/or a stability of the membrane segments of the H^+,K^+-ATPase looser than for bacteriorhodopsin, a protein which was used as a control in the course of all our experiments. In conclusion, the present work imposes a major overhaul of the models for the insertion into the membrane of the P-type ATPases.

W-Pos346

OLIGOMERIC INTERACTIONS STABILIZE THE ADP-SENSITIVE PHOSPHOENZYME IN ELECTROPHORUS Na,K-ATPase. ((Jeffrey P. Froehlich and R. Wayne Albers)). NIA, NIH, Baltimore, MD 21204, and NINDS, NIH, Bethesda, MD 20892.

The kinetic behavior of electroplax Na,K-ATPase demonstrates several complexities that cannot be explained by an Albers-Post scheme. Among these are differences between the rate coefficients in the pre-steady state and steady state of ATP hydrolysis. We have found from quenched-flow measurements of EP formation and P_i release at 21°C that the rate of conversion of E_1P to E_2P during the first turnover is $>1000\ s^{-1}$. The K^+-activated rate of hydrolysis of E_2P is only $300\ s^{-1}$ implying that E_2P is the predominant steady state acid-stabile intermediate. In contrast, dephosphorylation experiments with ADP and ATP revealed that E_1P and E_2P are present in roughly equal proportions. Solubilization of electroplax membranes with $C_{12}E_8$ and added phospholipids, conditions generating $\alpha\beta$ promoters in mammalian Na,K-ATPase, reduces the E_1P component to less than 15% of the total EP. We conclude that the detergent reduced the level of E_1P by destabilizing an interaction between adjacent subunits in an oligomer. The data are consistent with a model in which one subunit is delayed with respect to its neighbor during the normal catalytic cycle, leading to the accumulation of E_2P/E_1P in the steady state.

W-Pos347

cAMP PHOSPHORYLATES AND INHIBITS THE Na^+ PUMP AND RAISES INTRACELLULAR Na^+ ($[Na^+]_i$) IN AORTIC SMOOTH MUSCLE CELLS ((M.L. Borin and #R.W. Mercer)) Dept. of Physiol., Univ. of Maryland Med. Sch., Baltimore, MD 21201 and #Dept. of Cell Biology and Physiology, Wash. Univ, St. Louis, MO 63110.

Na^+ pump-mediated active efflux of Na^+ is the main mechanism for maintaining a low $[Na^+]_i$ in smooth muscle and other tissues. We demonstrated (Biophys. J. 66: A82) that 8-Br cAMP increases $[Na^+]_i$ in primary cultured rat aorta myocytes. This effect is due to the inhibition of Na^+ efflux and not to the activation of Na^+ influx. Here we present the results of studies designed to elucidate the mechanisms underlying this effect of cAMP on $[Na^+]_i$. **1)** The 8-Br cAMP-induced rise in $[Na^+]_i$ (measured with the fluorescent indicator, SBFI) was mimicked by other agents that raise cellular cAMP, namely, the β-adrenergic agonoist, isoproterenol, and the combination of adenylate cyclase activator, forskolin, and phosphodiesterase inhibitor, IBMX. **2)** The rise in $[Na^+]_i$ was directly correlated with the rise in cellular cAMP evoked by the test agents. **3)** Elevation of the cellular cAMP inhibited the Na^+ pump. At the cellular level it was manifested as a reduction in ouabain-sensitive Na^+ efflux. In native tissue (aortic rings) the same effect was demonstrated by inhibition of the ouabain-sensitive K^+ (^{86}Rb) uptake. **4)** Elevation of cellular cAMP triggered phosphorylation of the Na^+ pump. This was observed as an increase in phosphorylation of the Na^+ pump α-subunit immunoprecipitated from 8-Br cAMP-treated cells. Taken together, these results indicate that, in aortic smooth muscle cells, cAMP-dependent phosphorylation of the Na^+ pump α-subunit inhibits the pump and, thus causes $[Na^+]_i$ to rise. Supported by AHA, Maryland Affiliate, Grant-In-Aid and NIH HL-45215 Grant.

W-Pos348

ESTIMATION OF DISTANCE CHANGES BETWEEN CYS-457 AND THE NUCLEOTIDE BINDING SITE IN E_1 AND E_2 CONFORMATIONS OF Na,K-ATPASE. ((S.-H. Lin and L.D. Faller)) CURE, UCLA/VAMC Wadsworth, West Los Angeles, CA 90073

Na,K-ATPase from pig kidney was modified with 5'-iodoacetamidofluorescein (IAF) which reacts with Cys-457 in the α-subunit. Steady state fluorescence resonance energy transfer (FRET) was used to measure the distance between IAF (donor) and the binding site of TNPATP [2',3'-O-(2,4,6-trinitrophenyl) adenosine 5'-triphosphate] (acceptor) as a function of conditions that affect the enzyme's conformation. When IAF-enzyme is titrated with TNPATP in 20 mM NaCl, the maximum quench of IAF fluorescence is 32% with K_d = 50 nM. However, the maximum quench is only 28% and K_d increases up to 2.25 μM in 20 mM KCl. These results suggest that the distance between Cys-457 and the nucleotide binding site increases at least 1 Å when Na,K-ATPase changes from the $E_1(Na^+)$ to $E_2(K^+)$ conformation. The change in FRET efficiency caused by Na^+ and K^+ has been time-resolved in a stopped-flow instrument. All the traces could be fit with a single exponential function yielding one relaxation time. When the enzyme conformation shifts from E_1 to E_2, the observed rate is fast and the reciprocal relaxation time sigmoidally increases with increasing $[K^+]$. On the other hand, the reciprocal relaxation time is inversely related to $[Na^+]$. These observations are in excellent agreement with studies of FITC-modified Na,K-ATPase[1,2]. Although the reporter groups are different, these results suggest that the same event is being investigated by energy transfer and by changes in the fluorescence intensity of FITC-enzyme. Supported by AHA and NIH.

[1]Smirnova, I. N., & Faller, L. D. (1993) *J. Biol. Chem. 268,* 16120-16123.
[2]Faller, L. D. *et al.* (1991) *Biochemistry 30,* 3503-3510.

W-Pos349

CLONING OF THE α SUBUNIT OF THE SQUID SODIUM PUMP ((Y.G.-M. Covarrubias)) Department of Physiology, University of Pennsylvania, Philadelphia, PA 19104 (Sponsored by P. De Weer)

The kinetics and voltage dependence of several transport modes of the sodium pump of squid (Loligo) giant axon have been extensively studied. However, little has been published on the enzymatic or structure-function properties of Na^+,K^+-ATPase isolated from this mollusc. I have isolated a cDNA clone encoding the α subunit of the squid sodium pump by screening a cDNA library from Loligo pealei stellate ganglia with a full-length rat sodium pump α_1 subunit probe. This clone encodes a protein of ~110 KDa. The deduced amino acid sequence exhibits 70-75 % identity with that of other sodium pump α subunits, and 50-60 % identity with that of H^+-K^+ pumps. Sequence comparison of the putative ouabain binding domains (H1-H2 loop and H3-H4 loop) reveals interesting differences between the squid sequence and that of either ouabain-sensitive or -resistant forms of the sodium pump. Attempts are underway to express this clone in Xenopus oocytes to further investigate this divergence.
Supported in part by a University of Pennsylvania Research Foundation grant and NIH grant NS111223 (to P. De Weer).

W-Pos350

COMPARISON OF Na PUMP CURRENT AND TRANSIENT CHARGE MOVEMENT IN RAT AND GUINEA PIG CARDIAC MYOCYTES. ((R.D. Peluffo and J.R. Berlin)) Bockus Research Institute, Graduate Hospital, Philadelphia, PA 19146. (Spon. by R.L. Post)

Temperature, voltage and pH dependence of the Na pump current in rat (*R*) and guinea pig (*GP*) ventricular myocytes was studied in enzymatically isolated cells superfused with a (mM) 145 Na, 2.3 Ba, 0.2 Cd, Ca- and K-free Tyrode's solution and voltage-clamped with single patch electrodes containing 85 Na and Cs/TEA. Glycoside-sensitive Na pump current, activated by rapid application of 15 mM K, was 3.8 ± 0.4 pA/pF (Mean ± S.E.M., n = 6) in *R* myocytes (35°C, -40 mV) but only 1.2 ± 0.2 pA/pF in *GP* myocytes (n = 4); however, the voltage, temperature (see figure) and pH dependence of Na pump currents were similar. To examine the reason for the higher Na pump current density in *R* cells, the amount and the kinetics of glycoside-sensitive transient charge movement was studied in both cell types between 15°C and 35°C. The total amount of charge (24.7 ± 1.2 fC/pF, n = 9, *R*) and the voltage dependence of charge movement were similar, suggesting the Na,K-ATPase density is the same in *R* and *GP* myocytes. The time constant for charge movement (τ_{off}) was 4.3 ± 0.2 ms (25°C, -40 mV) in *R* vs. 5.6 ± 0.3 ms in *GP* myocytes (n = 3), but the Q_{10} of charge movement kinetics was similar. Thus, higher Na pump current density in *R* myocytes is difficult to explain by differences in the kinetics of charge moving reaction steps.

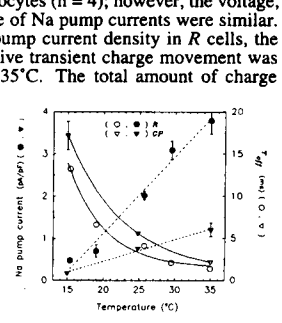

W-Pos351

PRESSURE AND LIGAND DEPENDENCE OF ANTHROYLOUABAIN BINDING TO (Na,K)-ATPase: EVIDENCE THAT PHOSPHOENZYME INTERMEDIATES HAVE DIFFERENT VOLUMES ((Michael K. Helms and P. A. George Fortes)) Dept. of Biology, University of California at San Diego, La Jolla CA 92093-0116

The fluorescent cardiac glycoside anthroylouabain (AO) binds with high affinity only to phosphorylated intermediates (EP) of (Na,K)-ATPase. The second order rate constant of AO binding (k_{on}) changes with the steady-state distribution of EP forms. The $EP(Na_2)$ form has the highest k_{on}. In order to study volume changes between different EP forms, we have measured k_{on} and k_{off} as a function of pressure (1 to 1000 bar, 23° C) under ligand conditions that change the distributions of EP forms at 1 bar. Mg + phosphate (Pi) stabilizes EP with no ions bound, whereas MgATP + Na stabilizes $EP(Na_n)$, where n = 0 to 3, and their distribution depends upon the Na concentration. Pressure up to 500 bar decreased k_{on} in the presence of Mg + Pi, but increased k_{on} at 1 kbar. With ATP, the responses of k_{on} depended upon [Na]. At 19 mM Na, pressure increased k_{on} between 100 and 1000 bar. At 0.4 M Na, pressure up to 500 bar increased k_{on}, but higher pressures decreased k_{on}. At 2 M Na, pressure (100-200 bar) increased k_{on}, but higher pressures decreased k_{on}. By contrast, k_{off} decreased with pressure, although it was less sensitive to pressure than k_{on}. Changes in AO binding rates with pressure may be due to redistribution of EP forms (each with different AO binding rates) if they have different volumes, as well as volume changes upon transfer of AO between the medium and the enzyme. The responses of k_{on} to pressure resemble the effects of increasing [Na] on k_{on} at 1 bar and the effect of pressure on Na-ATPase activity. The changes in k_{on} with pressure and [Na] are consistent with the idea that $EP(Na_2)$ and $EP(Na_3)$ are favored by pressure because they have a smaller volume. The increase in k_{on} with Mg + Pi at high pressure suggests that, in the absence of Na, protons may bind to EP to induce a low volume form, *e.g.* $EP(H^+_2)$, that would have enhanced AO binding rate analogous to the $EP(Na_2)$ form. (Supported by NIH grant GM47165)

W-Pos352

THE APPARENT AFFINITY OF THE NA^+/K^+ PUMP FOR CARDIAC GLYCOSIDES IN CARDIAC CELLS IS VOLTAGE DEPENDENT. ((A.N. Hermans, H.G. Glitsch°, F. Verdonck)) Univ. Leuven Campus Kortrijk, B-8500 Kortrijk, Belgium; ° Ruhr Univ., Bochum, FRG (Spon. by P.P. van Bogaert)

Cardiac glycosides (CG) inhibit the Na^+/K^+ ATPase, an effect that is antagonized by increasing external $[K^+]$ ($[K^+]_o$). Local changes of $[K^+]_o$ at the K^+ binding site may occur during variation of the membrane potential, Vm (Bielen et al. J Physiol 465, 699-714, 1993). Therefore it is expected that binding of CG may be affected by changes of V_m. To study the effect of V_m on CG binding we measured the Na^+/K^+ pump current (Ip) by whole cell voltage clamp in rat and guinea-pig ventricular cells and estimated the percentage of inhibition of Ip at different V_m and concentrations of the CG dihydroouabain (DHO). Ip was measured as the K^+_o activated current in the presence of blockers of other K^+ sensitive currents. The concentration-inhibition curves were shifted to higher DHO concentrations at more negative potentials. This effect was most evident in the presence of low $[K^+]_o$ (0.5 to 2 mM). When taking 0.26 as the fraction of the electric field accross the sarcolemma sensed by K^+_o (ref. above) local changes of $[K^+]_o$ at the K^+ binding site can be calculated by means of the Boltzmann equation. Experimental values were obtained for the affinity of the pump for DHO as a function of $[K^+]_o$ at 0 mV and for the changes in affinity at different V_m. When V_m is varied between 0 and -80 mV, calculations predict an 2.3x increase in $[K^+]_o$ at the K^+ binding site; from the shift of DHO affinity a factor of 2.2 was found. In conclusion, the dependence of CG affinity on V_m can be explained by the effect of V_m on $[K^+]_o$ at the K^+ binding site, affecting thereby the conformational state of the pump to which CG bind.

W-Pos353

MUTATION TYR763→GLY OF THE SR Ca^{2+}-ATPase UNCOUPLES ATP HYDROLYSIS FROM Ca^{2+} TRANSPORT. ((Jens Peter Andersen)) Institute of Physiology, University of Aarhus, DK-8000 Aarhus C, Denmark.

Site-directed mutagenesis was used to substitute glycine for residue Tyr763 located near the cytoplasmic end of transmembrane segment M5 of the Ca^{2+}-ATPase of sarcoplasmic reticulum. This created a new phenotypic variant of the Ca^{2+}-ATPase that catalyzed a high rate of Ca^{2+}-activated ATP hydrolysis without any net accumulation of Ca^{2+} in the microsomal vesicles. The ATPase activity of the mutant, like that of the wild type, was stimulated by Ca^{2+} at concentrations below 10 μM, and the mutant was able to form the ADP-sensitive and ADP-insensitive phosphoenzyme intermediates. However, there was no measurable accumulation of Ca^{2+} at Ca^{2+} concentrations up to 200 μM (the experimental upper limit of the Ca^{2+} transport assay), suggesting either that Ca^{2+} was never transported, even though ATP was hydrolyzed, or that transported Ca^{2+} leaked out from the microsomal vesicles through the mutant protein. While the ATPase activity of the wild type was enhanced 2-3 fold by incorporation of the calcium ionophore A23187 in the vesicles, the mutant ATPase activity was fully activated in the absence of the ionophore. These findings place Tyr763 as a central element in the gating mechanism controlling the closure of the transmembrane channel in the ATPase during Ca^{2+} pumping.

W-Pos354

PITUITARY ADENYLATE CYCLASE ACTIVATING PEPTIDE (PACAP) INHIBITS THE HUMAN ERYTHROCYTE CALCIUM PUMP. ((C. J. Allen, S.L. Jones, C. Gatto, M.A. Milanick)) Physiology, Univ. of Missouri, Columbia, 65212

The peptides XIP and C28 are inhibitors of the plasma membrane calcium pump. Both XIP and C28 contain several positively charged amino acid residues which are believed to be involved in the binding of these peptides to the pump and both peptides bind calmodulin. To gain further insight into the interactions of XIP and C28 with the calcium pump we performed experiments with other peptides (VIP, PACAP, H9685) that had several positively charged residues. Ca pump activity was assayed by the traditional 45Ca uptake into inside-out vesicles assay. In addition, a novel technique was used; Ca uptake into IOVs (~0.1 mg/ml) was measured using Fura-2 (1 μM) in the bulk solution. The advantages of using Fura-2 are that it does not require the use of radioisotopes, allows inhibition studies to be performed serially, and allows a continuous time course measurement. 25 μM Bachem peptide #H9685 (QRRQRKSRRTI) and 25 μM VIP did not inhibit. VIP binds calmodulin (Biochem. 22: 1995, 1983) and we have found that H9685 binds to dansyl-calmodulin. PACAP (1-38) inhibits with an IC50 of 20μM. PACAP (1-27) did not inhibit. Interestingly, the highly positively charged fragments of PACAP (16-38, 28-38) did not inhibit. Also, PACAP (1-27, 16-38) bind to dansyl-calmodulin. PACAP's inhibition of the calcium pump is interesting due to the fact that PACAP raises cytosolic calcium in target cells. Does PACAP become internalized in order to act as a Ca pump inhibitor in vivo? Does PACAP bind to the C28 binding site? If so, these results add additional constraints to the structural requirements for binding. However, PACAP may bind to a novel site on the pump. Supported by NIH DK37512 (MAM), a RCDA from NIH-DK (MAM), and AHA, MO Affl. (SLJ).

W-Pos355

INJURIOUS EFFECTS OF GLYCATED ALBUMIN ON Ca^{2+} REGULATION IN ENDOTHELIAL CELLS FROM THE PORCINE CORONARY ARTERY. ((G.M. Dick and M. Sturek)) Vascular Cell Biophysics Laboratory, Dalton Cardiovascular Research Center, and Department of Physiology, University of Missouri, Columbia, MO 65211.

Fura-2 loaded endothelial cells from the porcine right coronary artery were incubated in 40 mg/ml bovine serum albumin (BSA) or 10 mg/ml glycated BSA (plus 30 mg/ml BSA) for one hour at 37 ° C. Exposure to gBSA increased basal intracellular free Ca^{2+} (Ca_i) and attenuated the response of cells to 100 nM bradykinin (BK). The higher resting Ca_i does not appear to be due to increased influx of Ca^{2+}, as removing (10^{-5} M EGTA) or augmenting (10 mM) extracellular Ca^{2+} had the same effect on both groups of cells. In addition, the rate of Mn^{2+} quenching of fura-2 fluorescence, an estimate of unidirectional divalent cation influx, was not different. It has been reported that glycated albumin, via an interaction with specific cellular receptors, exerts an oxidative stress upon cells. Furthermore, it has also been reported that reactive oxygen species damage cellular Ca^{2+} pumps. The effect of glycated BSA on basal Ca_i and responsiveness to BK was mimicked by incubating cells in 100 nM thapsigargin, an inhibitor of the endoplasmic reticulum (ER) Ca^{2+} ATPase. The mechanism by which glycated BSA affects cells Ca^{2+} regulation remains to be elucidated, but may involve damage to the ER Ca^{2+} pump by reactive oxygen species. Supported by NIH RCDA HL02872, NIH Training Grant T-32 HL07094, and the American Diabetes Association.

W-Pos356

DIFFERENTIAL SCANNING CALORIMETRY STUDY OF THE THERMAL UNFOLDING OF SARCOPLASMIC RETICULUM Ca(II)-ATPase FROM RABBIT SKELETAL MUSCLE: EFFECT OF Ca(II) AND pH. **((J.Merino and C.Gutiérrez-Merino)) Depto. Bioquímica.Fac.Ciencias.UEX. 06080-Badajoz. Spain.**

The Ca(II)-ATPase from sarcoplasmic reticulum (SR) belongs to the E1/E2 ATPases. Ca(II) binding and pH changes between 6 and 8 shift the E1/E2 equilibrium of this ATPase. The thermal unfolding of this ATPase at pH 7 takes place between 47 and 55°C in the native membrane. Saturation of the Ca(II) transport sites (E1 state) increases the critical temperature (Tm) approx. 2°C with respect to the Tm obtained in the presence of EGTA (E2 state). In addition, the results at pH 7-8 can be fitted to one endothermic peak (Tm 53.5-54°C) at the Ca(II) concentrations that saturate the Ca(II) transport sites of the ATPase, and in the presence of millimolar Ca(II) concentrations (which inhibit the ATPase) a second endothermic peak with a Tm of 63-64°C is observed with ΔH values of 25-35% of that of the major endothermic peak. The E2 state is stabilized at pH 6, while E1 is more stable at pH 8 (Pick,U. and Karlish,S.J.D. (1982) J.Biol.Chem. 257, 6120). The scans run in the pH range 6-8 show that the Tm is 2-3°C higher at pH 8 than at pH 6, and also that the ΔHvH/ΔH ratio approaches unity at pH 6, while at pH 7-8 this ratio goes to 2-3. These results indicate that the interactions between ATPase monomers are weaker at pH 6 than at pH 7-8, and suggest that the increased stability of the E1 with respect to E2 state is largely due to stronger intermonomeric interactions.

Supported by Grants PB91-0311 (DGICYT) and SC1*-CT92-0783 (CE)

W-Pos357

HIGH ACTIVITY Ca TRANSPORT AND ATP HYDROLYSIS BY SERCA2a EXPRESSED IN SF21 INSECT CELLS. ((Joseph M. Autry and Larry R. Jones)) Krannert Institute of Cardiology, Indiana University School of Medicine, Indianapolis IN 46202

The cardiac SR Ca-dependent ATPase (SERCA2a) is postulated to transport two Ca ions into the SR lumen per molecule of ATP hydrolyzed; however, reported values of SERCA2a pumping stoichiometries in cardiac SR preparations are generally less than one. To determine the Ca/ATP pumping efficiency of the SERCA2a Ca-ATPase in the absence of endogenous cardiac SR Ca channels, we expressed canine cardiac SERCA2a cDNA in Sf21 insect cells. An improved method for isolating Sf21 microsomal membranes enriched in active SERCA2a was also developed. Microsomes from SERCA2a infected insect cells accumulated 7500 nmol Ca per mg protein, a value 2 fold greater than that attained by cardiac SR vesicles. In addition, Ca-dependent ATPase activity of the SERCA2a membranes was 10 times greater than the basal, Ca-independent ATPase activity. Simultaneous assays of Ca transport and ATP hydrolysis were performed over a range of Ca concentrations. The apparent Ca/ATP pumping stoichiometry of recombinant SERCA2a was 0.49 ± 0.17, less than the theoretical ideal of two. Co-expression of PLB with SERCA2a, under conditions in which the two proteins were functionally coupled, did not affect Ca/ATP stoichiometries significantly, and therefore, provided no evidence for PLB acting as a Ca efflux channel. Experiments are currently in progress to elucidate why pumping stoichiometries of two have not been achieved with this high-level expression system, which is functionally competent by several criteria.

W-Pos358

COMPARISON OF THE SARCOPLASMIC RETICULUM CALCIUM ATPase INHIBITED BY FLUORIDE AND MAGNESIUM IN THE PRESENCE AND ABSENCE OF BERYLLIUM. ((R. J. Coll and A. J. Murphy)) University of the Pacific, San Francisco, CA 94115

Many phosphate-utilizing proteins have been shown to bind strongly to mixtures of fluoride and metals such as Al^{3+} and Be^{2+}. The interaction of the ligands with the proteins (causing variously either activation or inhibition) is usually thought to proceed via negatively charged fluoro-metal complexes which mimic phosphate. We have previously shown that Mg^{2+} plus F^- together bind strongly to the SR calcium pump, causing reversible inhibition (Murphy & Coll (1992) J. Biol. Chem. 267, 5229 & 16990) which has also been reported by Daiho et al. (1993; Biochemistry 32 10021). This inhibition occurs at concentrations of Mg^{2+} and F^- below that necessary to form stable anionic complexes in solution. We have published a preliminary report concerning the effect of addition of Be^{2+}, F^- and Mg^{2+} to the SR calcium pump (Murphy & Coll (1993), J. Biol Chem. 268 23307); these three components also bind strongly, forming an inhibited complex with differences from those seen in the absence of Be^{2+}. Here we compare the two inhibited ATPases as to their similarities and differences. These include sidedness of inhibion/reactivation as judged by the effect of added ionophore, calcium concentration dependence in reactivation, and ligand stoichiometries. The results are discussed in relation to the presence/absence of beryllium, a metal known to form fluoride complexes under these conditions. (Supported by NIH grant GM31083)

W-Pos359

FUNCTIONAL MAPPING OF THE CARBOXY TERMINUS OF HPMCA4B AND HPMCA4A. ((A. Enyedi, A. K. Verma, A. G. Filoteo and J. T. Penniston)) Mayo Foundation, Rochester, MN 55905.

Isoforms 4a and 4b of the human plasma membrane Ca^{2+} pump (hPMCA) were expressed in COS-1 cells and their Ca^{2+} pumping activities were compared. These isoforms are produced by alternative splicing near the carboxy terminus which changes the structure of the calmodulin-binding domain and the downstream region. We have shown that this change in the structure results in enzymes with different calmodulin affinity, a difference which came from the change in the structure of the calmodulin-binding domain. We now report an additional consequence of the alternative splicing: in the absence of calmodulin the activity of hPMCA4a is higher than that of hPMCA4b. This altered self inhibition was further analyzed by studying the Ca^{2+} pumping activity of constructs containing different portions of the carboxy terminus. In both enzymes it appears that the inhibitory region is longer than the 28 residue calmodulin-binding domain. Constructs containing an additional 20 residues downstream of the calmodulin-binding domain (but lacking everything further towards the carboxy terminus) displayed nearly identical Ca^{2+} pumping activity and that activity in each case was identical to the activity of the full length hPMCA4a. This indicates that the greater self inhibitory properties observed in hPMCA4b must reside further towards the extreme COOH terminus of this isoform, a region which is not present in hPMCA4a. (Supported by NIH grant GM 28835)

W-Pos360

KINETIC EVIDENCE FOR A TETRAMER IN THE CATALYTIC MECHANISM OF THE SARCOPLASMIC RETICULUM Ca^{2+} PUMP. ((Jeffrey Froehlich, James Mahaney, and David D. Thomas)). National Institute on Aging, NIH, Baltimore, MD 21204, and Department of Biochemistry, University of Minnesota Medical School, Minneapolis, MN 55455.

The intermediate reactions of the Ca-ATPase in sarcoplasmic reticulum were investigated at 2°C using the quenched-flow technique. Addition of 100 μM ATP to the Ca^{2+}-equilibrated enzyme produced 3-3.5 nmols of phosphoenzyme per mg protein, representing 50% of the total site population in native membranes (6-7 nmol/mg). Dephosphorylation by ADP revealed that the ADP-sensitive (E1P) and ADP-insensitive (E2P) phosphoenzymes are present in equal amounts. Pre-steady state measurements indicated rapid conversion of E1P to E2P and slow reversal. These observations suggest a tetramer:

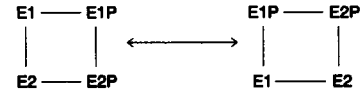

in which the four principle intermediates of the reaction cycle appear simultaneously in the functional transport unit during the steady state. The quaternary transformations are symmetry-conserving as required for alternating-site models with structurally identical subunits.

W-Pos361

CARBOXY-TERMINAL REGION OF THE P-TYPE ATPase CONTROLS THE AFFINITY FOR K^+. ((T. Ishii[a]*, F. Hata*, M.V. Lemas[a], D.M. Fambrough[a] and K. Takeyasu[b])) *Dept. Vet. Parmacol. Univ. Osaka Prefec. Sakai 591, Japan, [a]Dept. Biol. Johns Hopkins Univ. Baltimore, MD 21218, and [b]Neurobiotech. Ctr. Ohio State Univ. Columbus, OH 43210.

The Ca^{2+}-dependent and thapsigargin-inhibitable activity of the SECA-ATPase is not depending upon Na^+ and K^+ for its minimum activity, but further activated either by K^+ in a two-step fashion with high (ED50 ~20 mM) and low affinity (ED50 ~70 mM) or by Na^+ in a single step fashion with an ED50 value of ~50 mM. A replacement of the carboxy-terminal region (Ser_{800}-COOH) of SERCA1 ATPase with the corresponding region (Ser_{830}-COOH) of the Na^+/K^+-ATPase α1 subunit abolished the low-affinity regulation, and resulted in a single-step regulation (ED50 <10 mM) of the SERCA-ATPase activity by K^+ as seen in the wild-type Na^+/K^+-ATPase.On the other hand, the regulation by Na^+ was not affected by this chimeric recombination. Replacement of the middle (Gly_{354}-Lys_{712}) and the amino-terminal regions (Met_1-Asp_{162}) of the SERCA1-ATPase with the corresponding portions of the α1 subunit did not affect the K^+-sensitivity of the SERCA-ATPase activity, confirming that the carboxy-terminal regions of the SERCA1 and the Na^+/K^+-ATPase α1 subunit are critical for the K^+-effect. Further restriction of the donner region showed that carboxy-terminal 96 amino acids (Phe_{920}-Tyr_{1016}) of the α1 subunit are sufficient for the shift of the K^+-affinity in the regulation of the SERCA-ATPase activity. A substitution of the SERCA1 domain (Thr_{871}-Thr_{898}) with a short strech of extracellular 26 amino acids (Asn_{894}-Ala_{919}) of the α1 subunit that bind the Na^+/K^+-ATPase β1 subunit (J. Biol. Chem. (1994) 267, 20987) retained the two step regulation by K^+. Thus, the assembly and the K^+-sensitive domains are distinct within the carboxy-terminal region of the α1 subunit.

W-Pos362

AN UNEXPECTEDLY LARGE CATION CONDUCTANCE FOLLOWING RECONSTITUTION OF THE BACTERIAL F0 PROTON CHANNEL INTO BILAYERS. ((Dixon J. Woodbury, Stephen N. Alix and William S. A. Brusilow)) Departments of Physiology and Biochemistry, Wayne State University School of Medicine, Detroit, MI 48201. (Spon. by J. Ram)

The F_1F_0 proton translocating ATPase of *Escherichia coli* consists of an intrinsic membrane-bound F_0 sector to which an extrinsic F_1 sector is bound. The F_0 sector constitutes the transmembrane proton channel. We have isolated the F_0 complex by detergent extraction of *E. coli* membranes. The purified F_0 was reconstituted into vesicles by dialysis and prepared for fusion into bilayers according to the nystatin/ergosterol fusion technique.

A cation channel was reproducibly observed following the addition of 5 μl vesicles (containing only 50-100 ng protein) to one side of a bilayer chamber. Typically, the conductance was a multiple of 120 pS in symmetric 150 mM NaCl. The conductance was not affected by 80 μM DCCD and only had a mild pH dependence from pH 4.5 to 7.5.

Control experiments were performed by preparing vesicles the same way, but with an equal amount of protein from a strain of *E. coli* with a complete deletion of its F_1F_0 genes. Although occasional conductances were observed following addition of these vesicles, conductances were smaller and the gating kinetics were different. We conclude that this F_0 preparation can form a large cation channel. Because it is DCCD resistant, this channel is apparently not the proton channel naturally formed in *E. coli* membranes.

W-Pos363

RESONANCE-RAMAN SPECTROSCOPIC STUDY OF THE REDOX PROTEINS OF THE RESPIRATORY CHAIN OF *NATRONBACTERIUM PHARAONIS*.

(P. Hildebrandt*, B. Scharf and M. Engelhard) Max-Planck-Institut für Molekulare Physiologie, Postfach 10 26 64, 44026 Dortmund and *Max-Planck-Institut für Strahlenchemie, Stiftstr. 34-36, 45470 Mülheim/Ruhr, Germany

Two heme protein complexes which were isolated from the respiratory chain of *Natronobacterium pharaonis* have been studied by resonance Raman (RR) spectroscopy. Each of the complexes, cytochrome *b/c* and cytochrome b/a_3, includes two heme groups. Using various excitation lines it was possible to predominantly enhance the RR bands of the hemes *b*, *c*, and a_3, respectively. In this way structural information was obtained about the porphyrin geometry and the immediate protein environment of the individual redox sites in both proteins. In the cytochrome *b/c* complex, the RR bands of heme *c* indicate substantial structural differences of the heme pocket as compared to soluble mitochondrial cytochrome *c*. The cytochrome b/a_3 complex which may constitute the terminal oxidase in *N. pharaonis* includes a six-coordinated high-spin heme a_3 with a formyl substituent in a hydrophobic environment. The vibrational band pattern is closely related to that of heme a_3 of mitochondrial cytochrome *c* oxidase.

W-Pos364

CHARACTERIZATION OF THE QUINOL OXIDATION SITE OF THE *E. COLI* CYTOCHROME *BO* COMPLEX

((M. Sato-Watanabe, T. Mogi, H. Miyoshi, H. Iwamura and Y. Anraku)) Dept. Plant Science, Grad. Sch. Science, Univ. Tokyo, Hongo, Bunkyo-ku, Tokyo 113, Dept. Agricultural Chemistry, Kyoto Univ., Sakyo-ku, Kyoto 606, Japan.

The *E. coli* cytochrome *bo* complex is a heme-copper terminal quinol oxidase and functions as a redox-coupled proton pump. In contrast to the redox metal centers, a location and structure of the substrate oxidation site remain unknown. We have initiated the structure-function studies on the quinol oxidation site (Q_L) and identified new competitive inhibitors from screening of a series of quinone analogues, *p*-benzoquinones (BQ) and substituted phenols. Their inhibitory potencies were related to the *ortho*-substituents and the electron-withdrawing ability of the *para*-substituents. It indicates that the Q_L site has a higher affinity for one of the OH group. Among the potent Q_L site inhibitors, 2,6-dimethyl BQ, 2,6-dichloro-4-nitrophenol and 2,6-dichloro-4-dicyanovinylphenol were shown to be effective for isolation of quinone analogue-resisitant mutants of the cytochrome *bo* complex. Characterization of these mutations are now underway.

W-Pos365

UBIQUINONE BINDING DOMAIN IN CYTOCHROME *b*560 (QPs 1) OF BOVINE HEART MITOCHONDRIAL SUCCINATE-UBIQUINONE REDUCTASE

((Gyesoon Yoon Lee, Da-Yan He, Linda Yu and Chang-An Yu)) Oklahoma State University, Stillwater, OK. 74078.

Succinate-ubiquinone (Q) reductase (SQR), which catalyzes electron transfer from succinate to ubiquinone, contains five protein subunits. The two larger subunits compose succinate dehydrogenase (SDH) and the three smaller subunits, identified as QPs1, QPs2, and QPs3, serve as Q binding site and the membrane anchor for SDH. An azidoubiquinone, 3-azido-2-methyl-5-methoxy-6-[^{3}H]-decyl-1,4-benzoquinone ([^{3}H]-azido-Q) was used to identify the Q-binding domain in QPs1. When the Q-deficient SQR was incubated with an excess of [^{3}H]-azido-Q in the dark, no loss of activity was observed. Illumination of this azido-Q-treated sample with UV for 10 min at 0 °C caused a 35% decrease in SQR activity. The illuminated [^{3}H]-azido-Q treated SQR was subjected to SDS-PAGE after removal of non-protein-linked azido-Q by organic solvent extraction. Analysis of the radioactivity distribution among subunits of the complex found that QPs1 was heavily labeled, suggesting that QPs1 forms, in whole or in part, the Q-binding domain in the complex. The [^{3}H]-azido-Q labeled QPs1 protein was purified to homogeneity from the labeled SQR by preparative SDS-PAGE. When purified labeled QPs1 was subjected to reductive carboxymethylation prior to digestion by trypsin, two tryptic [^{3}H]-labled peptides were identified by HPLC. One of them (GLTISQ-) is located between the 2nd and 3rd transmembrane helices. This work was supported in part by a grant from NIH (GM 30721).

W-Pos366

SINGLE TURNOVER KINETICS OF CYTOCHROME aa_3 REDUCTION OF O_2.

((S. Bose and R. W. Hendler)) Laboratory of Cell Biology, NHLBI, NIH, Bethesda, MD 20892-0301

Multichannel optical spectra obtained with a 10 μs time-resolution spectrometer were analyzed by singular value decomposition. Formation of a heme-O_2 complex was seen with a τ of ~10 μs, followed by three steps of heme oxidation with τ's of 0.08, 1.0 and 30 ms. No evidence for an oxyferryl species was present. All heme oxidations were characterized by troughs at 446 and ~608 nm; none with a trough near 430 or 595 nm. The 0.08 ms species accounted for 100% of heme *a* (oxidized Soret peak at 427 nm). The other two species each accounted for 50 % of heme a_3 (oxidized Soret peaks at 416 nm). Because of the lack of evidence for oxidation of a low spin form of heme a_3, and because the amount of disappearance of the 446 nm peak accounted for the total oxidation, we believe that nearly all of the O_2 was held on Cu_B rather than heme a_3 during the oxidation. Our deconvoluted and actual difference spectra resemble the published spectra of Orii (JBC(1994)259:7187; Ann. NY Acad Sci(1988)550:105) for the corresponding time intervals. A tentative reaction scheme compatible with these findings will be presented.

W-Pos367

SITE DIRECTED MUTAGENESIS OF RESIDUES IN AND NEAR THE CUA CENTER OF CYTOCHROME *C* OXIDASE.

((Henry S. Speno, M. Reza Taheri, Hai Zhong, Craig T. Martin)) Department of Chemistry and Program in Molecular and Cellular Biology, University of Massachusetts, Amherst 01003. (Sponsored by C. Martin)

Recent developments have renewed interest in the structure and function of the Cu_A center in cytochrome *c* oxidase. In order to probe structural requirements at the Cu_A site and to test proposed interactions with cytochrome *c*, a variety of single and double mutations were introduced into subunit II of cytochrome *c* oxidase from the yeast, *S. cerevisiae*. A variety of modifications to conserved Cys and His residues proposed to be ligands to Cu_A not only eliminate cellular respiration, but also disrupt protein stability. These results are in contrast to analogous substitutions within blue copper sites, where even dramatic changes to ligands still allow protein folding. Despite the extreme sensitivity of cytochrome oxidase stability to modifications of proposed ligands to Cu_A, substitutions of nearby Glu-198 have no large effect on stability, and the effects on cytochrome *c* binding are consistent with the proposed role of Glu-198 as a surface-exposed contact for cytochrome *c*. The importance of the integrity of the Cu_A center is further established from nearby substitutions of conserved residues not predicted to be ligands, which likewise result in a lack of cellular respiration and a disruption of protein folding. Unlike blue copper proteins, the structure of this region of cytochrome *c* oxidase seems to be dependent on a highly specific coordination at the Cu_A center.

W-Pos368

METAL-METAL INTERACTIONS IN CYTOCHROME OXIDASE.

((M.P. Horvath)) The University of Chicago, Chicago, IL 60637

Electronic absorption spectroscopy of cytochrome oxidase was applied in combination with oxidation-reduction potentiometry to investigate electron transfer and metal-metal interactions of the enzyme. A method for the simultaneous analysis of absorption and second derivative absorption spectra was developed to quantify the amplitude of a component of the absorption spectrum of cytochrome oxidase that can serve as a specific marker for the Fe^{2+} oxidation state of cytochrome *a*. Analysis of oxidation-reduction titrations of the unliganded and carbon-monoxide-bound enzyme showed that carbon monoxide binding at cytochrome a_3 results in a –0.090 V change in the midpoint potential of cytochrome *a* in cytochrome oxidase purified from beef heart mitochondria and a –0.14 V change in the midpoint potential of cytochrome *a* in cytochrome oxidase purified from *Paracoccus denitrificans*. By studying a number of hybrid forms of the enzyme which differ in the oxidation and ligand state of cytochrome a_3, it was shown that cytochrome *a* interacts in an anti-cooperative manner with at least one other metal center in the enzyme. The energy of the interaction, measured as the change in midpoint potential of cytochrome *a* produced upon reduction of the interacting metal center, was –0.10 V for the mammalian enzyme and –0.06 V for the bacterial enzyme. The fraction of cytochrome *a* in the Fe^{2+} oxidation state at 50% reduction of total heme *a* in the mammalian enzyme was 0.51 ± 0.02 indicating that cytochrome *a* and cytochrome a_3 are reduced with equal probability. At 50% reduction of total heme *a* in the bacterial enzyme, the fraction of cytochrome *a* in the Fe^{2+} oxidation state was 0.94 ± 0.04 indicating that reduction at cytochrome *a* is favored. These results are discussed in terms of the possible roles which metal-metal interactions may play in electron transfer mechanisms of cytochrome oxidase.

W-Pos369

FREE FATTY ACID EFFECTS ON PROTEOLIPOSOMAL CYTOCHROME OXIDASE TURNOVER ARE DUE TO CHANGES IN THE PROTON MOTIVE FORCE

((Martyn Alun Sharpe and Peter Nicholls.)) Brock University, Ontario L2S 3A1, Canada.

Free fatty acids act as electroneutral H^+/K^+ exchange carriers and also as electrophoretic anions in biological membranes. The free fatty acid, oleic acid, is able to relieve respiratory control in cytochrome *c* oxidase containing vesicles (COV). This release from control can be calibrated to the dissipation of the inhibitory gradients, ΔpH and $\Delta\Psi$. Oleic acid is able to abolish both ΔpH and $\Delta\Psi$ in COV. Palmitic acid, although able to abolish ΔpH, is unable to dissipate $\Delta\Psi$ fully. The action of free fatty acids on transmembrane charge and cation gradients explains fully their proported action as mitochondrial decouplers. Although palmitic acid is more effective than oleic acid at relieving respiratory control at low concentrations, we find no evidence for a direct stimulation of enzyme turnover by palmitic acid.

Supported by NSERC (Canada) grant #A0412 to PN.

W-Pos370

CARBOCYANINE DYES WITH LONG ALKYL SIDE-CHAINS EXHIBIT A BROAD SPECTRUM OF INHIBITION OF MITOCHONDRIAL ELECTRON TRANSPORT CHAIN ACTIVITY. ((W. M. Anderson and D. Trogvcich-Zacok)) Ind. Univ. Sch. Med., N. W. Cent. Med. Ed. , 3400 Broadway, Gary, IN USA 46408

Certain carbocyanines dyes possessing short alkyl side-chains (one to five carbons) are potent inhibitors of mammalian mitochondrial NADH-ubiquinone reductase activity (Anderson. W.M., et al., Biochem. Pharmacol. 41, 677, 1991; Biochem. Pharmacol. 45, 691, 1993; and Biochem. Pharmacol. 45, 2115, 1993), and act similar to rotenone. Twelve carbocyanine dyes (six indo-, four oxa-, and two thiacarbocyanines) with alkyl side-chains of seven to eighteen carbons (both saturated and unsaturated side-chains) were tested for inhibiton of mitochondrial NADH, succinate and cytochrome c oxidase activities. Three of the indocarbocyanines inhibited respiratory chain activity, while three were non-inhibitory. Two of the oxacarbocyanines inhibited respiratory chain activity, while the other two were without effect. Both the thiacarbocyanines were non-inhibitory. In contrast to previous studies, the long alkyl side-chain carbocyanines exhibited a broad spectrum of inhibition of respiratory chain activity, effecting either oxidation of all three substrates or of NADH and cytochrome c, rather than specifically inhibiting NADH-ubiquinone reductase activity, indicating that there could be multiple binding sites for these compounds. The five inhibitory long side-chain carbocyanines inhibited reduction of ferricyanide and coenzyme Q_1 by NADH, using submitochondrial particles, but not with purified complex I, indicating that the mitochondrial inner membrane was an integral component in their inhibitory capacity. No general correlation of side chain length or degree of unsaturation and inhibitory capacity was discernable.

W-Pos371

INVESTIGATING THE NUCLEOTIDE BINDING SITES OF F_1-ATPase AND ITS SUBUNITS. ((Burgard, S., *Kagawa, Y., Wise, J.G., Trommer, W.E., Vogel, P.D.)) FB Biochemie, Universität 67663 Kaiserslautern, Germany, *Dep. Biochem. Jichi Medical School, Minamikawachimachi, Tochigi-ken 329-04, Japan

The F_1-ATPase from the thermophilic bacterium PS3 (TF1) consists of five different subunits with a stoichiometry of $\alpha_3\beta_3\gamma\delta\varepsilon$. The whole enzyme ($TF_1$-ATPase), the subassembly ($\alpha_3\beta_3$) as well as the isolated subunits and their assembly-behaviour were investigated using ESR-spectroscopy. For our studies we used $2N_3$-SL-ATP. The $\alpha_3\beta_3$ hexamer reflects the catalytic core of the enzyme. Up to five mol $2N_3$-SL-ATP can be bound per mol of $\alpha_3\beta_3$-subassembly resulting in ESR-spectra typical for highly immobilized radicals. Two distinct spectral components with $2A_{zz}$-values of 46G and 66G were observed indicating two different environments of the radicals. Isolated β-subunits can bind up to one mol/mol of the $2N_3$-SL-ATP. The resulting ESR-spectra show the unusual $2A_{zz}$-value of 53G. ESR-spectra of the α-subunit in complex with $2N_3$-SL-ATP show additional peaks in the high and low field region again indicating different environments of the spin-label with $2A_{zz}$ values of 48G and 65G. A dramatical change of the ESR-spectra was observed after addition of the isolated γ-subunit to the $\alpha_3\beta_3$-$2N_3$-SL-ANP complex.

W-Pos372

INTRAGENIC SUPPRESSOR ANALYSIS OF P-LOOP MUTANTS IN THE GENE CODING THE β-SUBUNIT OF THE YEAST MITOCHONDRIAL F_1-ATPase. ((H. Shen and D. M. Mueller)) Dept. of Biological Chemistry, FUHS/The Chicago Medical School, N.Chicago, IL 60064

The side chains of Gly192, Val194, and Val198 residues located in the P-loop of yeast F_1-ATPase β-subunit have been suggested to form steric or hydrophobic interactions with other residues of F1 (Shen, H., Yao, B.-y., and Mueller, D. M. (1994) *J. Biol. Chem.* 269, 9424-9428). To identify residues in the β-subunit that interact with the P-loop, suppression studies are being done on conditional mutants at positions 192, 194, and 198. Preliminary results demonstrate that three second-site mutations in the β-subunit, Thr237Ile, Pro353Leu, and Leu390Phe, suppressed the effects of three different P-loop mutations, Val194Tyr, Val194Met, and Val198Ser, respectively. Recent elucidation of the crystal structure of bovine F_1-ATPase showed that these suppressor residues are located at or near the nucleotide binding domain, and close to the original mutant residues. The P-loop and the regions containing suppressors Pro353Leu and Leu390Phe change conformations in βE, βDP and βTP states. These results suggest that the suppressors may produce their effects by interacting directly with the P-loop region. Because of the asymmetrical nature of the F_1 molecule, the interactions between the P-loop of the β-subunit and the other subunits, as well as the intrasubunit interactions, are important for the understanding of the catalytic mechanism of the enzyme. Further suppression studies are being done to identify more residues responsible for the conformational changes in the catalytic sites. Supported by grants from the NSF (DMB9020248) and the NIH (1R01GM44412).

W-Pos373

ALTERED DYNAMICS OF INTRAMITOCHONDRIAL CALCIUM IN CARDIAC MYOCYTES FROM DIABETIC RATS. ((D.B.Zorov, R.G.Hansford)) Lab. Cardiovasc. Sci., NIA, NIH, Baltimore, MD 21224.

Intramitochondrial free calcium (Ca_m), calculated from the fluorescence of indo-1-AM-loaded cells after selective quenching of cytosolic fluorescence by Mn^{2+}, was found to be higher in unstimulated myocytes from diabetic rats (Sprague-Dawley: iv injection of 65 mg/kg streptozotocin 4-6 weeks before experiment) than in controls (0.13 ± 0.01 and 0.07 ± 0.01 μM respectively). High frequency (4Hz) electrical stimulation (ES) resulted in a rise in Ca_m followed by a spontaneous decline. The maximal value of Ca_m achieved during ES and β-adrenergic activation (10^{-8} M isoproterenol) was significantly lower in myocytes from diabetic rats than in controls ($0.30+0.02$ and 0.45 ± 0.02 μM respectively). This was also true if elevated buffer Ca^{2+} (3.5 versus 1.5 mM) was used instead of isoproterenol to give the inotropic activation. The relative failure of diabetic cardiomyocytes to raise Ca_m in response to stimulation may limit the activity of Ca^{2+}-sensitive dehydrogenases and hence energy transduction in diabetic cardiomyopathy.

W-Pos374

NADH IN CARDIAC TRABECULAE DECREASES DURING ELECTRICAL PACING AND OVERSHOOTS UPON REDUCTION OF PACING RATE.

((Rolf Brandes and Donald M. Bers)), Loyola University, Maywood, IL 60153.

The oxidative phosphorylation rate, in isolated mitochondria, is stimulated by increased [ADP], resulting in decreased [NADH]. In vivo, however, increased mechanical work have not demonstrated increased [ADP], and increased [NADH] has instead been suggested to stimulate the phosphorylation rate. We have monitored [NADH] in isolated rat trabeculae (at 24°C) while changing pacing frequency, using fluorescence spectroscopy and accounting for oxygenation and motion artifacts. With glucose and/or pyruvate as substrate, [NADH] decreased with increasing pacing frequency (e.g., fluorescence fell by 35% at 3 Hz). When pacing was suddenly stopped, [NADH] increased above resting levels (by ~64%), and then slowly decreased. This NADH overshoot was enhanced by prolonged stimulation and increased ATP consumption (ADP production) rate, since reduced sarcomere length caused both reduced force and overshoot. We conclude: 1. The phosphorylation rate, during increased work, is not stimulated by increased [NADH] (since [NADH] decreased).

2. With sustained ATP consumption, NADH production is slowly stimulated to prevent further decline of [NADH] (as evidenced by the overshoot upon cessation of stimulation).

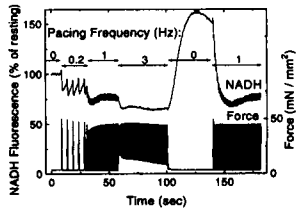

W-Pos375

CRITICAL CELLULAR OXYGEN IN MYOCARDIUM DETERMINED WITH 1H NMR SIGNALS OF MYOGLOBIN. ((T. Jue, U. Kreutzer, Y. Chung, S. Busse, and S. Brauer)) Biological Chemistry, University of California Davis, Davis, Davis, CA 95616-8635.

How the cell specifically regulates or signals a response to oxygen limitation is still somewhat unclear. Theories have postulated roles for metabolic products, such ADP or NADH, which form the feedback indicators in either a kinetic or equilibrium model. However experimental results are disparate and do not support convincingly any of the proposed biochemical paradigms. In particular the exact participation of myoglobin in skeletal or myocardial tissue remains also moot, despite the accepted view of its oxygen storage and facilitated oxygen transport activity.

We report that the 1H NMR signals of myoglobin are visible and provide a unique set of indices that mark the intracellular oxygen level. In myocardium, the critical oxygen point, where the cell no longer can sufficiently meet its needs through oxidative phosphorylation, hovers around 2-4 torr. However the specific cellular response is asynchronous, with lactate release and rate pressure product reflecting a change before oxygen consumption and phosphocreatine concentration. The results indicate that oxygen level alone does not solicit a singular response. Moreover, the data analysis does not produce results that conform to current biochemical paradigms.

The observation of the Mb signal in the cell offers also an opportunity to explore the physicochemical properties of a protein in its native environment. In the cell the Mb exhibits a rotational correlation time only a few times longer than in solution, but apparently not identical spectral features. Both the *in vivo* and *in vitro* NMR as well as physiological data have broadened our insight into the biochemical mechanism that mediates oxygen level and the cellular response.

W-Pos376

CREATINE KINASE EQUILIBRATION FOLLOWS SOLUTION THERMODYNAMICS IN MOUSE SKELETAL MUSCLE: ^{31}P-NMR STUDIES USING CREATINE ANALOGS. ((R.W. Wiseman[1], & M.J. Kushmerick[1,2,3])), Dept. of Radiology[1], Physiology and Biophysics[2] and Center for Bioengineering[3] University of Washington, Seattle, WA 98195

One of the key tenets of bioenergetics is the near-equilibrium property of creatine kinase (CK) coupled with cytosolic substrates which are freely mixing and available to the enzyme. However, existence of multiple CK isozymes and localization of these enzymes into subcellular compartments (perhaps with associated substrate pools), has suggested that the concept of freely diffusing metabolites in the cytoplasm may be too simplistic. We tested whether, in the presence of competitive inhibitors (PX and X, as well as PCr and Cr), the observed mass action ratio (Γ=[PX][Cr]/[PCr][X]) for CK could be predicted from combined equilibrium constants (K_{comb}) measured in solutions mimicking the intracellular ionic environment and temperature. Mice were fed cyclocreatine (cCr) or β-guanidopropionate (βGPA) for 3 weeks and substrates and products of the CK reaction were assayed in soleus (SOL) and extensor digitorum longus (EDL) muscles by ^{31}P NMR spectroscopy and HPLC. Γ was indistinguishable from K_{comb} in the SOL and EDL of mice treated with cCr, but different in both SOL and EDL due to a higher content of muscle βGPA that predicted by the solution K_{comb}. Feeding for periods of 8 - 9 weeks results in the agreement between K_{comb} and Γ suggesting transient metabolic stress is occurring at earlier time points. These competitive inhibitors of creatine kinase show that PCr/Cr and PX/X are at the same thermodynamic ratio in solution as in the muscles and therefore must have equilibrated with a constant and uniform cellular ATP/ADP ratio. It thus follows that in whole muscles, calculation of free ADP from the creatine kinase equilibrium for a heterogeneous population of cells with respect to total creatine and ATP content is correct only if the chemical potentials of these cells are uniform.

Supported by NIH grants F32 AR08105 and R29 AR41793 to RWW and AR36281 to MJK.

W-Pos377

INTRACELLULAR P_i CONTENT IS SUFFICIENT FOR SHORT-TERM (4 HR) OXIDATIVE PHOSPHORYLATION IN PERFUSED HEART. ((N. M. Doliba, X. G. Gao, K. Wroblewski, and M Osbakken)) Biochemistry/Biophysics, U of PA, Philadelphia, PA 19104 and Bristol-Myers Squibb, Princeton, NJ 08543

Free intracellular inorganic phosphate (P_i) is important for oxidative phosphorylation (ox-Phos). With this in mind, there is controversy concerning the addition of KH_2PO_4 to perfusion buffer for hearts studied via ^{31}P NMR because this extracellular source of P_i can mask the changes of intracellular P_i, thus making it difficult if not impossible to monitor pH changes by ^{31}P NMR. This has led many investigators to eliminate KH_2PO_4 from the perfusion buffer during ^{31}P NMR experiments. The criticism related to this deletion is that a P_i deficit will inhibit ox-phos. To evaluate the effect of removal of KH_2PO_4 from the perfusion buffer on ox-phos, state 2, 3, and 4 respiratory rates were determined on mitochondria (Mito) isolated from hearts which either were not perfused (Group 1) or were perfused for 20 min (Group 2) or 4 hrs (Group 3) without KH_2PO_4 containing Krebs Henseleit buffer. State 3 and 4 rates, respiratory control rate (RCR), and rate of ox-phos (ROP) were similar in Groups 1 & 2, and slightly decreased (15-20% depending on substrate) in Group 3 during the oxidation of pyruvate + malate, glutamate + malate, α-ketoglutarate, and succinate. P/O was the same in all 3 groups. In addition, ^{31}P NMR (ATP, PCR, P_i) data obtained on hearts perfused 4 hour showed stable ATP, PCr and P_i. These data indicate that intrinsic P_i is sufficient for normal ox-phos and that deletion of KH_2PO_4 from perfusion buffer does not adversely affect the cardiomyocytes.

ELECTRON TRANSPORT PROTEINS

W-Pos378

CRYSTALLIZATION OF MITOCHONDRIAL ELECTRON TRANSFER CHAIN PROTEINS - A PROGRESS REPORT. ((Edward A. Berry, Li-shar Huang, Vladimir M. Shulmeister, and Sung-Hou Kim)) Lawrence Berkeley Laboratory, Berkeley, CA 94720.

Ubiquinol:cytochrome c reductase (E.C. 1.10.2.2) has been crystallized in a new orthorhombic space group ($P2_12_12_1$) as well as the previously reported ($C222_1$ and $P6_1{}_{(5)}22$) crystals. The unit cell parameters of the new crystals are a, b, c =178, 183, 244 Å. The new crystals diffract to about 3.0 Å, whereas our best hexagonal crystals diffract to only 3.5 Å. The short cell axes reduce spot overlap and so allow more accurate data collection with imaging plates and multiwire detectors.

One strong heavy atom site has been located in a TAMM derivative of hexagonal bovine cytochrome reductase crystals by correlation search (XPLOR, Hercules) and independently by PATSOL Patterson search program. A possible second site was located by correlation search only. The phasing power of this derivative is too weak to make interpretable SIR density maps with the present data.

Bovine mitochondrial cytochrome oxidase (EC 1.9.3.1) has been crystallized in an orthorhombic space group by vapor diffusion in the presence of octyl glucoside, with polyethyleneglycol as precipitant. The cell parameters are 127, 129, and 354 Å and the space group is $P2_12_12$. Diffraction is presently limited to 6-7 Å.

We will present results from heavy atom searches and MAD data collection using the new cytochrome reductase crystals, and progress in improving the order of the oxidase crystals.

W-Pos379

IN VITRO RECONSTITUTION OF *R. SPHAEROIDES* CYTOCHROME *b-c1* COMPLEX FROM RECOMBINANT THREE-SUBUNIT CORE ENZYME AND OVER-EXPRESSED SUBUNIT IV. ((Yeong-Renn Chen, Chang-An Yu, and Linda Yu)), Oklahoma State University, Stillwater, OK 74078.

The cytochrome *b-c1* complex from *Rhodobacter sphaeroides (Rs.)* is composed of four protein subunits, cytochromes *b*, c_1, ISP and subunit IV (S4). The gene encoding S4 (*fbcQ*) has been deleted from the wide type and the resulting mutant is capable of photosynthetic growth after adaptation. The mutant has a partially active three-subunit cytochrome *b-c1* complex (core complex). Purified core complex showed less detergent tolerance, higher K_ms for Q_2H_2 and cytochrome c_2. than those of the wild-type four-subunit complex. S4 has been expressed in *E. coli* by fusing the *fbcQ* gene to the structural gene of glutathione S transferase in the expression vector of pGEX-2T. The fusion protein (MWr 40.5 kDa) reacts with antibodies against S4 in Western bloting analysis. An active S4 (Mr 14.4 kDa) can be released from the expressed fusion protein by proteolytic cleavage with thrombin. The recombinant S4 is soluble in 50 mM Tris-Cl, pH 8.0 and stable for several weeks at 0° C. When it was reconstituted with the core complex, antimycin sensitive ubiquinol-cytochrome *c* reductase (QCR) activity was restored to the same level of the wild-type complex. Titration of the core complex with S4 showed a saturation behaviour with the maximal QCR activity restored at one mole S4 per mole complex. Reconstitution between S4 and core complex not only restored the detergent tolerance but also restored K_ms for Q_2H_2 and for cytochrome c_2. There results suggest that S4 plays a role in the structural integrity and in interaction with substrates. This work was supported by a grant from NSF (MCB-93-05455).

W-Pos380

THE ROLE OF PHE-166 OF THE CYTOCHROME *b* PROTEIN OF UBIQUINOL CYTOCHROME *c* REDUCTASE FROM *R. SPHAEROIDES* IN UBIQUINONE BINDING. ((M. W. Mather, Lisa M. McReynolds, L. Yu, and C.-A. Yu)) Oklahoma State University, Stillwater, OK 74078.

Previous photoaffinity studies of mitochondrial ubiquinol cytochrome *c* oxidoreductase (cyt bc_1) have identified potential Q-binding regions in the cytochrome *b* (cyt *b*) protein and another subunit. One Q-binding peptide of cyt *b* corresponds to amino acid residues 158-171 of cyt *b* of the *R. sphaeroides* (*R.sph.*) cyt bc_1 complex. These residues may form part of a putative amphipathic helix thought to participate in the formation of the quinol oxidizing (Q_o) site. Much attention has been focused on the amino-terminal end of this helix as several inhibitor resistance mutations are located in that region. In *R. capsulatus*, it was found that substitution of Gly158 with an amino acid larger than Ala resulted in an inactive cyt bc_1 complex. It was speculated that Gly158 forms part of the Q-binding pocket accommodating the portion of the benzoquinone ring near the 2-methoxy group. A Gly158Ala mutation was constructed in *R. sph.* cyt *b*, and the activity of the mutated cyt bc_1 complex in chromatophore membranes was assayed with Q analogs having a larger substituent in the 2, 3 or 5 position, but no effect on the relative activities was observed. In contrast, a mutation near the other end of the putative amphipathic helix, Phe166Leu, exhibited increased tolerance of a larger substituent group at position 5 of the benzoquinone ring. The purified cyt bc_1 from this mutant appeared to contain normal cyt *b*, but displayed about 35% of the normal specific activity and has a lower K_m for QH_2, suggesting tighter quinol binding. Supported in part by grants from NIH (GM30721) and OCAST (HN3-008).

W-Pos381

***In Situ* Photo-Reduction of Bovine Cytochrome *c* Reductase using a Novel Ru(II)(*tris* bipyridine)/EDTA/Ubiquinone Reducing System** ((S. L. Niu and R. W. Larsen))[1] Department of Chemistry, University of Hawaii at Manoa, Honolulu HI, 96822.

We present a new method for the investigation of electron transfer reactions associated with bovine cytochrome *c* reductase by photo-generating ubiquinol *in situ*. Photo-generation of ubiquinol from ubiquinone is achieved by photolyzing a solution containing ruthenium (II) *tris*-bipyridine and EDTA in the presence of ubiquinone. Steady-state photolysis of a solution containing ruthenium (II) *tris*-bipyridine, EDTA, and ubiquinone-2 results in a decrease in the absorption maxima of the ubiquinone bands consistent with ubiquinol formation. This species can be air oxidized back to a species with spectral properties identical to those of the original ubiquinone. In the presence of cytochrome *c* reductase, photolysis of this system results in an initial reduction of cytochrome *b* followed by reduction of cytochrome c_1 on longer time scales. In the absence of ubiquinone photo-reduction occurs primarily at the cytochrome c_1 site. Our data will be discussed in the context of the Q-cycle model for proton translocation in cytochrome *c* reductase.

W-Pos382

PHOTODISSOCIATION OF SYNTHETIC CAGED DIOXYGEN CARRIERS. A TOOL TO STUDY FAST BIOLOGICAL REACTIONS INVOLVING O_2. ((A. Sucheta, R. MacArthur and Ó. Einarsdóttir)) Department of Chemistry and Biochemistry, University of California, Santa Cruz, CA 95064

The reduction of dioxygen to water by heme-copper oxidases is so fast that studies by conventional stopped-flow techniques are impractical. This reaction is generally studied by a flow-flash method involving photodissociation of the heme-CO complex. Time-resolved spectroscopic evidence indicates that these experiments are potentially compromised by the fate of the photodissociated CO and by photolability of intermediates. A novel approach to study the rapid reactions of heme-copper oxidases with dioxygen involves O_2 production *in situ* by photodissociating synthetic caged dioxygen carriers. An ideal system would utilize a source of dioxygen that does not react prematurely with the reduced unliganded enzyme but would release oxygen upon photodissociation on any relevant time scale. We have found that a (μ-peroxo)(μ-hydroxo) bis[bis(bipyridyl)cobalt(III)] complex in aqueous solutions and at physiological pH releases dioxygen upon photolysis. The quantum yield was 0.04 upon irradiation at 355 nm at 25°C. The photoproduct was generated on a nanosecond or faster time scale as determined by time-resolved optical absorption spectroscopy. Oxyhemoglobin was formed from deoxyhemoglobin upon photodissociation of the (μ-peroxo)(μ-hydroxo)bis[bis(bipyridyl) cobalt(III)] complex. This complex and other related compounds may provide a method to study fast biological reactions involving O_2, including the reduction of dioxygen to water by cytochrome oxidase, the key enzyme in respiration. Supported by NIH grant R29 GM45888.

W-Pos383

INTRAMOLECULAR ELECTRON TRANSFER IN CYTOCHROME BO of E. COLI. ((A. Sucheta, J.N. Rumbley, R.B. Gennis and Ó. Einarsdóttir)) Department of Chemistry and Biochemistry, University of California, Santa Cruz, CA 95064 and School of Chemical Sciences, University of Illinois, Urbana, Illinois 61801.

The photolysis intermediates of partially and fully reduced CO bound cytochrome *bo* of *E. coli* were investigated at room temperature. Transient absorption difference spectra were collected in the visible and Soret regions on time scales of nanoseconds to milliseconds using a gated optical spectrometric multichannel analyzer. The time-resolved data were analyzed at all wavelengths and times simultaneously combining exponential fitting and singular value decomposition procedures. Global analysis of the fully reduced transient difference spectra in the Soret region shows that at least two processes are present with apparent lifetimes of 12 μs and 15 ms. These are attributed to a conformational change and CO recombination at the cytochrome *o* site, respectively. The global analysis indicates that at least two processes, with apparent lifetimes of 19 μs and 23 ms, are present following photodissociation of the mixed-valence CO enzyme. The spectral changes associated with the microsecond process reflect electron transfer from cytochrome *o* to cytochrome *b*. A third process, attributed to a conformational change, may occur with approximately the same lifetime as the electron transfer process. The millisecond lifetime is attributed to CO recombination. The difference between the 40 ns mixed-valence and fully reduced transient difference spectra indicates that intramolecular electron transfer between the two hemes also occurs prior to 40 ns. Supported by NIH grant R29 GM45888.

W-Pos384

RESONANCE RAMAN STUDIES OF WILD TYPE AND MUTANT RHODOBACTER CAPSULATUS bc_1 COMPLEXES.

((F.Gao[a], H. Qin[b], D.B.Knaff[b], K.A. Gray[c], F.Daldal[c]. M.C. Simpson[d], J.A. Shelnutt[d] AND M.R. Ondrias[a])) a: Dept. of Chem., Univ. of N.M., Albuquerque, NM 87131. b: Dept. of Chem. and Biochem., Texas Tech Univ., Lubbock,TX 79409. c: Dept. of Biol.,Plant Science Institute, Univ. of Penn., Philadelphia,PA 19104, d: Sandia National Lab, Albuquerque, NM 87185

We report the results of our resonance Raman(RR) investigation of the heme active sites of bc_1 complexes. Comparision of spectra obtained from wild type and cM183L mutant shows that while the c_1 spin and coordination states are the same, the mutant exhibits behavior consistent with a much lower c_1 redox potential. The effects of several classes of inhibitors on RR spectra of the b hemes were also examined using both Q- and B-band excitation. Our results will be discussed within the context of current views of bc_1 active site structure and function.

(Supported by the NIH GM 33330 (to MRO), USDA (to DBK), DOE Dist. Postdoc Fellowship (to MCS), and DOE DE-AC04-94AL 85000 (to JAS))

W-Pos385

RESONANCE RAMAN SPECTROSCOPY OF CYTOCHROME *b* MAQUETTES ((W. A. Kalsbeck[1], D. E. Robertson[2], F. Rabanal[2], P. L. Dutton[2], R. K. Pandey[3], K. M. Smith[3], and D. F. Bocian[1])) [1]Department of Chemistry, University of California, Riverside, CA 92521, [2]Johnson Research Foundation, Department of Biochemistry and Biophysics, University of Pennsylvania, Philadelphia, Pennsylvania 19104, [3]Department of Chemistry, University of California, Davis, CA 95616 (Spon. by R. Cardullo)

The structure of the heme cofactor in a synthetic cytochrome model has been investigated using resonance Raman spectroscopy. The protein, described by Robertson *et al* (*Nature*, **368**, 425-432 (1994)), binds one heme via bis histidine ligation of the iron atom, the protein dimerizes in solution to form a four helix bundle. Previous work has shown that the two hemes are electrochemically inequivalent, with their redox couples separated by 115 mV. In effort to determine the factors governing the redox coopertivity, a detailed resonance Raman study of the protein reconstituted with several different hemes, including 2- and 4-monovinyl-substituted hemes as well as protoheme IX has been undertaken.

W-Pos386

PHOTOOXIDATION OF TRP-191 IN CYTOCHROME *C* PEROXIDASE BY RUTHENIUM-CYTOCHROME *C* DERIVATIVES

((Rui-qin Liu, S. Hahm, M. Miller+, N. Peffer, S. McKee, C. Chen, B. Durham and F. Millett)) Dept. Chem. Biochem., Univ. Arkansas, Fayetteville, AR & +Dept. Chem., Univ. California at San Diego, La Jolla,CA

A novel photoinduced electron-transfer reaction in complexes between resting state cytochrome *c* peroxidase (CcP) and several cytochrome *c* (CC) derivatives labeled at single lysine amino groups with (bisbipyridine)(dicarboxybipryidine) ruthenium(II)[Ru(II)] is reported. Photoexcitation of Ru(II) in Ru-CC results in formation of a metal-to-ligand charge-transfer state, Ru(II*), which is a strong reducing agent and rapidly transfers an electron to heme Fe(III). The resulting Ru(III) is a strong oxidizing agent with a redox potential of 1.3 V for the Ru(III)/Ru(II) couple, which can then oxidize heme Fe(II). In previous studies of interprotein electron transfer between Ru-CC and cytochrome *c* peroxidase compound 1 (CMPI), a sacrificial electron donor such as EDTA or aniline was used to reduce Ru(III) and prevent the back reaction. However, it was discovered that photoexcitation of a complex between resting state CcP and Ru-CC in the absence of a sacrificial donor resulted in reduction of the heme Fe(III) of Ru-CC by Ru(II*), followed by oxidation of the indole ring of Trp-191 by Ru(III). The cycle is completed by electron transfer from Fe(II) to the Trp-191 radical. This new method allows the study of the electron transfer reaction between CC and the radical on Trp-191 in the complete absence of hydrogen peroxide. We have used the method to characterize the electron-transfer properties of the indolyl radical on Trp-191 utilizing a wide range of CcP mutants.

Supported by NIH grant GM20488(FM&BD) and NSF grant MCB9119292(MM&JK)

W-Pos387

DESIGN OF A RUTHENIUM-CYTOCHROME *C* DERIVATIVE TO MEASURE ELECTRON TRANSFER TO THE INITIAL ACCEPTOR IN CYTOCHROME *C* OXIDASE

((L. Geren, J. Beasley+, B. Fine+, A. Saunders+, S. Hibdon, G. Pielak+, B. Durham and F. Millett)) Dept. Chem. Biochem., Univ. Arkansas, Fayetteville, AR & +Depts. Chem. Biochem. & Biophysics, Univ. North Carolina, Chapel Hill,NC

A ruthenium-labeled cytochrome *c* derivative was prepared which will rapidly transfer an electron to the cytochrome *c* heme group without altering the interaction with cytochrome *c* oxidase. Site-directed mutagenesis was used to replace His-39 on the backside of yeast C102T iso-1-cytochrome *c* with a cysteine residue which was then labeled with (4-bromomethyl-4 methylbipyridine)(bisbipyridine)ruthenium(II) to form Ru-39-cyt *c*. There is an efficient pathway for electron transfer from the ruthenium group to the heme group of Ru-39-cyt *c*. Electron transfer from the excited state Ru(II*) to ferric heme occurred with a rate constant of $(6.0 \pm 2.0) \times 10^5\ s^{-1}$, followed by electron transfer from ferrous heme *c* to Ru(III) with a rate constant of $(1.0 \pm 0.2) \times 10^6\ s^{-1}$. Laser excitation of a complex between Ru-39-cyt *c* and beef cytochrome *c* oxidase in low ionic strength buffer resulted in electron transfer from photoreduced heme *c* to Cu_A with a rate constant of $(6 \pm 2) \times 10^4\ s^{-1}$, followed by electron transfer from Cu_A to heme a with a rate constant of $(1.8 \pm 0.3) \times 10^4\ s^{-1}$. Increasing the ionic strength to 100 mM leads to bimolecular kinetics as the complex is dissociated. The second-order rate constant is $(2.5 \pm 0.4) \times 10^7\ M^{-1}s^{-1}$ at 230 mM ionic strength, nearly the same as that of wild-type iso-1-cytochrome *c*.

Supported by NIH grants GM20488(FM&BD), GM42501(GJP),&GM08332(JRB)

W-Pos388

LIGHT-INDUCED SPECTRAL CHANGES IN FULLY OXIDIZED CYTOCHROME OXIDASE IN THE PRESENCE OF OXYGEN. ((J. Brooks and Ó. Einarsdóttir)) Department of Chemistry and Biochemistry, University of California, Santa Cruz, CA 95064

Fully oxidized bovine heart cytochrome oxidase in the presence of oxygen undergoes spectral changes in the Soret and visible regions upon continuous illumination with a deuterium lamp in the presence of oxygen. The spectral change is driven by wavelengths lower than 300 nm and the rate is proportional to the light intensity. The Soret band undergoes a red shift upon illumination with a peak and a trough at 438 nm and 414 nm, respectively in the light-induced difference spectrum (after minus before illumination). The difference spectrum in the visible region shows a peak at ~606 nm and a shoulder at ~580 nm. The light-induced spectral change did not occur in the fully reduced enzyme. The spectral change follows a sigmoidal curve, indicating the existence of an intermediate in equilibrium with the initial and final products. The time required to reach half the maximum absorbance change was ~800 s. The enzyme reverts to its original resting state on a much longer time scale. The light-induced spectral changes are inhibited by the presence of cyanide, suggesting the involvement of cytochrome a_3. The spectral changes were larger at higher pH with a pK_a of ~ 7.8. The shift was found to be dependent on the pK_a of the buffer, with a larger change being observed when the pK_a of the buffer was lower than the pH of the measurement. This indicates that the light-induced shift may involve a deprotonation of the protein with the buffer being the proton acceptor. Supported by NIH grant R29 GM45888.

W-Pos389

FLOW-FLASH STUDIES OF THE REACTION BETWEEN CYTOCHROME c OXIDASE AND OXYGEN USING MULTICHANNEL TRANSIENT ABSORPTION SPECTROSCOPY. ((Ó. Einarsdóttir, A. Sucheta and K.E. Georgiadis)) Department of Chemistry and Biochemistry, University of California, Santa Cruz, CA 95064

The reaction of fully reduced bovine heart cytochrome c oxidase with oxygen has been studied using flash photolysis of the CO complex. The transient absorption difference spectra in the Soret and visible regions were collected from 50 ns to 50 ms after photolysis by a gated optical spectrometric multichannel analyzer system. The transient difference spectra in the visible region indicate a conformational change on an early microsecond time scale as is observed upon photolysis of the fully reduced CO-bound enzyme in the absence of oxygen. This is followed by the formation of the cytochrome a_3-O_2 complex. Electron transfer from cytochrome a to the binuclear site occurs with an apparent half-life of ~20-30 μs. A peak at ~580 nm in the transient 100 μs minus 20 μs difference spectrum indicates the formation of a ferryl compound in agreement with previous results of Orii[1]. Cytochrome a becomes reoxidized with an apparent half-life of ~100 μs. The product present 5 ms after photolysis has a considerably more intense alpha band than the fully oxidized resting enzyme. Analysis of the difference spectra using a global fitting procedure combined with a singular value decomposition method is in progress to determine the kinetics and the absorption spectra of the intermediates present during the reduction of dioxygen to water. Supported by NIH grant R29 GM45888.

1. Orii, Y. (1988) Ann. N.Y. Acad. Sci. 550, 105-117.

W-Pos390

pH-DEPENDENT CARBOXY CYTOCHROME OXIDASE SPECTRA.

((H. James Harmon)) Dept. Microbiology and Molecular Genetics, Oklahoma State Univ. Stillwater, OK 74078

The kinetics of CO recombination to fully ferrous cytochrome oxidase in beef heart mitochondria are dependent on CO concentration indicating that one CO is bound to the heme Fe while the other is bound at another site in the heme pocket, possibly at or near Cu_B. pH-dependent CO binding kinetics are due to changes in energy barriers encountered by CO during rebinding, possibly indicative of structural alterations in the heme pocket. CO concentration-dependent spectra differences are observed. The difference spectra of ferrous carboxy-oxidase minus ferrous oxidase in the presence of 1 CO/aa_3 at low temperature show significant pH-dependent differences. At pH 5 and 7 the λ_{max} is at ~430 nm while at pH 9 λ_{max} is at ~425 nm. At pH 9, the a_3^{2+}CO peak is markedly decreased while the 446 intensity decrease due to loss of a_3^{2+} is unaffected by pH. The absolute absorbance of a_3^{2+}CO at 417 nm increases and 430 nm absorbance decreases at pH 5 compared to pH 7/9. This suggests that unliganded oxidase can release H^+ at a site with pK>7 or that oxidase binds OH^-. Release/binding of H^+ or OH^- could occur at a_3^{2+}, or CuB.

Supported by a grant from the Oklahoma Center for the Advancement of Science and Technology.

W-Pos391

THE TRINUCLEAR IRON-SULFUR CLUSTER IN *BACILLUS SUBTILIS* SUCCINATE:MENAQUINONE OXIDOREDUCTASE.

((C. Hägerhäll, V. Sled, L. Hederstedt* and T. Ohnishi)) Dept. of Biochem. and Biophys., Univ. of Penn., Philadelphia, PA, USA. *Dept. of Microbiol., Univ. of Lund, Sweden.

The carboxyterminal portion of the iron-sulfur protein subunit of succinate: quinone oxidoreductases (SQR) and quinol:fumarate reductases (QFR) contains two fully conserved cysteine motifs, stereotypical for ligands of [3Fe-4S] and [4Fe-4S] clusters. In *Escherichia coli* QFR, introduction of an additional cysteine in the putative ligation motif of the tri-nuclear iron-sulfur cluster resulted in a tri- to tetra-nuclear conversion (Manodori *et al.*, 1992, Biochemistry 31; 2703). We have found that the introduction of a cysteine at the corresponding position in the iron-sulfur protein subunit of *B. subtilis* SQR did not result in cluster conversion. However, the EPR properties of the trinuclear cluster changed and the enzyme activity and stability was affected by the mutation. The data indicate that although the *B. subtilis* and *E. coli* enzymes are structurally similar, and catalyze the same reactions *in vitro*, there are differences between the trinuclear iron-sulfur clusters that may reflect these enzymes reverse function *in vivo*. In the presence of methanol, but not ethanol, the wild type *B. subtilis* S-3 signal changed dramatically, from broad and fast relaxing to narrow and slow relaxing, whereas the mutant enzyme S-3 signal was not affected by methanol. (This work was supported by NSF grant MCB-9119300 to T. Ohnishi)

W-Pos392

EXPRESSION OF THE COFACTOR BINDING SUBUNITS OF THE PROTON-TRANSLOCATING NADH-QUINONE OXIDOREDUCTASE (NDH-1) OF *PARACOCCUS DENITRIFICANS*.
((1Yano, T., 2Sled', V.D., 1Takano, S., 3Crouse, B., 3Finnegan, M.G., 3Johnson, M.K., 2Ohnishi, T., and 1Yagi, T.,)) 1TSRI, La Jolla, CA 92037, 2Univ. of Pennsylvania, Philadelphia, PA 19104-6089, 3Univ. of Georgia, Athens, GA 30602-2556.

A Gram negative and soil bacterium, *Paracoccus denitrificans* possesses the proton-translocating NADH-quinone oxidoreductase (NDH-1) whose enzymatic and molecular properties are very similar to those of mitochondrial Complex I. The *P. denitrificans* NDH-1 is composed of at least 14 dissimilar subunits (designated as NQO1-14) and contains one molecule of non-covalently bound FMN and at least 5 EPR-visible FeS clusters (N1a, N1b, N2, N3, and N4) as prosthetic groups. However, little is known as to which subunits contain these cofactors at the present time. On the basis of the deduced primary sequences of the *P. denitrificans* NDH-1 subunits and results of resolution experiment of bovine Complex I, we hypothesize that the NQO1, 2, 3, 6, and 9 are cofactor binding subunits. In order to verify the supposition, we have attempted to express these putative cofactor binding subunits in *E. coli*.

The expressed subunits have been purified and then subjected to several physicochemical analyses to characterize bound cofactors. Thus the following results have been obtained so far:

(1) The NQO2 subunit contains a single [2Fe-2S] cluster and the NQO3 subunit houses a [2Fe-2S] cluster and a [4Fe-4S] cluster. Based on the EPR properties of FeS clusters in the expressed subunits, we may suggest that the [2Fe-2S] clusters in NQO2 and NQO3 subunits correspond to N1a and N1b center, respectively. Furthermore, the [4Fe-4S] cluster in NQO3 subunit seems to be a N4 center.

(2) The expression of *P. denitrificans* FP subcomplex which is composed of the NQO1 and NQO2 subunits is successful. The two subunits are expressed as soluble proteins and stoichiometrically form the subcomplex *in situ*. Although the purified FP subcomplex contains less amounts of FMN and FeS clusters, these cofactors are sufficiently incorporated *in vitro*. The expressed-reconstituted FP subcomplex houses FMN, a [2Fe-2S] cluster (N1a), and a [4Fe-4S] cluster (N3) and shows the NADH oxidizing activity with a variety of electron acceptors. The kinetic analysis revealed that enzymatic property of the expressed FP subcomplex is very similar to that of bovine FP subcomplex.

(3) The NQO6 and NQO9 subunits are also expressed in *E. coli*. Chemical analyses of the expressed subunits suggest that both subunits contain FeS clusters. The characterization of the FeS clusters is in progress.

W-Pos393

EFFECTS OF CALCIUM ON MITOCHONDRIAL NAD(P)H IN PACED RAT VENTRICULAR MYOCYTES.((Roy L. White† and Beatrice A. Wittenberg‡)) †Temple University Medical School, Philadelphia, PA 19140 and ‡Albert Einstein College of Medicine, Bronx, NY 10461.

The response of the steady–state level of mitochondrial NAD(P)H of individual cardiac myocytes to substrate, and to pharmacological alteration of calcium channels in the sarcolemma, sarcoplasmic reticulum, and mitochondrial membrane was investigated using a defined pacing protocol. Supplementation of glucose medium with βOH butyrate significantly increased NAD(P)H in slowly–paced (0.5 Hz) and rapidly–paced (5 Hz) cells. Rapid pacing reversibly decreased the NAD(P)H level with both substrates. Ruthenium red blockade of Ca^{++} entry into mitochondria did not block contraction but significantly decreased NAD(P)H levels in both slowly–paced and rapidly–paced cells. Verapamil plus $NiCl_2$ blockade of calcium channels abolished contraction. NAD(P)H levels did not change during stimulation. Ryanodine, which maintains sarcoplasmic reticulum calcium channels in the open position, also stopped cell contraction. NAD(P)H levels also did not change during stimulation. Blockade of sarcolemmal K^+ channels did not stop contraction, and NAD(P)H levels reversibly decreased during rapid pacing. Thus rapid contractions are associated with a reversible decrease in NAD(P)H levels. The simplest explanation of these data is that the steady–state reduction of NAD(P)H is strongly dependent on rate of ATP utilization and not on sarcoplasmic Ca^{++} levels, when oxygen and substrate supply are not limiting. An effect of intracellular Ca^{++} on NAD(P)H is observed only when Ca^{++} entry into mitochondria is blocked with ruthenium red.

W-Pos394

ELECTRON TRANSFER REACTIONS WITHIN YEAST FLAVOCYTOHROME B_2 AND ZUCCHINI ASCORBATE OXIDASE: CONTROL OF RATE CONSTANTS BY THE REDOX STATE OF THE ENZYME.
((J. T. Hazzard and G. Tollin)) Department of Biochemistry, University of Arizona, Tucson, AZ 85721.

Intramolecular electron transfer reactions occurring within two distinctly different multi-center redox enzymes have been studied using laser flash photolysis. We have determined rate constants for electron equilibration within the one-electron reduced species, as well as equilibration following one-electron oxidation of the fully reduced enzymes. In both enzymes we observe a significantly larger electron transfer rate constant in the one-electron oxidized enzyme than in the one-electron reduced species. In the case of the flavocytochrome, an increase of 10-fold is observed, whereas for ascorbate oxidase the rate constant increases 100-fold. These results suggest that the communication between redox sites in multi-center enzymes is dependent upon the overall redox state of the enzyme, and that the more fully reduced species is more "active". The results are consistent with the concept that, if the rate limiting step involves intramolecular electron transfer, turnover will occur at a faster rate in the more reduced species. Interpretation of the data in terms of the known tertiary structures will be discussed.

W-Pos395

CRYSTAL STRUCTURE OF *E. COLI* PHOTOLYASE AT 2.3Å RESOLUTION.
((H.W.Park1, S.T.Kim2, A.Sancar2, J.Deisenhofer1,3)) 1Molecular Biophysics Program,UT Southwestern Med., Dallas, TX, 2Dept of Biochemistry and Biophysics, UNC, Chapel Hill, NC, 3Howard Hughes Med Institute, Dallas, TX (Spon. by J. Deisenhofer)

DNA photolyase from *E. coli* (Mr. 54,000) consists of a polypeptide chain of 471 amino acids and the non-covalently bound cofactors, methenyltetrahydrofolate (MTHF) and flavin adenine dinucleotide ($FADH^-$). The enzyme recognizes and repairs thymine dimers using light of wavelength about 400 nm. The crystal structure has been determined by x-ray diffraction methods with a final model R-factor of 17.4% at 2.3Å resolution. The overall structure consists of two domains, an αβ domain and an α domain. The α domain forms a flat surface. In the center of this surface a hole large enough to accommodate a thymine dimer leads to a cavity in which the $FADH^-$ is bound. A patch of surface around the hole is at positive electrostatic potential. Based upon these observations we propose that DNA containing a thymine dimer is bound to this surface with the dimer occupying the hole. This configuration would be favorable for electron transfer between $FADH^-$ and substrate. The distance between $FADH^-$ and MTHF appears consistent with energy transfer through dipole-dipole interactions. This structure provides a model for studying DNA binding, energy transduction, and electron transfer.

W-Pos396

TIME RESOLVED TRANSIENT RAMAN AND ABSORPTION SPECTROSCOPY: PHOTOINDUCED ELECTRON TRANSFER IN PORPHYRIN-QUINONE DONOR ACCEPTOR PAIRS.
((T. Buranda1, Shui-Lin Niu2, Randy Larsen2 and Mark R. Ondrias1)) 1Chemistry Department University of New Mexico, Albuquerque, NM. 87131. 2Department of Chemistry, University of Hawaii, Honolulu, Hawaii 96822.

Transient absorption and two color resonance Raman time resolved spectroscopies have been used to probe the electron transfer dynamics between 2,3-dimethoxy-5-methyl-1,4-benzoquinone and various porphyrin electron donors (e.g.. $ZnTTS_4$). Since redox potentials of various quinone species are widely known to be pH dependent, we have also examined the influence of acidic media on the electron transfer quinone-porphyrin electron transfer dynamics. Laser excitation of the porphyrin donor leads to the formation of a triplet state which is subsequently quenched by the quinone. The time resolved spectroscopic features, indicate the initial formation of the triplet state followed by the appearance of charge separated species, which later decay to the ground state in tens of microseconds. The measured return electron transfer rates show a decrease with increasing $\Delta G°$ (increasing pH) - a manifestation of the Marcus inverted region. **This research is funded by the National Institutes of Health (GM33330 (to MRO).**

W-Pos397

PROTON TRANSFER IN BIOLOGICAL SYSTEMS: A SIMPLE MODEL ((P.M. Kiefer and V.B.P. Leite)) Department of Physics, University of California at San Diego, La Jolla, CA 92093.

A simple model is presented for the study of proton transfer in hydrogen bonds. The energetics and dynamics of a simplified unidimensional proton coordinate under the presence of an effective potential is considered. The transfer of a proton from one nucleus to another depends on the effective potential at each site and the coupling between the two electronic states. The model describes these features with three factors: the geometry of the system, the non-bonding interaction, and the electronic coupling strength. The validity of a two level approximation for proton transfer is considered. The transition from a two level to a non-two level system is dependent on the effective hydrogen bond length R used, the electronic coupling T_{AB}, and the non-bonding interaction strength represented by $\Delta\nu$. For a reasonable range of T_{AB} $(0.5 - 2.5eV)$ and $\Delta\nu$ $(350 - 550cm^{-1})$ the transition occurs for $R = 2.6 - 2.9\text{Å}$ The application of the model to biological systems is discussed. Of particular interest is is proton transfer coupled to electron transfer, as in photosynthetic reaction centers. The possible mechanisms for such a reaction is presented.

* VBPL is partially supported by CNPq Brazilian agency. PMK is supported by NIH Grant HG00005 (Human Genome Training Grant, UCSD).

W-Pos398

AXIAL LIGAND CAVITY MUTATIONS TO THE PRIMARY DONOR OF THE PHOTOSYNTHETIC REACTION CENTER ((Joshua O. Goldsmith and Steve G. Boxer)) Dept. of Chem., Stanford University, Stanford, CA 94305

Histidine serves as the axial ligand to Mg of bacteriochlorophyll in the photosynthetic reaction center and other photosynthetic systems. A series of axial ligand cavity mutations to the primary donor (P_MP_L) of the RC from *Rb. sphaeroides* which include (M)H202G, (L)H173G, and the double mutant (M)H202G/(L)H173G, have been prepared in an effort to bind exogenous ligands inside the cavity to probe the primary donor. This strategy has been exploited with the proximal histidine of myoglobin.[1] The absorption and stark spectra of M202HG are similar to that of the wild type protein, with the exception of a ~5 nm blue shift of the primary donor absorption band at 77K. The rate of the recombination reaction $P^+Q^-_A \rightarrow PQ_A$ is slower in (M)H202G, with a $P^+Q^-_A$ lifetime at 298K of 144 ms ± 4 ms and 119 ms ± 4 ms in the mutant and wild type proteins, respectively. Growth or dialysis in exogenous imidazole has no effect on the properties of (M)H202G and thus we conclude the cavity is not accessible. The data are consistent with the primary donor in (M)H202G being a "pseudo homodimer" with an unidentified fifth ligand coordinated to the Mg atom of P_M. The longer lifetime of the charge separated state for (M)H202G is consistent with a more polar environment around the primary donor that better solvates P^+, lowering its free energy. Thus, we propose that the cavity left by removal of the histidine side chain at position (M)202 contains single or multiple water molecules, one of which serves as the axial ligand to P_M. The role of these ligands in modulating the properties of the primary donor is discussed as is the relevance of this work to the efforts in identifying axial ligands of chlorophyll binding proteins in photosystem II. It is clear that axial coordination from the protein by histidine is not required for chlorophyll binding.

[1]DePillis, G.D., *et al*, (1994) *JACS*, 116,6981-6982

W-Pos399

TIME-RESOLVED OPTICAL STUDIES ON THE ELECTRON TRANSFER STRUCTURAL DYNAMICS OF RUTHENIUM POLYPYRIDINE MODIFIED MICROPEROXIDASES ((B. Fan[1], Randy W. Larsen[2], Shui-Lin Niu[2], L. Martinez,and M. R. Ondrias[1])) [1]Department of Chemistry, University of New Mexico, Albuquerque, NM 87131; [2]Department of Chemistry, University of Hawaii at Manoa, Honolulu, HI 96822.

We have recently begun a series of time dependent spectroscopic studies of the dynamics associated with electron transfer (ET) in heme systems. Ruthenium polypyridine complexes have been widely used as photoinitiators in transient absorption studies of the ET in a veriety of heme proteins. We have extended this general protocol to include RR and luminescence studies of photoinitiated ET in heme-peptide systems obtained from the enzymatic digestion of cytochrome c (microperoxidase). Ruthenium modified octapeptide (MP-8) gives a well defined donor/acceptor system between heme and the ruthenium group. Since its sixth coordination site is open, this also gives us a opportunity to study the ligation state dependence of ET processes. Ruthenium bisbipyridine-4-methyl-4'-carboxylic acid succinimide ester has been used for the modification at the N-terminal amino group. Characterization of the HPLC purified product show a 1:1 modification. Significant photoreduction is observed in the 10ns transient RR spectra as indicated by the behavior of the high frequency heme modes. Initial time-resolved RR experiments indicate that the population of the photoreduced species peaks up around 200ns. Further detailed investigations are on-going. [Supported by NIH GM33330 to MRO and PRF 28510-G4 to RWL]

PEPTIDES/MODEL PROTEINS

(See also W-Pos504)

W-Pos400

FACTORS AFFECTING FOLDING AND DISULFIDE BOND FORMATION OF A SMALL BIOACTIVE PEPTIDE ((K.Mattila[1], A.Annila[2], J.J.Schmidt[3], M.Hyvönen[1], T.Kivistö[1], T.T. Rantala[1], J.J.McArdle[4] and L.C.Sellin[1])) [1]Dept. of Physical Sciences, University of Oulu, Oulu, Finland; [2]Chemical Technology, VTT, Espoo, Finland; [3]Toxinology Division, USAMRIID, Frederick, MD, USA; [4]Dept. of Pharmacology, N.J.Medical School, Newark, NJ, USA.
E-mail: kkmattil@phoenix.oulu.fj

The 3-D structure of a toxic (0.37 mg/kg i.p.) peptide, WTX1 (GGKPDLRPCHPPCHYIPRPKPR), from the SE Asian snake Trimeresurus wagleri was studied using 2-D NMR (600 MHz spectrometer) and computer simulations. From NOE-spectra of the peptide, a group of distance restraints were obtained and CHARMm force fields were applied to do simulations for the conformational search. The structure was found to be extended with an angle determined by the rigid loop region formed by the disulfide bond. Single amino acid substitutions within this loop region at position 10 altered the bioactivity of the peptide through an effect on disulfide bond formation. Substituting Gly for His resulted in an inactive product due to preferential formation of an intermolecular disulfide bond. The inability to form an intramolecular disulfide bond was due to an increase in flexibility leading to different bending of phi- and psi- angles or cis-trans isomeria at position 10. The overall result was a decrease in the probability that the peptide would assume a structure favoring intramolecular oxidation of the cysteine residues. The Phe10 analogue formed the intramolecular bond but at a considerably slower rate than WTX1 (52 and 7 hours, respectively for 85% oxidation). These data suggest that even subtle changes in the steric or electrostatic environment within this disulfide region can result in a significant alteration in activity. (Supported by NIH grant 5R01 NS31040).

W-Pos401

CHARACTERIZATION OF THE CALMODULIN BINDING OF DERIVATIVES OF A 22 mer PEPTIDE FROM A M13 PHAGE LIBRARY. ((B. K. Kay[1], J. D. Brennan[2], & A. G. Szabo[2])) [1]Department of Biology, Univ. of North Carolina, Chapel Hill, NC, 27599-3280, [2]Department of Chemistry and Biochemistry, University of Windsor, Windsor, Ontario, N9B 3P4, Canada. (Spon. by I. Clark).

The modulation of the activity of a number of proteins by Calmodulin in a Ca^{2+} dependent manner is the subject of considerable interest. By screening a M13 phage library which displays random peptides consisting of 22 amino acids, the sequence determinants of high affinity interaction with Calmodulin were explored. Acid-elutable phage which bound to bovine brain calmodulin were recovered, amplified, and rescreened twice to yield binding phage. These isolates bound three orders of magnitude stronger to Calmodulin coated plates than to BSA coated plates. When the isolates were sequenced they were found to be the same recombinant with a common insert sequence, one residue of which was a tryptophan. The peptide had some similarity to the calmodulin binding domain of skeletal muscle light chain kinase and had a dissociation constant of ca. 2 μM. To improve the binding properties of this particualr peptide sequence, several codons of the phage insert were randomized and recombinants were selected for higher affinity binders. Four derivative sequences were confirmed to bind 5 - 25 fold better than the parental peptide. This demonstrates the utility of phage display libraries in identifying and engineering peptide antagonists to CaM. The interaction of the original synthetic 22mer peptide and the four derivative peptides with bovine brain calmodulin was studied by steady state and time-resolved fluorescence methods. It was shown that each peptide bound to Calmodulin in a Ca^{2+} dependent manner, and that there were significant changes in the structure of the various peptides on binding to calmodulin.
This work was supported by Cytogen Corp., Princeton NJ (B.K.K.) and the Natural Science and Engineering Research Council of Canada (A. G. S.).

W-Pos402

THE IMPORTANCE OF AMINO ACID ORDER FOR THE FORMATION OF α-HELICES IN SHORT PEPTIDES ((D.V. Waterhous and W.C. Johnson, Jr.)) Dept. of Biochemistry and Biophysics, Oregon State University, Corvallis, OR 97331-7305.

There is fair agreement between Chou-Fasman theoretical predictions for secondary structure propensities of the 20 common amino acids and the measured ability of the 20 amino acids to stabilize that secondary structure in isolated peptide sequences. However, it has been noted in these measurements that the rank ordering of the stabilization energy of the different amino acids for that secondary structure depends on the primary sequence of these peptides. We have been studying a series of peptides with a variety of sequences in different solvent environments to determine the importance of the bulk environment for the development of specific secondary conformations. In general, we have noted that the solvent environment is as important as the sequence for the formation of a specific secondary structure. Of course, the sequence is also important. We have found that even interchanging the order of two amino acids can make a large difference in the amount of α-helix formed. Specifically, Y(VATAK)3 achieves a maximum 93% α-helix in alcoholic solvents, whereas Y(VTAAK)3 only achieves a maximum of 58% α-helix under the same conditions. These results will be presented and discussed (This is supported by NIH grant GM 21479).

W-Pos403

STRUCTURE OF A COMPACT PEPTIDE DETERMINED BY CIRCULAR DICHROISM AND NMR.
((M.W. Maciejewski and M.H. Zehfus)) Department of Biochemistry, The Ohio State University, Columbus, OH 43210 USA

Structural domains are regions of proteins that fold spontaneously, even when removed from the intact protein. Several studies have linked the presence of structural domains with physically compact regions in proteins (M.H. Zehfus, *Prot. Eng.* **7**: 335-340, 1994). If this is true then a compact region excised from the protein should closely resemble the structure in the intact protein. To test this theory, a compact peptide corresponding to residues 129-142 of staphylococcal nuclease (Ac-EAQAKKEKLNIWS-NH_2) was synthesized and its solution structure determined by circular dichroism (CD) and NMR. In aqueous solution, the peptide exhibits CD spectra characteristic of a nascent helix. This structure can be stabilized with the addition of 2,2,2-trifluoroethanol (TFE). Under these conditions, the chemical shift index of the $^1H\alpha$ and $^{13}C\alpha$ resonances, temperature coefficients of amide protons, and noe constraints, are all consistent with the peptide's structure being a helix-turn. This structure is almost identical to that found in the intact protein.

W-Pos404

NMR STUDIES OF A SYNTHETIC LYTIC PEPTIDE.
((Karol Maskos and Kathleen M. Morden)) Dept. of Biochemistry, Louisiana State University, Baton Rouge, LA 70803

The secondary structure and the aggregation of the synthetic lytic peptide $(KLAKLAK)_3$ in a solution of 15% hexafluoroisopropanol has been investigated using nuclear magnetic resonance spectroscopy. Even with the repetitive nature of this peptide the resonance assignments for all the backbone protons has been possible using 2D DQF COSY, TOCSY and NOESY experiments. Circular dichroism and 2D NOESY data indicate that this peptide forms an amphipathic helix. Amide exchange experiments using 2D TOCSY experiments reveal that there are several extremely slowly exchanging amide protons (> 8 days) located in the center of the hydrophobic face of this helical peptide. Protection factors have been determined for all the amide protons using 1D and 2D NMR experiments. When mapped against the sequence of the peptide these protection factors show a periodicity reminiscent of a coiled coil. A model for the aggregation state of this peptide based on amide exchange will be discussed.

Supported by NSF/LEQSF (1992-96)-ADP-01.

W-Pos405

Investigating Association of Helical Peptides in Solution by 2D HEXSY.
((Chris J. Stenland and Glenn L. Millhauser)) Department of Chemistry and Biochemistry, University of California, Santa Cruz, CA 95064

We have been developing a time domain EPR technique called two dimensional Heisenberg exchange spectroscopy (2D HEXSY) to study how helical peptides associate in solution. Using spin labeled peptide models we plan to probe collision events that simulate the early phases of protein folding. One question investigated here is how the helical macrodipole influences the N to N terminal collision rates of helical peptides. We will present results of an N-terminally labeled alpha helical peptide, called sym 3R-N, shown below.

(Sym 3R-N) **SL-AAAARAAAARAAAARAAAA-NH_2**

The 2D HEXSY experiments have been run at physiological conditions at several concentrations. These experiments have been repeated in chemical and thermally denaturing conditions to eliminate or reduce the effect of the helical macrodipole on the rate of association. Preliminary results indicate a significant effect of the helical macrodipole on the N to N association of helical peptides and the free energy of interaction has been calculated.

W-Pos406

SuperHelices: Learning to control peptide secondary structure via the primary sequence.
((Paul Hanson, Eric Praatz, Glenn Millhauser.)) Department of BioChemistry and Chemistry, Univerisity of California at Santa Cruz, Santa Cruz, Ca. 95064 (Sponsored by G. Millhauser)

A review of proteins with known crystal structures show that over 40% of the amino acids contained therein are in helical domains. Consequently, there is large interest in developing models of these regions to serve as a foundation for how proteins adopt these structures. By adaptation of alanine based peptides that previously have been shown to be helical[1], we attempt to show how to apply some observations made in this lab and in the recent literature towards the control of peptide secondary structure. We set out to build the most helical 13 residue peptide by using a variety of N-capping boxes[2] as well as using various amino acids, such as arginine, to control the helical domain towards the C-terminus[3]. The various peptides were characterized by circular dichroism and electron spin resonance experiments. Initial results indicate that we have succeeded in setting a literature record for the most helical 13 residue peptide built by design or nature. The most influential factor on the helicity of the peptide is what residue is placed at the C-terminus. Arginine was found to be the most helical promoting and the lysine the least. Modifications of the N-capping box are also examined in terms of their effect upon the helicity of the peptide.
(1)Marqusee, S.; Robbins, V. H.; Baldwin, R. L. *Proceedings Of The National Academy Of Sciences USA* **1989**, *86*, 5286-5290. (2)Rose, G. D.; Wolfenden, R. *Annual Review Of Biophysics And Biomolecular Structure* **1993**, *22*, 381-415. (3)Fiori, W. R., Lundberg K.M., Millhauser, G.L. *Nature Structural Biology* **1994**, *1*, 374-377.

W-Pos407

ASSESSING THE USE OF 2° STRUCTURE SEQUENCE-BASED ALGORITHMS AND MOLECULAR DYNAMICS FOR CONSTRUCTING 3D STRUCTURES OF PEPTIDES.
((T.F. Kumosinski and J.J. Unruh)) ERRC, USDA. Philadelphia, PA 19118.

Determination of the three dimensional (3D) structure of proteins by X-ray crystallography and 2D NMR is imperative for developing quantitative structure/function relationships. However, many biologically important proteins can not be crystallized, nor successfully analyzed by 2D NMR. Therefore, a project to develop molecular modeling techniques for construction of 3D working models with a high degree of predictability for structure/function relationships has been initiated. Here secondary structure sequence-based prediction algorithms, global secondary structure analyses from Fourier transform infrared spectroscopy (FTIR) or circular dichroism (CD), molecular dynamics techniques, and knowledge-based experimental information were employed in an iterative fashion. Success (which was determined via superposition analysis of the backbone atoms of the models verses the X-ray 3D structures) decreased markedly with increasing number of intra-molecular disulfide bridges primarily because of the lack of information concerning the angles of disulfide bonds. Predicted 3D models of biologically relevant proteins are presented and assessed for validity by comparison with X-ray crystallographic structure. The results clearly indicate that this combination methodology yields predicted structures which are more comparable with the X-ray structure than the traditional de novo calculations.

W-Pos408

Salt Induced Structural Transitions of a Helical Peptide and the Influence of an N-Terminal Capping-Box on Helix Content.
((Darren A.Thompson, Karen Lundberg, Glenn L. Millhauser)) Department of Chemistry and Biochemistry, University of California at Santa Cruz, Santa Cruz, CA 95064

In order to explore the effect of a helical capping box on helix structure [Harper, E. T., Rose, G. D. *Biochemistry* **1993**, *32*, 7605.] we designed the peptide SE3K: **Ac-SAAEAKAAAAKAAAAKA-NH_2** and placed methanethiosulfonate spin labels in 4 peptides at positions 5&9, 5&8, 10&14, and 10&13 to determine the α and 3_{10} helical composition. The design is similar to the 3K peptide upon which much work has been published [Miick, S. M., Martinez, G. V., Fiori, W. R., Todd, A. P., Millhauser, G. L. *Nature* **1992**, *359*, 653.] [Marqusee, S., Robbins, V. H., Baldwin, R. L. *Proc. Nat. Acad. Sci.* **1989**, *86*, 5286.]. Circular dichroism (CD) experiments show a 45% increase in MRE for SE3K in 1M NaCl versus MOPS buffer alone. The peptide design allows for 3 possible salt bridges which would break-up the helical structure. Elecron spin resonance (ESR) double label spectra indicate a C terminal structural distortion rather than an N-terminal distortion. The proposed distortion is one of random coil going to helix upon the addition of NaCl, with the salt acting as an electrostatic shield. We attempt to quantify the relative proportion of each possible bridge to the ensemble of structures and reinforce the calculation with MD. ESR also indicates that SE3K has a greater α helical component than the 3K peptide. CD shows a substantially higher MRE for the SE3K peptide (when in 1M salt) than the 3K peptide. There is no change in CD signal for the 3K peptide in salt solutions.

W-Pos409

ANTIFREEZE PROTEINS: A COMPUTATIONAL PERSPECTIVE.
((Jeffry D. Madura, Mark S. Taylor, Andrzej Wierzbicki, J. P. Harrington and Frank Sönnichsen)) Department of Chemistry, University of South Alabama, Mobile, AL 36688 and Protein Engineering Network of Centres of Excellence, Department of Biochemistry, University of Alberta, Edmonton, Alberta, T6G 2S2 Canada

Antifreeze peptides (AFPs) and glycopeptides (AFGPs) found in cold-water fishes have been studied experimentally for two decades and computationally the last eight years. Our goal is to test recent conjectures by Knight et al. and Laursen et al. on the mechanism of binding by type I AFPs and to investigate the binding of a Type III AFP. Computer modeling methods have been employed to study the binding of winter flounder (WF, *Pseudopleuronectes americanus*), short-horn sculpin (SHS, *Myozocephalus scorpius*), and ocean eel pout (suborder *Zoarcoidei*) a Type III AFP to various ice-Ih surfaces. The ice surfaces were constructed from the asymmetric fractional coordinates of ice using CERIUS 3.2. The direction vector [102] on (201) and $(2\bar{1}0)$ were also identified. Initial structures for the AFPs along with the positioning of the AFPs on the ice surface were done using QUANTA 4.0 while all energy minimizations were performed using CHARMM 23. The results of these calculations will be presented along with a description of the role the different residues of Type I and III AFPS play in binding to ice.

W-Pos410

SYNTHETIC PEPTIDES AS INHIBITORS OF ICE RECRYSTALLIZATION. ((A. Chatterjee, A. Wierzbicki, C.S. Sikes and J.P. Harrington)) Department of Chemistry, University of South Alabama, Mobile, Alabama 36688

Ice crystal growth is responsible for cellular damage within biological materials. Inhibitors or modifiers of ice crystal growth, analogous to the functional behavior of native antifreeze proteins and glycoproteins, have been studied as to their effectiveness in reducing ice recrystallization. Use of the splat cooling recrystallization method of Knight et al (1988) has been coupled to a photo-cryomicroscopy technique for a quantitative assay of the comparative effectiveness of synthetic polypeptide analogs and proteins investigated. Our study of 18 different polypeptides and proteins showed significant differences in their ability to inhibit ice recrystallization as determined by ice crystal sizes after 2 hrs. of growth at -8°C. $(Ala_2Thr)_7$ was the most effective synthetic peptide along with the protein, α-casein, in reducing ice recrystallization growth. Crystal diameters were 2.03 ±0.96 and 1.90 ±0.92 mm respectively, compared to 11.76 ±7.0 mm for pure ice crystal diameters after 2 hrs. of recrystallization. The effect of concentration (10-0.1 mg/ml) of these peptides and proteins, as well as the addition of NaCl to the peptide solutions were also studied. NaCl did not effect ice recrystallization inhibition activity of winter flounder. From all effective recrystallization inhibitors studied only α-casein and $(Ala_2Thr)_7$ activity was not changed by addition of 0.1-1.0 mg/ml NaCl. Effect of pH on ice recrystallization inhibition was also studied for the winter flounder, α-casein, and $(Ala_2Thr)_7$.
(Supported by NOAA Grant # NA16RG0115-03).

W-Pos411

RECOMBINANT HUMAN α - SPECTRIN PEPTIDES. ((Denise M. Lusitani, Nasser M. Qtaishat, Mark R. Kelley and L. W.-M. Fung)) Department of Chemistry, Loyola University of Chicago, Chicago, IL, 60626.

Spectrin, a human red blood cell skeletal protein, is known to contain a repeating homologous amino acid sequence, approximately 106 amino acids in length, which is believed to fold into repeating structural domains. With the advent of molecular biology and biophysical techniques, structural studies of these spectrin 106-amino acid repeats became approachable. However, one of the difficulties in such an approach is the determination of the correct reading frame of the structural domains, which may or may not coincide with the sequence motifs. In order to prepare stable spectrin peptides for molecular studies it is necessary to identify the correct reading frame of the structural domains. Based on recombinant peptides and proteolytic digestion studies, we have determined that the first structural repeat of human α-spectrin begins at amino acid 52 and ends at amino acid 156. Employing this knowledge of the correct reading frame we have prepared several recombinant α-spectrin peptides for biophysical studies to provide structural and functional information about spectrin. β-spectrin isolated from human intact spectrin was obtained for binding studies with α-spectrin peptides. α-spectrin peptides containing different structural domain sequence were used for structural studies. (Supported by NSF, American Heart Association and Loyola University of Chicago.)

W-Pos412

SYSTEMIN IS A POLY(L-PROLINE)II HELIX ((A.Toumadje and W.C. Johnson, Jr.)) Department of Biochemistry and Biophysics, Oregon State University, Corvallis, OR 97331

The proline pairs in the sequence, the fact that DPPK is found in poly(L-proline)II (PPII) helices in proteins, the PPII-type CD in aqueous buffer, and the precedent of SH3 ligands as a PPII helix all point to a PPII structure for the central portion of systemin.

W-Pos413

KINETIC CHARACTERISATION OF THE COMPLEX OF RAS.GTP AND NEUROFIBROMIN. ((T. JENKINS AND J.F. ECCLESTON)) NAT. INST. MED. RES., LONDON, NW7 1AA, U.K.

A complex of the small G-protein Ras with the fluorescent analogue of GTP, 2'(3')-O-(N-methylanthraniloyl) GTP (mantGTP), has been prepared and it's interaction with the catalytic domain of neurofibromin has been studied by a combination of stopped-flow fluorescence and quenched-flow techniques. On mixing Leu61Ras.mantGTP with excess neurofibromin and monitoring mant fluorescence, an increase in fluorescence occurs which can be fitted to a single exponential. The rate constant is proportional to [neurofibromin] and gives a second-order binding rate constant of $2.0 \times 10^7\ M^{-1}\ s^{-1}$ (20mM Tris.HCl pH 7.5, 1mM $MgCl_2$, 1mM dithiothreitol, 30°C). On mixing wild-type Ras.mantGTP with excess neurofibromin, a biphasic process is observed. An initial increase in fluorescence first occurs which is [neurofibromin] dependent with a second-order rate constant of $3.7 \times 10^7\ M^{-1}\ s^{-1}$, followed by a first-order decrease in fluorescence of $13\ s^{-1}$. The effect of temperature and ionic strength on these processes were determined and the results compared to those from quenched-flow methods where the cleavage step of GTP hydrolysis is determined directly. The results are interpreted on the basis of the model for the wild-type protein:

Ras.mantGTP + neurofibromin ⇌ Ras.mantGTP.neurofibromin
⇌ Ras*mantGTP.neurofibromin

W-Pos414

ENHANCEMENT OF $GABA_A$ AND GLYCINE CURRENTS BY WAGLER TOXIN I. ((J.-H. Ye, J.J. McArdle)) Dept. of Anesthesiology and Pharmacology, UMD, New Jersey Medical School, Newark, NJ 07103. (Spon. by K.J. Friedman).

The effect of a peptide Wagler Toxin I (WTXI, GGKPDLRPCHPPCHYIPRPKPR) stimulation on $GABA_A$ and glycine receptors/channels currents was studied in acutely dissociated hypothalamic neurons of mice. WTXI consistently augmented currents activated by $GABA_A$ (IGABA) and glycine (IGly) in nystatin perforated whole-cell recordings. This effect is rapid in onset and recovered upon washing out of the WTXI solution. TWXI dose dependently enhanced both these inhibitory currents with EC50s of 1.2 μM and 1.8 μM for IGABA and IGly, respectively. This effect is voltage dependent; WTXI stimulated IGABA and IGly more prominently when held at hyperpolarized than at depolarized potentials. However, the reversal potentials of both these currents were not affected. WTXI had a stronger effect when these Cl^- currents were induced by lower concentrations (10^{-4} M or below) than with higher concentrations (3×10^{-4} M or above) of GABA or glycine, suggesting that WTXI may compete with the agonists. In contrast, the toxin has no effect on kainate induced current recorded in these neurons, indicating that WTXI acts selectively. (Supported by NIH grant NS31040).

W-Pos415

WAGLER TOXIN I BLOCKS THE NICOTINIC ACETYLCHOLINE RECEPTOR. ((J.J. McArdle[1], J.J. Schmidt[2], S.A. Weinstein[2] and L.C. Sellin[3])) [1]Dept. of Pharmacology, New Jersey Medical School, Newark, NJ; [2]Toxinology Division, USAMRIID, Frederick, MD; [3]Dept. of Physical Sciences, University of Oulu, Oulu, Finland.

Wagler toxin I (WTXI) is a lethal peptide (GGKPDLRPCHPPCHYIPRPKPR) having a mouse LD50 of 0.37 mg/kg i.p. In an early study (Pharmacol. Tox. 70:459), we showed that WTXI reversibly blocks neuromuscular transmission. That study suggested a pre- and post-synaptic action of WTXI. In order to further explore this issue, we examined the effects of WTXI on the function of the nicotinic acetylcholine receptor (nAChR). To do this, we iontophoretically applied ACh to motor end-plates in the Triangularis sterni muscle isolated from adult mice; ACh potentials in response to maximal iontophoretic pulses (0.5 Hz) were recorded before, during and after fast application of WTXI. Within 1 sec of applying 1 μM WTXI to a superficial motor end-plate, the ACh response declined in amplitude; at 10 sec, the ACh response was completely blocked. In our study of the concentration dependency of this effect of WTXI, we found that lower concetrations have a slower onset of peak effect. Therefore, we selected a 2 min exposure time to assay ACh sensitivity. Under this condition, WTXI inhibits the ACh response with an IC50 of approximately 75 nanoM. Upon washout of WTXI, we found full recovery of the ACh response. Longer washout times are required for higher concentrations of WTXI. WTXI also suppresses spontaneous neurally evoked end-plate potentials (mepps). The effect of WTXI on mepps was slower in onset than that on ACh-evoked potentials; presumably, WTXI encounters greater diffusion barriers to the nAChRs directly apposed to active zones of the motor nerve terminal. These data demonstrate that WTXI reversibly interacts with the nAChR with a high affinity. (Supported by NIH grant NS31040)

W-Pos416

THE pKa VALUES OF MELITTIN IN SOLUTION AND IN LIPID MICELLES. ((Lingyang Zhu*, Marvin D. Kemple*, and Franklyn G. Prendergast†)) *Department of Physics, Indiana University - Purdue University Indianapolis, Indianapolis, IN 46202 and †Department of Pharmacology, Mayo Foundation, Rochester, MN 55905.

Melittin (MLT) is a 26-amino acid peptide which is known to exist as an α-helical tetramer or as a monomeric random coil depending on solvent conditions. The charge state of MLT is believed to be a major factor in determining its aggregation properties and its interaction with lipids. Several contradictory indirect measurements of the pK_a values of the three lysine groups in MLT have been reported. In this study, high resolution ^{15}N-NMR at 50.6 MHz was used to find the pK_a's of MLT. The pH dependence of MLT ^{15}N chemical shifts were measured for the isotopically labeled backbone α-^{15}N of gly-1 and the side chain ζ-^{15}N's of lys-7, lys-21, and lys-23 at a MLT concentration of 1.2 mM and a temperature of 23°C for MLT in phosphate buffer, in neat water, and in MMPC lipid micelles. The results show that each lys residue has a pK_a of 10.2 and gly-1 has a pK_a of 8.1 in phosphate buffer. Similar results were obtained for MLT in 48 mM MMPC. The pK_a values were somewhat lower for MLT in water with gly-1 at 7.6 and lys-21 and lys-23 at 9.9 and 9.8 respectively. These pK_a values indicate that the lysine residues are primarily positively charged when MLT forms a tetramer at pH values between 8.5 and 10 contrary to prevailing expectations. This work was supported in part by NSF Grant DMB-9105885 to MDK and by PHS Grant GM34847 to FGP.

W-Pos417

A COMPARISON OF THE BIOLOGICAL ACTIVITY OF A NATURAL AND DESINGED AMPHIPATHIC PEPTIDE AND THEIR STRUCTURAL PROPERTIES
((M. Dathe, J. Seydel*, K. Matsuzaki+, M. Beyermann, E. Krause, M. Bienert)) Research Institute of Molecular Pharmacology, Berlin, Germany, *Research Institute Borstel, Germany, +Faculty of Pharmacy, University of Kyoto, Japan

Analogues of different helical proponsity of Magainin-II-amide, a linear peptide with antibacterial activity have been synthesized. Additionally, a $(KLA)_n$-peptide has been developed with double-D substitutions at different positions of the 18 residue-long chain generating sequences of varying helical proponsity.
By CD, the unmodified peptides are found to be mainly α-helical in TFF and in the presence of SDS micelles and charged lipid vesicles. The two peptides show a pronounced antibacterial activity. The reduction of the activity of the Magainine analogues as well as their decreased bilayer disturbing effect properly correlate with the impaired helicity of the sequences. The differentiated helical propensity of the KLA-peptides as shown in structure inducing TFF solution is also reflected in the biological effect. However, almost no differentiation was found in the structural properties of the double D-substitued analogues interacting with SDS, vesicles and at the air-water interface as well as in their effect on dye release from negatively charged liposomes .The results show that the antibacterial activity of the peptides correlates best with their helicity in TFE.

W-Pos418

A COMPARISON OF THE EFFECTS OF MAGAININ AND ALAMETHICIN ON MEMBRANE STRUCTURE ((S.J. Ludtke, K. He, T. Harroun, W.T. Heller, and H.W. Huang)) Rice University, Houston, TX 77251-1892.

The magainins are 23-residue (nonhemolytic) antibiotic peptides discovered in the skin of xenopus laevis. Alamethicin is a 20 residue (hemolytic) antibiotic peptide. Both peptides interact with lipid bilayers in a similar fashion: At low concentrations and in low hydration states, the peptides lie parallel to the surface of the bilayer. At high concentrations/hydration the peptides insert perpendicular to the bilayer. Membrane composition is also a strong factor in determining degree of insertion. At high concentrations/hydration, magainin will insert completely in bilayers with charged headgroups while it inserts only slightly into neutral bilayers. Alamethicin, on the other hand, will also insert into neutral bilayers. In DPhPC, magainin remains primarily on the surface even at concentrations high enough to cause alamethicin to be completely inserted. Using lamellar x-ray diffraction we have studied how these peptides affect membrane structure at various concentrations and hydration states. We have found that both magainin and alamethicin cause the membrane to become thinner in high hydration states. In these states, change in membrane thickness is proportional to the peptide concentration. In addition DPhPC has a low hydration phase which appears to be unaffected by either peptide even at high concentrations. There are noticeable differences between the effects of the two peptides in the transition between the high and low hydration states. Results for other lipid systems will also be presented.

W-Pos419

X-RAY DIFFRACTION STUDY OF ALAMETHICIN INTERACTING WITH DIPHYTANOYL PHOSPHATIDYLCHOLINE BILAYERS. ((K. He, S. J. Ludtke, Y. Wu and H. W. Huang)) Rice University, Houston, TX 77251.

We have shown in our previous publications that amphiphilic helical peptides undergo a phase transition from a state of adsorbing on a bilayer surface to a state of insertion across the bilayer as their concentrations increase over a critical peptide to lipid ratio, P/L. By x-ray lamellar diffraction we examined the bilayer thickness (the phosphate to phosphate distance) t as a function of the lamellar spacing D at various values of P/L. At low P/L the peptide molecules are primarily adsorbed at the hydrophobic-hydrophilic interface, separating the headgroups laterally. As P/L increases, t decreases in proportion to P/L, until P/L reaches the critical value. Presumably because the thickness of the chain region becomes equal to alamethicin's hydrophobic length, at this critical P/L, the peptide starts to insert into the bilayer. And the bilayer ceases further thinning with increasing P/L as long as there are inserted peptides. Above the critical P/L we are able to examine the peptide both in the inserted state and in the surface state due to hysteresis. If the bilayers are dehydrated, the inserted peptide comes out of the bilayer and DPhPC forms a unique gel phase independent of the peptide concentration. (Thus we observed two different phase transitions in this experiment.) If the dehydrated bilayers are slowly hydrated, the peptide remains in the surface state. In this state, the bilayer thickness continues to decrease as the peptide concentration increases.

W-Pos420

HYDRATION DEPENDENCE OF ALAMETHICIN'S PHASE TRANSITION IN ALIGNED LIPID BILAYERS ((W.T. Heller, K. He, T. Harroun, S.J.Ludtke, and H.W. Huang)) Rice University, Houston, TX 77251-1892.

Alamethicin undergoes a phase transition from adsorption on the bilayer surface to insertion across the bilayer as a function of the peptide concentration and the water content. In order to study the hydration dependence, we built a humidity chamber in which an aligned multilayer sample is exposed to a continuously variable humidity. Our method for varying the relative humidity involves changing the temperature of a water bath relative to that of the sample using a feedback circuit responding to a measurement from a humidity probe. The orientation of the peptide is monitored by oriented circular dichroism (OCD) once the chamber has reached equilibrium. Using this technique, we mapped out the coexistence region of the inserted state and the surface state of the peptide in concentration-humidity phase space. OCD measurements at a given peptide concentration were taken as the value of the relative humidity was increased and then as the relative humidity was decreased. We observed that the coexistence region for the process of increasing the relative humidity does not match the coexistence region for the process of decreasing relative humidity. Hysteresis was observed. The OCD measurement was correlated with a corresponding measurement of lamellar x-ray diffraction.

W-Pos421

STUDIES OF INTERACTION BETWEEN GELSOLIN(150-169) AND PIP_2 IN MIXED MICELLES. ((W. Xian, W.H. Braunlin)) Universtiy of Nebraska-Lincoln, Lincoln, NE 68588-0304

The interaction of the actin binding protein gelsolin with phosphotidylinositol 4,5-bisphosphate (PIP_2) is a crucial step in biological signal transduction that leads to modification of the cytoskeleton. A 20 amino acid PIP_2 and actin-binding domain G(150-169) is found in gelsolin. A peptide with the same sequence has been synthesized. Previous CD and NMR experiments have shown that the peptide adopts α-helical conformation in >20% trifluoroethanol (TFE). CD experiments of this peptide in SDS-PIP_2 mixed micelle solution show that the peptide adopts partially α-helical conformation in SDS micelle solution. Increasing the SDS concentration does not change the helicity significantly, but addition of PIP_2 induces a more helical conformation of the peptide. When PIP_2 was added to SDS to form mixed micelles, NMR NOESY experiments show that while no dramatic chemical shift changes ocurred, additional NOE cross peaks were observed, suggesting proximity between peptide protons and PIP_2 protons. ^{31}P NMR experiments suggest that the head group conformation is more homogeneous in the presence of the peptide.

W-Pos422

STRUCTURAL STUDIES OF A LIPID-ASSOCIATING DOMAIN OF SURFACTANT PROTEIN A. ((A.J. Waring, L.M. Gordon, and F.J. Walther)) Departments of Pediatrics, Drew University/King Medical Center & UCLA, 12021 South Wilmington Ave. Los Angeles, CA 90059.

Surfactant protein A (SP-A) is a 248 residue, water soluble, lipid associating protein found in lung surfactant. Analysis of the amino acid sequence of human SP-A indicates that residues 115-120 have high hydrophobic moments typical of lipid-associating amphipathic protein molecular domains. The folding and secondary structure of this SP-A domain was studied by synthesis of a thirty-one residue synthetic peptide analog of the protein sequence. The secondary structure of the SP-$A_{114-144}$ was measured in a number of structure promoting solvents using circular dichroism and FTIR. Measurements in trifluoroethanol, SDS micelles, and surfactant lipid dispersions (DPPC:unsatPG:palmitic acid, 66:22:9, wt:wt) indicate the peptide had a dominant helical content. Contrarily, the peptide had a lower helix content and greater disordered conformation in saline solution. Complimentary FTIR measurements of lipid-peptide films dried on the surface of germanium ATR crystals show that the peptide assumes largely helical conformations in these molecular environments and the helical axis is at an oblique angle to the surface of the film. These observations suggest that this SP-A domain is an amphipathic helical segment in membrane mimic environments.

Supported by RCMI-NIH Grant 2G12 RR 3026 and RO1 HL 40666

W-Pos423

THE INTERACTIONS OF LYTIC PEPTIDE ANALOGUES WITH LIPOSOMES: BINDING AND MEMBRANE PERMEABILITY STUDIES ((T. Jamil, S.M. Bishop, P. S. Russo and M. D. Barkley)) Department of Chemistry, Louisiana State University, Baton Rouge, LA 70803.

The interactions of three synthetic amphipathic peptides $(KLAKKLA)_3$, $(KLAKLAK)_3$ and $(KLGKKLG)_3$ with differently charged model membranes are described. These positively charged peptides were designed to cause cell membrane lysis. $(KLAKKLA)_3$ and $(KLAKLAK)_3$ showed high lytic activity against bacteria and animal cells. Unilamellar liposomes of uniform size and of either neutral or negative charge were prepared from different phospholipids (DLPC, DLPG, DOPC, DOPG, DPPC) by the standard extrusion technique. The binding properties of $(KLAKKLA)_3$ were studied via fluorescence methods after derivitization of the N-terminus with an appropriate fluorophore. Using NBD labeled $(KLAKKLA)_3$, binding isotherms were obtained showing a strong association for DLPC/DLPG liposomes, i.e. surface partition coefficient of $2.5x10^5$ M^{-1}. Deviation of the isotherm from linearity at lower lipid:peptide ratios was consistent with peptide aggregation within the bilayer. CD spectroscopy indicated that the secondary structure of this peptide was α-helix or random coil when bound to negatively charged or neutral bilayers, respectively. Binding was also demonstrated via the fluorescence photobleaching recovery (FPR) method with carboxyfluorescein labeled $(KLAKKLA)_3$. The translational diffusion coefficient decreased from 10^{-6} cm^2s^{-1} to 10^{-8} cm^2s^{-1} upon association with both DOPC and DOPC/DOPG liposomes, indicating significant binding. The permeability of all membranes upon association with each of the three peptides was investigated via leakage of entrapped sodium fluorescein using FPR. At a lipid to peptide ratio of 40:1 $(KLAKKLA)_3$ and $(KLAKLAK)_3$ produced rapid dye leakage whereas $(KLGKKLG)_3$ induced a much slower membrane permeability. In all of these studies, light scattering showed that the liposome size was unaltered by treatment with peptide. It is thus shown that the nature of the peptide-lipid interaction is dependent upon vesicle surface charge and peptide conformation which also correlates with the degree of dye leakage in entrapment experiments. Possible mechanisms of membrane disruption by these novel lytic peptides will be discussed.

W-Pos424

INTERACTION OF LIPID BILAYERS WITH *de novo* MEMBRANE PEPTIDES. ((Laura A. Chung and T. E. Thompson)) Department of Biochemistry, University of Virginia, Charlottesville, VA 22908.

The insertion of proteins into membrane bilayers is a necessary step for the biogenesis of both secreted proteins and integral membrane proteins. Certain proteins (eg. apocytochrome C, colicin E1, M13 procoat protein, toxins) do not require accessory proteins for their membrane insertion. We are studying the problem of spontaneous protein insertion using *de novo* peptide sequences designed to be soluble in aqueous solution and also capable of interacting with lipid bilayers. Starting with polyalanine as our base sequence, we added polylysine as a hydrophilic 'carrier' sequence and included leucine residues to increase the hydrophobic membrane interactions. A tyrosine residue was included for optical detection. The resulting sequences, H_2N-Ala_{27}-Tyr-Lys_6-$CONH_2$ and H_2N-Ala_2-Leu_3-Ala_{22}-Tyr-Lys_6-$CONH_2$, are soluble in aqueous solution and bind to lipid vesicles. We are currently studying the solution and membrane bound structures of these peptides using spectroscopic methods. (This work is funded by NIH grant GM-14628)

W-Pos425

A PREDICTED 3-D WORKING MODEL OF PLANT PLASMA MEMBRANE H^+-ATPASE. ((Shu-I Tu, Thomas F. Kumosinski, and Deidre Patterson)) USDA, ARS, NAA, Eastern Regional Research Center, 600 E. Mermaid Lane, Philadelphia, PA 19118

The plasma membrane H^+-ATPase of plant cells provides the energy needed to transport nutrients. Using the nucleotide sequence as a guide, predicted amino sequence of the *A. thaliana* plasma membrane H^+-ATPase is now available (Harper, et al., Proc. Natl. Acad. Sci. *86*, 1234-1238, *1989*). The hydropathy plots of the primary sequence of 949 amino acids indicated the presence of two helix-rich regions (61-305 and 670-846, 4 helices in each region), a long stretch between helix 4 and 5 (306-669), and the N and C-terminal regions. We have constructed a 3 d working model of this enzyme by a variety of molecular modeling techniques. The applied approaches involve (1) docking 2 α-helical boundless (4 helix each) to construct a trans- membrane channel (2) constructing the non-helical portion using 2^o structural sequence-based algorithms, (3) building the peptide loop (306-669) linking the helical boundless based on its sequence and structural homology to fructose-1,6-bisphosphatase, and (4) restricting the motion of ATP binding regions in the loop. All of these individual pieces as well as total structure were energy minimized using a Tripos force field modified by an experimentally based hydrophobic attractive force and were equilibrated via molecular dynamics at a variety of temperatures. The final model contains essential structure features of a transmembrane ion pump. This approach was also used to verify the known structure features of a well-studied membrane protein (bacteriorhodopsin).

W-Pos426

HOMOLOGY MODELING OF HUMAN 5-, 12- AND 15-LIPOXYGENASES ((S. T. Prigge, J. C. Boyington, B. J. Gaffney and L. M. Amzel)) The Johns Hopkins School of Medicine, Baltimore, MD 21205

Lipoxygenases are a class of non-heme iron dioxygenases which catalyze the hydroperoxidation of fatty acids for the biosynthesis of leukotrienes and lipoxins. The structure of the 839-residue soybean lipoxygenase-1 was used as a template to model human 5-, 12- and 15-lipoxygenases. A distance-based algorithm for placing side chains in a low homology environment (only the four iron ligands were fixed during side chain placement) was devised. Twenty-five of the fifty-one conserved lipoxygenase residues were found to interact in four distinct regions of the enzyme. These regions were analyzed in the models to discern whether the interactions were duplicated or whether alternate conformers were viable. Charged residues were analyzed to identify conserved buried salt bridges. The effects of site directed mutagenesis variants were rationalized using the models of the human lipoxygenases. In particular, variants which shifted positional specificity between 12- and 15-lipoxygenase activity were analyzed. A detailed analysis of the active site produced a model which accounts for observed lipoxygenase regiospecificity and stereospecificity. (Supported by NIH grant GM 44692)

W-Pos427

THE MOLECULAR BASIS OF HUMAN OTCASE DEFICIENCY. ((H. Morizono, X. Yuan, M. Tuchman[1] and N. M. Allewell)). Department of Biochemistry, University of Minnesota, St. Paul MN 55108. [1]Department of Pediatrics, University of Minnesota Medical School, Minneapolis MN 55455.

Deficiencies in the activity of ornithine transcarbamylase (OTCase), an enzyme of the urea cycle, are among the most common causes of hyperammonemia, which is toxic to the brain. Many different mutations that result in neonatal or late onset have been identified through PCR cloning. The sequence similarity of human OTCase and the catalytic subunit of E. coli ATCase is 46%, secondary structure predictions and distributions of hydrophobic/hydrophilic residues are similar, and residues at the carbamyl phosphate binding site are conserved, suggesting that their three-dimensional structures may be similar. We have developed a model of the OTCase structure by aligning human OTCase and E. coli ATCase catalytic subunit sequences and energy minimizing by the method of steep descent. All known mutations that result in neonatal onset are at the active site of the model, while more distant mutations are associated with late onset. A putative divalent metal ion binding site that may be analogous to the Zn(II) binding site in E. coli OTCase has been identified at the interdomain, interchain interface. The wild type enzyme and two common mutants have been cloned into E. coli, overexpressed and purified to homogeneity, making possible future biochemical and structural studies. Supported by NIH grant DK-17335 to NMA.

W-Pos428

A MODEL OF THE THREE-DIMENSIONAL STRUCTURE OF PARAFUSIN BASED ON SEQUENCE HOMOLOGY TO PHOSPHOGLUCOMUTASE.

((S. Levin, B.H. Satir, S.C. Almo)) Albert Einstein College of Medicine, Bronx, NY 10461.

Parafusin (PFUS) is a 63 kD protein hypothesized to be a new type of signal transduction molecule associated with regulation of membrane fusion in exocytic events. Despite high sequence homology (up to 51.7% identity) to phosphoglucomutase (PGM), PFUS is a functionally different protein of a PGM superfamily. A model of 3-dimensional structure of parafusin from *Paramecium tetaurelia* was constructed based on multiple sequence alignments of a number of PGM from human, rat and yeast and the known 3-dimensional structure of rabbit muscle PGM (Dai et al, J. Biol. Chem. 267:6322, 1992). Two major deletions and four major insertions (from 4 to 9 amino-acids) were allocated in all domains of the PGM molecule. Most deletions and insertions in PFUS occurred in surface exposed loops connecting elements of the secondary structure. Surprisingly, one 9 amino-acid deletion appears to be consistent with the deletion of a complete β-strand from the middle of a parallel β-sheet. The model is consistent with, and provides structural interpretations for, experimental results obtained from biochemical studies. Predictions are made concerning the changes of functionally important sites leading to alteration of protein function while retaining high sequence homology to PGM.

RHODOPSIN—BACTERIORHODOPSIN

W-Pos429

STRUCTURAL MODELS OF RHODOPSIN AND BATHORHODOPSIN BASED ON NMR CONSTRAINTS. ((M. Han and S.O. Smith)) Yale University, Dept. Mol. Biophys. & Biochem., New Haven, CT 06520.

Rhodopsin is the photoreceptor in vertebrate rod cells responsible for vision at low light intensities. The photoreactive chromophore in rhodopsin is 11-*cis* retinal bound to the protein via a protonated Schiff base with Glu113 as the counterion. We have used the observed ^{13}C NMR chemical shifts of the conjugated retinal carbons in combination with semiempirical molecular orbital calculations to establish the major charge interactions in the retinal binding site of rhodopsin and its primary photoproduct, bathorhodopsin. In rhodopsin, the NMR data constrain one of the carboxylate oxygens of Glu113 to be ~ 3 Å from the C_{12} position of the retinal with the second oxygen oriented away from the conjugated retinal chain. The bathorhodopsin retinal binding site structure is generated from the rhodopsin model by isomerization of the C_{11}=C_{12} bond and incorporation of C-C single bond twists from C_8 to C_{15}. The resulting structure yields a moderate fit to both the chemical shift data and the 543 nm λmax of bathorhodopsin. Finally, the retinal binding site structure derived from the NMR constraints is used to position the 11-*cis* retinal chromophore in the interior of the rhodopsin apoprotein recently proposed on the basis of sequence analysis of G-protein coupled receptors. The resulting model can also explain the following experimental observations: the opsin shift of rhodopsin, the spectral shifts in mutants E113D and G90D/E113Q, crosslinking between the ring and helix VI, the position and orientation of the retinal based on fluorescence energy transfer and linear dichroism data.

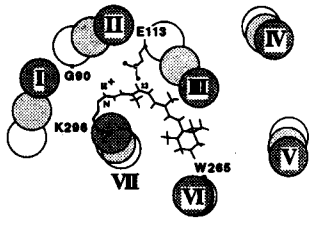

W-Pos430

LOCALIZATION OF THE TRANSMEMBRANE HELICES IN THE THREE-DIMENSIONAL STRUCTURE OF FROG RHODOPSIN. ((V.M. Unger, P.A. Hargrave and G.F.X. Schertler)) Laboratory of Molecular Biology, Hills Rd. Cambridge/U.K., CB2 2QH (Spon. by R. Henderson)

The visual pigment, rhodopsin, is a member of the family of G protein-coupled receptors. Electron cryo-microscopy was used to determine the three-dimensional structure of frog rhodopsin from tilted two-dimensional crystals embedded in vitrified ice. At present, the effective resolution cut-offs in a map calculated from 38 images are about 8Å horizontally and approximately 30 Å normal to the plane of the membrane. Compared to the three-dimensional map of bovine rhodopsin obtained previously (Unger and Schertler, Biophys. J., submitted), the improved vertical resolution now allows the approximate positions of all the helices to be established within the structure. In particular, the direction of tilt for the three more strongly tilted helices, located within the "arc-shaped" feature in the projected structure (Schertler, Nature 1993), is now defined unambigiously and supports the tentative model obtained from the three-dimensional map of bovine rhodopsin. In this model, the likely arrangement of all the helices creates a structure in which an "arc " formed by the four more highly tilted helices, is flanked by a single helix on the outer side and a pair of helices on its inner side. All three of these flanking helices are oriented almost perpendicular to the plane of the membrane and the triangle formed between them clearly indicates the structural differences between rhodopsin and the light driven, archaebacterial proton pump bacteriorhodopsin.

W-Pos431

BR-ATCASE: A FUSION STRATEGY FOR CRYSTALLIZATION OF MEMEBRANE PROTEINS. ((G.J. Turner, L.J. Miercke, A. Mitra, C. Schafmeister, M. Betlach and R.M. Stroud)) Department of Biochemistry and Biophysics, UCSF, San Franscisco, CA 94143.

A novel method is reported for attempting generation of high quality 3-dimensional crystals of integral membrane proteins. The strategy employs addition of a large soluble domain to the membrane protein to promote crystal contacts. Our first attempt has been the production of a fusion between Bacteriorhodopsin (BR) and the catalytic subunit of the catalytic subunit of *E.coli* aspartyl transcarbamylase (i.e. ATCase). ATCase was initially chosen for the BR fusion since both proteins are nearly spherical with similar diameters, both trimerize *in vivo*, and the ATCase crystal structure is known. The fusion protein (termed BRAT) was initially expressed in *E.coli* at 5mg/liter to yield active ATCase and an unfolded BO component. BRAT was solubilized with SDS, and after high pressure size excusion chromatography (HPSEC) was 40% pure. BRAT expressed in *Halobacterium salinarium* yielded a purple membrane consisting of 90-100% BRAT, at 3 mgs/L. The purple fusion protein was solubilized in SDS, to near homogeneity, delipidated by HPSEC in 0.1% SDS and refolded in tetradecyl maltoside (TDM). The visible absorption properties of BRAT are essentially identical to BR impling that the ATCase has no effect on BR structure. The high TDM concentrations (>20mM), required to maintain BRAT solubility, has hindered initial crystallization trials.

W-Pos432

RHODOPSIN UNDERGOES AN INCREASED HYDROGEN-DEUTERIUM EXCHANGE UPON PHOTOEXCITATION

((Parshuram Rath, Willem J. DeGrip§ and Kenneth J. Rothschild)) Department of Physics and Molecular Biophysics Laboratory, Boston University, Boston, MA 02215 and §Department of Biochemistry, Center for Eye Research, University of Nijmegen, 6500 HB, Nijmegen, The Netherlands

FTIR difference spectroscopy was used to investigate the kinetics of hydrogen-deuterium (H/D) exchange in bovine rhodopsin films before and after photoexcitation. Films exposed to D_2O for more than 24 hours in the dark exhibit a very slow H/D exchange as indicated by changes in the intensity of the amide II and amide II' bands at 1545 and 1460 cm^{-1} respectively. Upon photoexcitation, the time-resolved FTIR difference spectra have contributions from the Rho→Meta II transition along with the refolding of rhodopsin structure (Rothschild et al.(1987), Biophys. J., 51, 345-350) which at 10°C has a $t_{1/2}$ of 30 minutes. An additional component is also detected that reflects a sudden increase in the hydrogen-deuterium exchange which continues for more than 10 hours. These data indicate that a portion of the rhodopsin structure becomes accessible to H/D exchange after photoexcitation.

W-Pos433

EFFECT OF ALCOHOL CHAIN LENGTH ON METARHODOPSIN II FORMATION AND ACYL CHAIN PACKING FREE VOLUME

((Drake C. Mitchell, John T. R. Lawrence, & Burton J. Litman)) Laboratory of Membrane Biochemistry & Biophysics, N.I.A.A.A., N.I.H., Rockville MD 20852.

Rhodopsin is a member of the superfamily of G protein-coupled receptors. The MII (metarhodopsin II) photointermediate is synonymous with the form of bleached rhodopsin which activates the ROS G protein, transducin (G_t). The effect of ethanol, butanol, hexanol, octanol, and decanol on MII formation was studied in POPC and PDPC vesicles and ROS disk membranes. Modulation of MII formation by these alcohols was studied by resolving the post bleaching spectral contributions of MI and MII. In all three membranes, equilibrium MII concentration was increased by alcohols shorter than heptanol in the order ethanol > butanol > hexanol, whereas longer chain alcohols decreased MII concentration with decanol being more effective than octanol. The effect of all alcohols on MII formation in ROS disks and PDPC were similar and greater than those observed in POPC. The influence of these alcohols on acyl chain packing was assessed by deriving a fractional volume parameter, f_v, from dynamic fluorescence anisotropy measurements of the probe DPH. The disk membrane is about 40%, 42%, and 16% of PC, PE, and PS respectively. The similar behavior observed for rhodopsin in disk membranes, which have about 50% of their phospholipid acyl chains as 22:6, and PDPC, suggests that the differential effect of alcohols with varying chain length is due to the acyl chain packing properties of the various phospholipids and not to differences in head group composition.

W-Pos434

PRESSURE AND VISCOSITY DEPENDENCE IN THE BACTERIORHODOPSIN PHOTOCYCLE.

((G.S. Harms, Q. Song, C.K. Johnson)) *Department of Chemistry, University of Kansas, Lawrence, KS 66045*

We have studied the effect of solvent viscosity on the kinetics of the bacteriorhodopsin photocycle in the purple membrane of *Halobacterium salinarium*. The effect of viscosity was isolated from the possible influence of the activity of water by the isopiestic method, whereby the activities of solutions whose viscosities are vastly different are equilibrated. A viscosity dependence of the kinetics of bacteriorhodopsin was observed at constant water activity. Although the kinetics of the intermediate steps were sensitive to viscosity, the amplitudes of reorientational motions as measured by the optical anisotropy did not change with viscosity.

Pressure dependent kinetic data have been recorded for the ground state, L-state, and K-state at pressures up to 4 kbar. Higher pressure (.1 to 5 kbar) impedes the K→L→M steps and the BR recovery of the photocycle, revealing a positive volume of activation. Volumes of activation of +30 ml/mole and +8 ml/mole have been determined for the BR recovery and the L→M transition, respectively.

W-Pos435

SITE-DIRECTED ISOTOPE LABELING OF BACTERIORHODOPSIN

((Sanjay Sonar[‡], Chan-Ping Lee[§], Matthew Coleman[‡], Cheryl F.C. Ludlam[‡], Xiao-Mei Liu[‡], Thomas Marti[#], H. Gobind Khorana[#], Uttam L. RajBhandary[§] and Kenneth J. Rothschild[‡])) [‡]Physics Department and Molecular Biophysics Laboratory, Boston University, Boston MA 02215; [§]Department of Biology, and [#]Departments of Chemistry and Biology Massachusetts Institute of Technology, Cambridge, MA 02139

FTIR-difference spectroscopy can provide detailed information about changes in the hydrogen bonding, protonation state and orientation of specific chemical groups in a membrane protein. However, this approach is limited by the absence of a general method for placing isotope labels at specific positions in a protein. We report site-directed isotope labeling (SDIL) of an integral membrane protein: bacteriorhodopsin (bR) (Sonar *et al.*, (1994) *Nature Struct. Biol.* 1, 512-518). SDIL-Analogs of bR were produced by expressing bR in an in vitro system containing a tyrosine suppressor tRNA aminoacylated with isotopically labeled tyrosine followed by refolding. SDIL-analogs containing ^{2}H and ^{13}C isotopes at both specific tyrosine and backbone peptide carbonyl groups were produced and have properties almost identical to native bR. FTIR analysis of the bR →K, L, M and N steps in the photocycle of these SDIL-analogs has led to the identification of structurally active groups which may be involved in proton transport and in the coupling of chromophore isomerization to protein conformational changes, in an essentially unperturbed system.

W-Pos436

EVALUATION OF INTERHELICAL DISTANCES OF A BACTERIORHODOPSIN MUTANT USING A HETEROBIFUNCTIONAL CROSS-LINKER.

((T. L. Bishop, Y. Feng, B. Katz, K. Schey, D. Knapp, and R. K. Crouch)) Medical University of South Carolina, Charleston, SC 29425.

Bacteriorhodopsin (BR), the sole protein found in the purple membrane of *Halobacteria salinarium*, is one of the few transmembrane proteins for which a probable 3-D map has been obtained. Of the many techniques used to determine BR structure, very few methods using a molecular ruler have been reported. By using the heterobifunctional cross-linker 4-(maleimido)-benzophenone (MBP), interhelical distances of BR can be examined. By using a BR mutant containing a single cysteine residue, MBP can be linked to BR in a predetermined region. MBP can then be photoactivated to a triplet excited state which will react with C-H bonds. The BR mutant we have prepared contains a threonine point mutation to cysteine at position 121 (T121C). The absorbtion maxima (558 nm) and the proton pumping activity of T121C are found to be close to that of the wild type BR which suggests there are few conformational changes of the protein by the point mutation. MBP synthesized containing a C-14 label has been cross-linked to the protein, and T121C digested by CNBr has been mapped by MALDI mass spectrometry. The sites of cross-linking will be discussed.

Supported by EY04939, EY08239, and Research to Prevent Blindness.

W-Pos437

RAPID LONG-RANGE PROTON DIFFUSION ALONG THE SURFACE OF THE PURPLE MEMBRANE AND DELAYED PROTON TRANSFER INTO THE BULK.

((U. Alexiev[1], P. Scherrer[1], R. Mollaaghababa[2], H.G. Khorana[2] and M.P. Heyn[1])). [1]Biophysics Group, Dept. of Physics, Freie Universität Berlin, D-14195 Berlin, Germany. [2]Dept. of Biology, Massachusetts Inst. of Technology, Cambridge, MA 02139, USA.

The pH-indicator dye fluorescein was covalently bound to the surface of the purple membrane in position 72 on the extracellular and in positions 101, 105 or 160 on the cytoplasmic side of bacteriorhodopsin by reacting 5-(bromomethyl)fluorescein with the sulfhydryl group of cysteine residues introduced by site-directed mutagenesis. We verified that the kinetics of the rise of the M-intermediate is not affected by either the mutation or the labeling. At position 72 on the extracellular surface the light-induced proton release was detected 71 ± 4 μs after the flash (pH 7.3, 22°C, 150 mM KCl). For the cytoplasmic side with the dye in positions 101, 105 and 160 the corresponding values were 77, 76 and 74 ± 5 μs, respectively. Under the same conditions the proton release time in the bulk medium as detected by pyranine was around 880 μs, i.e. more than ten times slower. The fact that the proton which is released on the extracellular side is detected much faster on the cytoplasmic surface than in the aqueous bulk phase, demonstrates that it is retained on the surface and migrates along the purple membrane to the other side. Based on the small difference between the proton detection times with labels on opposite sides of the membrane, we estimate that at 22°C the proton surface diffusion constant is larger than $3 \times 10^{-5} cm^2/s$. These findings support models of local proton coupling.

W-Pos438

STRUCTURAL INVESTIGATIONS OF BACTERIORHODOPSIN USING RF-DRIVEN RECOUPLING NMR SPECTROSCOPY.

((J. M. Griffiths [1, 2], A. E. Bennett [1, 2], K. V. Lakshmi [1, 3], J. Raap [4], J. Lugtenburg [4], M. Engelhard [5], J. Herzfeld [3] and R. G. Griffin [1, 2])) [1] Francis Bitter National Magnet Laboratory and [2] Department of Chemistry, Massachusetts Institute of Technology, Cambridge, MA 02139; [3] Department of Chemistry, Brandeis University, Waltham, MA 02115; [4] Rijksuniversiteit te Leiden, NL-2300 R A Leiden, The Netherlands; [5] Max-Planck-Institut für Ernährungsphysiologie, Rheinlanddamm 201, D-46 Dortmund, Germany.

We apply a new solid state NMR technique -- RF-Driven Recoupling (RFDR) -- to probe conformation-dependent geometries and measure ^{13}C-^{13}C distances in the membrane protein bacteriorhodopsin (bR). RFDR is a method for the recoupling and observation of homonuclear dipolar interactions in magic angle spinning experiments. 2D RFDR spectra of [14-^{13}C-retinal], [ε-^{13}C-lys]-bR demonstrate the configuration of the retinal-protein Schiff base linkage via dipolar correlation. This study has confirmed the relative differences between the conformers comprising dark-adapted bR (bR_{555} and bR_{568}) and yields distance information consistent with Rotational Resonance (R^2) NMR spectroscopy. Likewise, we apply dipolar correlation spectroscopy to elucidate the proximity of aspartic acid residues to the retinal. 2D RFDR spectra of [14-^{13}C-retinal], [4-^{13}C-asp]-bR indicate that the 14-^{13}C-retinal is farther from the closest 4-^{13}C-asp in bR_{555} than in bR_{568}. These applications illustrate the utility of RFDR in examining geometric changes in the retinal and surrounding protein, and in clarifying the role of the aspartic acid residues, during the bR photocycle.

W-Pos439

SOLID STATE NMR DETECTION OF MULTIPLE M-INTERMEDIATES IN BACTERIORHODOPSIN ((J.G. Hu, B.Q. Sun, R.G. Griffin and J. Herzfeld)) Dept. of Chemistry, Brandeis University, Waltham, MA 02254 and Dept. of Chemistry and Francis Bitter National Magnet Laboratory, Massachusetts Institute of Technology, Cambridge, MA 02139.

In order to enforce vectorial proton transport in bacteriorhodopsin (bR), it is necessary that there be a change in molecular structure between deprotonation and reprotonation of the chromophore --- i.e., there must be at least two different M-intermediates in the functional photocycle. We present here the first detection of multiple M-intermediates by solid-state NMR. Illumination of light adapted [ε-^{15}N-Lys]-bR at low temperatures shifts the ^{15}N signal of the Schiff base downfield by about 150 ppm, indicating a deprotonated photointermediate. In 0.3 M guanidine-HCl at pH=10.0, two diffferent M states are obtained, with a 7ppm chemical shift difference, depending on the temperature during illumination. The M state prepared at the lower temperature decays to the other as the temperature is increased. Both relax to bR_{568} at room temperature. The state trapped at the higher temperature in 0.3 M guanidine-HCl at pH=10.0 is not seen in 0.2 M KCl at pH 10.0. This suggests that this state is not necessary for pumping and may be an M_N-type photointermediate such as is seen in the D96N mutant for which the proton uptake pathway is also severely perturbed. For the M intermediate trapped at the lower temperature, ^{13}C CP/MAS spectroscopy of [14-^{13}C-ret],[ε-^{13}C-Lys]-bR shows two different 14-^{13}C chemical shifts. This implies two different substates. Further studies are underway to clarify the structures of these states and their relationships to each other and to the L and N states.

W-Pos440

SOLID STATE NMR DETECTION OF BACKBONE STRUCTURAL CHANGE IN THE BACTERIORHODOPSIN PHOTOCYCLE ((J.G. Hu, B.Q. Sun, M. Bizounok, R.G. Griffin and J. Herzfeld)) Department of Chemistry, Brandeis University, Waltham, MA 02254 and Department of Chemistry and Francis Bitter National Magnet Laboratory, Massachusetts Institute of Technology, Cambridge, MA 02139. (Sponsored by J.N. Han)

It has been suggested that proline residues play key roles in the active transport of cations by membrane proteins. In bacteriorhodopsin (bR), which functions as a light-driven proton pump, there are eleven proline residues. Three of them (Pro-50, 91 and 186) are deeply embedded in the middle of α-helices B, C, and F, respectively. FTIR difference spectra indicate that at least one of the three X-Pro peptide bonds participates in conformational changes during the photocycle. In order to examine such changes, we performed NMR experiments on isotopically labeled bR. The ^{15}N CP/MAS spectrum of [^{15}N-Pro]-bR shows 5 resolved spectral lines at RT. The chemical shifts of particular proline residues were assigned using doubly labeled [1-^{13}C-X],[^{15}N-Pro]-bR's (X=Thr, Tyr) and a REDOR pulse sequence. The ^{15}N chemical shifts of Pro-91 and Pro-186, relative to saturated (5.6 M) NH_4Cl, are 109.0 ppm and 105.8 ppm, respectively, in bR_{568}, and move downfield to 110.8 ppm and 106.3 ppm, respectively, in the M-intermediate. These shifts suggest that the bR_{568} and M states differ more at Pro 91 than at Pro-186. At Pro-91, the chemical shift change could reflect a *trans* to *cis* isomerization of the peptide bond in the bR_{568} to M transition. Further studies are underway to determine the conformation of this bond in the bR_{568} and M states.

W-Pos441

INTERACTIONS BETWEEN THE PROTONATED SCHIFF BASE AND ITS COUNTERION IN THE PHOTOINTERMEDIATES OF BACTERIORHODOPSIN ((J.G. Hu, R.G. Griffin and J. Herzfeld)) Dept. of Chemistry, Brandeis Univ., Waltham, MA 02254-9110 and Dept. of Chemistry and Francis Bitter National Magnet Lab., MIT, Cambridge, MA 02139-4307.

In a previous study, we have shown that halide salts of the protonated Schiff base (pSB) of all-*trans* retinal with aniline crystallize in the 6-s-*trans* conformation. These compounds are therefore better solid state models for the chromophores of the all-*trans* states of bacteriorhodopsin (bR) than the butylimine compounds. We have now extended these studies to the halide salts of the pSB of 13-*cis* retinal with aniline. The ^{13}C-5 chemical shift again indicates a 6-s-*trans* conformation. These compounds are thus good models for the chromophores of the 13-*cis* states of bR. As for the all-*trans* compounds, the 13-*cis* compounds show that the frequencies of maximum visible absorbance and the ^{15}N chemical shifts are linearly related to the strength of the counterion interaction as measured by ($1/d^2$) where d is the center-to-center distance between the pSB charge and the counterion charge. With these calibrations, we estimate values of d for K, L, N and bR_{555} of about 3.99, 3.73, 3.62 and 3.75 Å, respectively. These distances compare with similarly determined values of about 4.15 and 4.66 Å for the all-*trans* bR_{568} and O states, respectively. The results suggest that the H-bonding is stronger in all the 13-*cis* photocycle intermediates, including the red-shifted K intermediate, than in bR_{568}. This is consistent with models of the early photocycle in which electrostatic attractions between the pSB and counterions constitute an important constraint.

W-Pos442

STUDIES OF THE ELECTRIC FIELD-INDUCED CHANGES IN THE OPTICAL PROPERTIES OF BACTERIORHODOPSIN. ((Yuan-chin Ching, Satoshi Takahashi, and Denis L. Rousseau)) AT&T Bell Laboratories, Murray Hill, NJ 07974.

To advance the use of bacteriorhodopsin as a bio-electronic device, it is important to gain an understanding at the molecular level of the relationship between its electrical and optical properties. To determine the influence of an electric field on the optical properties we applied fields of up to ~3x10^7 Volts/cm across polyvinyl alcohol films of bacteriorhodopsin. We measured the difference spectrum generated by the electric field as a function of the degree of hydration. The degree of hydration was established by controlling the atmosphere surrounding the films and its effect on the bacteriorhodopsin was confirmed by monitoring the optical absorption spectrum. Just as in dried films made in the absence of polyvinyl alcohol the maximum in the optical absorption spectrum shifted by over 25 nm to the blue as the relative humidity was reduced to a low level. The electric field-induced optical changes as a function of the film hydration will be reported and mechanism of the changes discussed.

W-Pos443

CHANGE IN CARBOXYL GROUP ENVIRONMENT LINKED TO DEHYDRATION BLUE SHIFT OF BACTERIORHODOPSIN. ((N. Gracia and R. Renthal)) U. of Texas, San Antonio, TX 78249

The bacteriorhodopsin (bR) proton pump contains water-filled channels that connect the purple membrane (PM) surfaces with the protonated retinal Schiff base at the membrane center. The volume of each channel could accomodate 5-10 water molecules, several of which may be tightly bound as part of the Schiff base complex counter ion. The dehydration of PM causes a shift of the 570 nm retinal absorbance maximum to 530 nm, and the blue shift is cooperative with water concentration. Most of the change occurs below 15% relative humidity, in the hydration region where the membrane surface is left with small clusters of water. The 530 nm pigment may result from removal of water from the channels, or it may occur when tightly bound water is removed from the Schiff base. We have now examined dehydrated PM by FTIR difference spectroscopy. In dehydrated minus hydrated PM, a negative band is observed at 1742 cm^{-1} and an equal-sized peak is observed at 1737 cm^{-1}. We measured the magnitude of the FTIR difference between 1737 cm^{-1} and 1742 cm^{-1} as a function of relative humidity between 50% and 4%. The fractional change exactly coincides with the appearance of the 530 nm pigment. This suggests that as a result of dehydration a protonated carboxylic acid group undergoes a change in environment that is linked to the appearance of the 530 nm pigment.

W-Pos444

PHOTOCHEMISTRY OF THE BLUE LIGHT DRIVEN PROTON PUMP BACTERIORHODOPSIN D85X. ((Martin Wahl, Jörg Tittor and Dieter Oesterhelt)) MPI Biochemie, D-82152 Martinsried, Germany

In halorhodopsin (HR), the occurence of proton pump activity in opposite direction of that from BR was shown in a two photon process involving the deprotonated form of the Schiff base in HR called HR410 (1). This finding guided further experimentation with bacteriorhodopsin (BR) mutants lacking asp85. In all these mutants the pK of the Schiff base is lowered to a value around 8.5 and actually proton translocation occured in a one photon driven process starting from the deprotonated Schiff base (2). Therefore the photoreactions occuring in these mutants should provide a base to understand the sequence of events leading to proton translocation. In BR mutants D85N and D85T the reaction cycle initiated by a blue photon is characterized by the sequence of states (numbers represent the absorbance maxima) 410 (hv)-> 430 -> 610 -> 410 with the rate-limiting step at the 610 to 410 transition, i.e. the deprotonation of the Schiff base. In the double mutant D85N96N the reaction from the 430 to 610 state is impaired but can be restored upon addition of azide. Obviously this reaction represents the protonation of the Schiff base which is mediated by D96 or if absent, by azide.

(1) Bamberg et al. 93, *PNAS* 90, 639-643
(2) Tittor et al 94, *Biophys. J.* 67, 1682-1689

W-Pos445

A New Ultrasensitive Nanosecond Linear Dichroism Technique: Application to Early Bacteriorhodopsin Intermediates.

((Raymond M. Esquerra, Diping Che, Daniel B. Shapiro, James W. Lewis, Roberto A. Bogomolni, Jorge Fukushima, and David S. Kliger)) Department of Chemistry and Biochemistry, University of California at Santa Cruz, Santa Cruz, CA 95064.

We introduce a sensitive and simple technique to measure time-resolved linear dichroism. A description of this pseudo-null technique and its sensitivity is presented using Mueller Calculus. The photoselection induced time-resolved linear dichroism of aqueous bacteriorhodopsin in purple membrane across the spectral region of 350 nm to 750 nm is presented. In combination with time-resolved absorption measurements, we determine the reorientation of the chromophore through the temporal range of 50 ns to 100 us. The intermediates corresponding to these times are the K to the early formation of M in the photocycle. An appropriate analysis of the photoselection induced linear dichroism and absorption shows that the anisotropy does not vary throughout the entire spectral region within our resolution limits. This implies that excited chromophores rotate less than 8 degrees with respect to non-excited chromophores during this time span.

W-Pos446

TIME-RESOLVED INFRARED SPECTRA REVEAL PHOTOCYCLE DIFFERENCES BETWEEN HALORHODOPSIN AND THE ACID PURPLE FORM OF BACTERIORHODOPSIN. ((K.G. Victor, Q.M. Mitrovich, and M.S. Braiman)) Biochemistry Dept., Univ. of Virginia Health Sciences Center, Charlottesville, VA 22908. (Spon. by A. Dioumaev)

It has been proposed that at pH 1 bacteriorhodopsin ($bR_{acid\ purple}$) mimics the function of halorhodopsin (hR) by binding halide ions, and possibly also by using light energy to pump them across the membrane. However, measurements of their FTIR difference spectra ~15 ms after photolysis indirectly indicate that these two proteins cannot have identical chloride pumping mechanisms. A positive band at 1753 cm^{-1} and a negative band at 1732 cm^{-1} in the COOH carbonyl region of the $bR_{acid\ purple}$ difference spectrum have no analogs in the hR difference spectrum. These bands are assignable to Asp-85, -96, and -212 based on effects of site-directed mutations to asparagine. Our results demonstrate that Asp-85 and -96 both undergo substantial changes in their hydrogen-bonding environment during the photocycle of $bR_{acid\ purple}$. This is in contrast to the hR chloride pumping cycle, in which neither protonation nor hydrogen bonding changes of carboxylic acid groups play a significant role. Furthermore, the negative and positive bands located at 1692 cm^{-1} and 1682 cm^{-1}, respectively, in the $bR_{acid\ purple}$ difference spectrum are not sensitive to deuterium exchange. These bands, therefore, cannot be due to an arginine residue, as analogous bands are thought to be in hR. We conclude that details of the Cl^- transport mechanism of hR probably cannot be deduced by studying bR at low pH.

W-Pos447

THERMAL EFFECTS IN RESONANCE RAMAN SCATTERING: ANALYSIS OF THE RAMAN INTENSITIES OF RHODOPSIN AND THE TIME-RESOLVED RAMAN SCATTERING OF BACTERIORHODOPSIN. ((Andrew P. Shreve[#] and Richard A. Mathies[+])) [#]CST-4, MS G755, Los Alamos National Laboratory, Los Alamos, NM 87545; [+]Department of Chemistry, University of California, Berkeley, CA 94720.

We model the results of two experiments, the Raman intensity analysis of rhodopsin[1] and transient Raman scattering from bacteriorhodopsin (bR).[2] To illustrate important effects on resonance Raman scattering resulting from the thermalization of strongly displaced vibrations, a model molecule with large electron-phonon coupling (S=2) is first considered. An increase in temperature causes a nearly symmetric broadening of the absorption spectrum, a decrease in Stokes intensities and complex changes in anti-Stokes intensities that depend on wavelength and mode frequency. In rhodopsin, several low-frequency modes are Raman active. Previous modeling[1] used a linear-dissociative potential in the excited electronic state, while here we present a thermalized fully harmonic model. The resulting parameters are used to examine the contribution of low-frequency modes to the Gaussian homogeneous electronic absorption line shape. In bR, transient anti-Stokes experiments show that the chromophore is vibrationally excited after completion of its subpicosecond isomerization. Comparison of the calculated anti-Stokes spectra at various molecular temperatures with the experimental spectra indicates that the vibrational energy distribution in bR is likely non-Boltzmann for the first few picoseconds following excitation, suggesting that vibrational energy redistribution is incomplete on this time scale.

[1] G.R. Loppnow and R.A. Mathies, *Biophys. J.*, **1988**, *54*, 35.

[2] S. Doig, P. Reid and R.A. Mathies, *J. Phys. Chem.*, **1991**, *95*, 6372.

W-Pos448

MEMBRANE LIPID CONTROL OF THE BACTERIORHODOPSIN PHOTOCYCLE: AN FTIR STUDY. ((S.M. Barnett[a], S. Dracheva[b], A. Mukhopdhay[b], R.W. Hendler[b], and I.W. Levin[a])) [a]Laboratory of Chemical Physics, NIDDK, [b]Laboratory of Cell Biology, NHLBI, NIH, Bethesda, Md., 20892-0510.

Exposure of purple membrane (PM) to 0.05% Triton for 2 min destroys the ability of bacteriorhodopsin (BR) to modulate the proportion of M_f to M_s intermediates in response to changing levels of actinic light and alters the decay path of M_f without affecting the BR trimer structure (Mukhopdhay *et al.* (1994) Biochem. 33:10889). FTIR was employed to detect subtle changes in lipid-BR interactions and/or BR conformation. Distinct differences in the vibrational spectrum of BR were detected after this Triton treatment. Difference spectra between native and Triton-treated PM were correlated with the spectra of individual lipids extracted from PM. It appears that the lipids most affected are squalene and glycolipid sulfate. A small amount of phospholipid was also perturbed. Concurrent with these changes, an alteration of BR conformation was seen. A parallel study employing lipid analytical chemistry and TLC chromatography correlates with the FTIR results (Dracheva and Hendler poster, this session).

W-Pos449

MEMBRANE LIPID CONTROL OF THE BACTERIORHODOPSIN PHOTOCYCLE: A CHEMICAL STUDY. ((S. Dracheva, and R. W. Hendler)) Laboratory of Cell Biology, NHLBI, NIH, Bethesda, MD 20892-0301. (Spon. by P. D. Smith)

Exposure of purple membrane (PM) to 0.05% Triton for 2 min destroys the ability of bacteriorhodopsin (BR) to modulate the proportion of M_f and M_s intermediates in response to changing levels of actinic light and alters the decay path of M_f without affecting the BR trimer structure (Mukhopdhay et al. (1994) Biochem. 33:10889). Purple membrane (PM) lipids contain approximately by weight 5% squalenes, 62% phospholipids (PG, PGP, and PGS), and 30% glycolipids (glycolipid sulfate and triglycosyl diether), in addition to retinal and vitamin MK-8. We have determined time courses for release of the various lipid classes during exposure to 0.1% Triton using quantitative analytical techniques for unsaturation, carbohydrates, phosphorous, and sulfate, combined with silica TLC chromatography. The lipids most susceptible to removal are squalene and glycolipid sulfate (and possibly PGS). These findings correlate well with a parallel FTIR study (Barnett et al. Poster, this session).

W-Pos450

ON THE ABILITY OF ACTINIC LIGHT TO MODIFY THE BACTERIORHODOPSIN PHOTOCYCLE: HETEROGENEITY AND/OR PHOTOCOOPERATIVITY? ((R. I. Shrager[a], R. W. Hendler[b], and S. Bose[b])) [a]Laboratory of Applied Studies, DCRT, [b]Laboratory of Cell Biology, NHLBI, NIH, Bethesda, MD 20892-0301. (Spon. by M. R. Bunow)

The bacteriorhodopsin (BR) photocycle responds to actinic light by altering proportions of fast M (M_f) which decays through O, and slow M (M_s) which does not. Several cooperative models (Ohno's, Tokaji's, and Shrager's), one noncooperative, heterogeneous (Hendler's), and a mixed cooperative, heterogeneous model were tested with actual experimental data. The Ohno and Tokaji models could not account for the data but the Shrager, Hendler, and mixed models could. Although models which can not account for the BR response to light, must be altered or eliminated, it is demonstrated that the real explanation for the phenomenon can not be determined by modeling alone. Based on the facts that BR photocycles are in fact heterogeneous (Eisfeld et al., (1993) Biochem. 32: 7196) and that BR exists in a highly regular trimer structure, suggestive of cooperativity, we believe that a mixed heterogeneous, cooperative model is most probable.

W-Pos451

Over-expression of a new halorhodopsin in a photo-active state. ((Jun Otomo)) PRESTO, JRDC and Advanced Research Laboratory, Hitachi, Ltd., Hatoyama, Saitama 350-03, Japan.

A new haloopsin gene from a new halobacterial strain shark was cloned and its nucleotide sequence was determined. The deduced amino acid sequence showed that three amino acid residues (Arg-52, Arg-58, His-95; numbering as in halobium HR) in A-B and B-C interhelical loop segments were conserved. A shark haloopsin gene was over-expressed in *Halobacterium salinarium* (*halobium*) by using a halobacterial transformation system. The anion pumping activity of shark halorhodopsin expressed in *H. salinalium* was almost the same as that for halobium halorhodopsin. However, its anion selectivity was different from that for halobium halorhodopsin. Furthermore, its absorption maximum in the absence of chloride was shifted to around 600nm in contrast to that for halobium halorhodopsin. Several charged residues were different in A-B and B-C interhelical loop segments between shark halorhodopsin and halobium halorhodopsin, showing that these residues probably affect the anion binding site around the retinal Schiff base.

W-Pos452

ROLE OF ARGININE-134 IN BACTERIORHODOPSIN: EFFECTS ON PURPLE MEMBRANE RECONSTITUTION ((Y. Feng, N. Chen, E.S. Hazard, S. Misra, T.G. Ebrey, D.R. Menick, and R.K. Crouch)), Medical University of South Carolina, Charleston, SC 29425 and University of Illinois, Urbana, IL 61801

The homologous expression of mutant bacteriorhodopsin (bR) in *H. salinarium* has been utilized to examine the role of arginine-134. Visible absorption was not observed for the Arg134Ala and Arg134Gln bR mutants, even in the presence of exogenous *all-trans* retinal, although the protein is present in the membrane. These membranes were termed "white membranes". For Arg134Lys, both purple and white membranes were obtained. The Arg134Lys purple membrane has photocycling and proton pumping functions which suggest Asp85 has moved slightly closer to the Schiff base and that there may be a slight decoupling of the proton release components. Western analysis of the white membranes of all three mutants showed a significant decrease in the ratio between folded bR in the membrane to unfolded bR in the cytoplasm. Circular dichroism showed that the mean residue molar ellipticities of three mutants at 208 nm and 222 nm were much smaller than for wild type, indicating a decrease in the transmembrane α-helix. The distribution of Arg134Ala, Arg134Gln, and Arg134Lys across the sucrose gradient was more diffuse than for wild-type, implying a decrease of mutant in the membrane. We conclude that arginine-134 plays an important role on stabilizing the structure of the transmembrane α-helices in bR which is critical to retinal assembly. Sponsored by NIH (EY04939), DOE (DE-7002-88 13948) and Res. to Prevent Blindness.

W-Pos453

ASP-46 CAN SUBSTITUTE FOR ASP-96 AS THE PROTON DONOR FOR THE SCHIFF BASE IN THE M→N TRANSITION OF BACTERIORHODOPSIN. ((M. Coleman, A. Nilsson, P. Rath, T. S. Russell, S. Ali, R. Pandey, K.J. Rothschild)) Physics Department and Molecular Biophysics Laboratory, Boston University, Boston, MA 02215

The double-mutant Thr-46→Asp/Asp-96→Asn (T46D/D96N) was expressed in *Halobacterium salinarium* (strain MPK40). Time-resolved visible absorption spectroscopy reveals that T46D/D96N exhibits an M decay at pH 7 close to wild-type. In contrast, the single mutant Asp-96→Asn (D96N) exhibits a very slow M decay under identical conditions. However, the overall photocycle of this mutant is significantly slower than wild-type due to the presence of a slowly decaying species. Resonance Raman spectroscopy shows that this species has an N-like chromophore structure. The bR→N FTIR difference spectrum of T46D/D96N exhibits a new negative band at 1716 cm^{-1} in the carboxylic acid C=O stretch region. These data indicate that Asp-46 can substitute for Asp-96 as the donor group in the reprotonation of the Schiff base during the M→N transition. In addition, the slow N decay of this mutant may be explained by a decrease in the reprotonation rate of this group from the cytoplasmic medium.

W-Pos454

pK_a OF ASP85 IS HIGHER IN TRANS- THAN IN 13-CIS-BACTERIORHODOPSIN ((S. P. Balashov, R. Govindjee, E.S. Imasheva, M. Sheves*, and T.G. Ebrey)) Center for Biophysics and Dep. of Cell and Struct. Biol., UIUC, Urbana, IL 61801 and *Dep. of Org. Chem., Weizmann Inst. of Science, Rehovot, 76100, Israel

Light adaptation of purple membrane with 400-550 nm light at pHs between 4 and 2 causes an increase in the fraction of the blue membrane. We suggest that trans-bR has slightly higher pK_a of the purple-to-blue transition (a higher pK_a of Asp85) than 13-cis-bR and that the light-induced purple-to-blue transition occurs in two steps: i) 13-cis-bR-purple is phototransformed into trans-bR-purple and ii) the latter converts into blue-bR. The pK_a of purple-to-blue transition in the dark (pK_a=2.6) is approx. 0.3 pH unit lower than that in the light (pK_a = 2.9 in 150 mM KCl). We suggest that the latter value is close to the pK_a of Asp85 in trans-bR. To estimate the pK_a of Asp85 in 13-cis-bR we developed a model which describes the pH dependencies of equilibrium fractions of the blue and purple forms of trans and 13-cis-bR and the fraction of the light-induced blue membrane. The model is based on the assumption that thermal 13-cis<=>trans isomerization occurs in the blue membrane (upon transient protonation of Asp85) rather than in the purple membrane. From the fit of the experimental and published data we determine that the pK_a of Asp85 in 13-cis-bR is about 0.6 pH unit less than that in trans-bR, and that the rate constant of isomerization of 13-cis-bR in the blue membrane is ca. 2.8 times larger than that of the trans-bR. In agreement with this estimate the pK_a of the purple to blue transition in 13-desmethyl-bR (which contains 85%13-cis-isomer and 15% trans-isomer) is 0.2 pH units lower than in the native dark adapted bR.

W-Pos455

TWO pKs OF ASP85 IN BACTERIORHODOPSIN (bR): IMPLICATIONS ON CATALYSIS OF PROTON RELEASE AND CHROMOPHORE ISOMERIZATION ((S.P. Balashov, E.S. Imasheva, R. Govindjee, T.G. Ebrey, Y. Feng*, R.K. Crouch* and D.R. Menick*)) Center for Biophysics and Dept. of Cell and Struct. Biology, UIUC, Urbana, IL 61801, and * Med. Univ. of S. Carolina, Charleston, SC 29425.

Asp85, the proton acceptor and a part of the counterion to the Schiff base in bR, is deprotonated in the purple membrane and becomes protonated upon decreasing the pH and forming the blue membrane. We have recently proposed that the pK_a of Asp85 depends on the state of an unidentified residue X'; deprotonation of X' (pK 9.6 in 150 mM KCl) causes an increase in the pK_a of D85 by several pH units (Balashov et al., *Biochemistry 32*, 10331, 1993). This hypothesis predicts that D85 has a complex titration curve. In order to test this we determined spectroscopically the fraction of blue membrane (and thus the fraction of protonated Asp85) in the R82K mutant of bR over a wide pH range (from 2 to 9). R82K mutant was used since the blue membrane is easier to detect at high pH in this mutant partially because the pK_as of Asp85 and X' are closer in R82K than in the wild type (3.5 and 8.0 in R82K versus 2.6 and 9.6 in the WT). We find that the fraction of protonated Asp85 as a function of pH in dark adapted R82K has two inflection points, 3.5 and 8.0. The fit of the experimental curve with the D85/X' model indicates that deprotonation of residue X' causes a shift in the pK of D85 from 3.5 to 6.1. Conversely protonation of D85 decreases the pK of residue X' by about 2.2 units in R82K. We suggest that Arg82 in the wild type bR and Lys82 in R82K is a likely candidate for the residue X' and that it can act as a part of the proton release complex in the photocycle. We also find that the rate constant of thermal isomerization of the chromophore (dark adaptation) is directly proportional to the fraction of protonated D85 in R82K which proves that isomerization proceeds through the transient protonation of D85.

W-Pos456

EFFECTS OF STERIC CONSTRAINTS AND PROTEIN DYNAMICS ON PHOTO-ISOMERIZATION YIELD OF RETINAL IN RHODOPSIN. ((A. Xie, M. L. Weber, Q. He, R. B. Needleman[1], M. R. Chance)). Dept. of Physiology & Biophysics, Albert Einstein College of Medicine, Bronx, NY 10461. [1]Dept. of Biochemistry, Wayne State University, Detroit, MI 48201.

Steric constraints and protein dynamics are two of the key elements regulating protein reactivity. We investigate how these two elements are coupled and influence the photo-isomerization yield of retinal in rhodopsins. In particular, why the photo-product yields (80 - 300 K) of sensory rhodopsin I, like bacteriorhodopsin (BR) and rhodopsisn, is high and independent of temperature above 220 K, but reduces dramatically below 220 K [1]? We assume that (1) strong steric constraints on retinal binding will prevent retinal from photo-isomerization; (2) freezing of protein motions will enforce such steric constraints. To test our hypothesis, we have designed and selected BR mutants and analogs that induce strong steric constraints (by virtue of a bulkier group) in retinal-protein interactions, namely L93F and M145H mutants, and the 13-ethyl-BR analog. The photo-product yield of L93F mutant at 80 K is found to be only half as much as that of BR. We are examing the temperature dependence of photo-product yield of L93F, M145H, 13-ethyl-BR and wild type halorhodopsin, so as to elucidate relations between quantum yield reduction and freezing of protein motions.

1. Yan, B., A. Xie, G. U. Nienhaus, Y. Katsuta, and J. L. Spudich. Steric constraints in the retinal binding pocket of sensory rhodopsin. 1993. *Biochemistry*, **32**: 10224-10232.

W-Pos457

13-ACETOXY-13-DESMETHYLRETINAL: SYNTHESIS, INCORPORATION INTO BACTERIORHODOPSIN, AND ITS APPARENT DARK-INHIBITORY EFFECT ON THE PIGMENT.
((S. Seltzer)) Chemistry Department, Brookhaven National Laboratory, Upton, NY 11973

The title compound (**1**), was designed to test for the involvement of nucleophilic catalysis, presumably by asp-212, in the dark cis-trans isomerization of retinal in bacteriorhodopsin (bR). ß-Ionylidenacetaldehyde (**3**) was condensed with acetylacetaldehyde dimethyl acetal to form 1,1-dimethoxy-7-methyl-9-(2',6',6'-trimethyl-1-cyclohexen-1-yl)-4E,6E,8E-nonatrien-3-one (**4**). Treatment of **4** with base followed by acetic anhydride and 4-(dimethylamino)-pyridine furnished 13-acetoxy-13-desmethylretinal dimethyl acetal (**5**) which upon controlled acid-catalyzed hydrolysis yielded **1**. 13-*cis*-**1** forms a pigment (13-Ac-bR) in the dark with bacterioopsin which initially absorbs at 559 but within an hour moves to 573 nm. Added *all-trans*-retinal slowly replaces **1** in 13-Ac-bR to form bR^{DA}. In the absence of light 13-Ac-bR slowly loses its 573 absorption and in place develops absorption at 406 nm signaling an alteration in the chromophore's binding to the protein. After a substantial drop in the 573 nm absorption the analogue can not be removed from the protein by the standard ethanol-delipidation method which otherwise removes retinal from bR or retinal oxime from bleached membrane. [Research funded by the Department of Energy and supported by its Division of Chemical Sciences, Office of Basic Energy Sciences, contract DE-AC02-76CH00016.]

W-Pos458

BINDING OF EXTERNAL CHLORIDE TO HALORHODOPSIN INDUCES AN ARGININE STRUCTURAL PERTURBATION DETECTABLE WITH INFRARED SPECTROSCOPY.
((J.R. Lewis and M.S. Braiman)) Biochemistry Department, University of Virginia Health Sciences Center, Charlottesville, VA 22908.

To characterize structural changes of halorhodopsin (hR) occurring when it binds Cl^-, ligand-induced IR difference spectroscopy was performed using a flow-through attenuated total reflection (ATR) cell with hR membranes adsorbed on the Ge prism surface. In ^2H_2O at constant ionic strength and p^2H=7.4, we observed Cl^--induced difference bands at ~1602 and ~1585 cm^{-1}. These bands are not observed in similar Cl^--titration spectra of bacteriorhodopsin, which transports H^+ rather than Cl^- ions. The Cl^--induced positive difference peaks of hR at 1606 and 1590 cm^{-1} match negative difference peaks observed previously in the hR→hL photolysis difference spectrum. They also correspond to known guanidino C-N stretch vibrations observed for arginine-HCl in ^2H_2O, and for ethylguanidinium chloride in deuterated organic solvent. The Cl^--induced difference bands of hR at ~1602 and ~1585 cm^{-1} are thus likely due to arginine(s) in the halide binding pocket. Cl^--titration-induced FTIR difference spectra may provide a general method for identifying chloride-arginine interactions in anion transport proteins. *Supported by NIH Grant GM46851.*

W-Pos459

THE PHOTORECEPTOR SENSORY RHODOPSIN I IS A TWO-PHOTON-DRIVEN PROTON PUMP ((Ulrich Haupts, Christina Haupts and Dieter Oesterhelt)) Max-Planck-Institut f. Biochemie, D-82152 München).

Proton translocation experiments with intact cells of *Halobacterium salinarium* overproducing sensory rhodopsinI (SRI) revealed transport activity of SRI in a two photon process. The vectoriality of proton translocation depends on pH, being outwardly directed above and inwardly directed below pH 5.7. Activation of the transport cycle requires excitation of the initial dark state of SRI, SRI_{590}, to form the intermediate SRI_{380}. Action spectra identify the photocycle intermediates SRI_{380} and SRI_{520} as the two photochemically reactive species in the outwardly directed transport process. As shown by flash photolysis experiments, SRI_{520} undergoes a so far unknown photochemical reaction to SRI_{380} with a half-time smaller than 200 µs. Mutation of aspartic acid 76 to asparagine in SRI, the residue which is equivalent to the proton acceptor D85 in bacteriorhodopsin, leads to inactivation of proton translocation. This demonstrates that the underlying mechanisms of proton transport in both retinal proteins share similar features. However, SRI is the first case where photochemical reactions between two thermally instable photoproducts of a retinal protein constitute a catalytic ion transport cycle.

W-Pos460

THE NATURE OF THE J INTERMEDIATE IN BACTERIOHODOPSIN'S PHOTOCYCLE ((D. Xu and K. Schulten)) Beckman Institute, UIUC, Urbana, IL 61801.

Molecular dynamics simulations have been carried out to study the J intermediate of bacteriorhodopisn's (bR's) photocycle. Starting from a refined structure of bR_{568} (Humphrey et. al., Biochemistry, 33:3668, 1994), retinal was assigned, for 250 fs, a charge distribution which corresponds to that of its excited state, and afterwards, was reassigned the ground state charge distribution. During the first 250 fs the protein responded through a strong polarization which reversed again. However, the reversal involves an "overshooting" such that at about 500 fs a polarization opposite to the direction of the dipole moment induced by the photoexcitation results, the polarization decaying with an approximate time of 150 fs. The polarization induces a bathochromic shift which shifts the spectrum of retinal by 32 nm, a value which is close to the spectral shift of 35 nm observed for the J intermediate. Accordingly, we suggest that the J intermediate is due to an intermediate polarization of bR.

W-Pos461

THE NATURE OF THE M INTERMEDIATE IN BACTERIOHODOPSIN AS REVEALED BY MOLECULAR SIMULATION ((D. Xu, M. Sheves and K. Schulten)) Beckman Institute, UIUC, Urbana, IL 61801.

Molecular dynamics simulations have been carried out to study the M intermediate of bacteriorhodopsin's (bR's) photocycle. Starting from a refined structure of bR_{568} (Humphrey et. al., Biochemistry, 33:3668, 1994), the all-trans to 13-cis photo isomerization process and K intermediates were modelled. A simulated annealing protocol exployed to reach L and M. Our simulations revealed that the M intermediate implies a sequence of states connected with protein conformational change as well as diffusion of water into bR and reconfiguration of water hydrogen bonding. Retinal's Schiff base becomes disconnected from Asp-85. An F helix tilt allows two water molecules to diffuse into the space between the Schiff base and Asp-96, and together with three water molecules in that space in bR_{568} to form a water chain. Accordingly M acts as a proton switch which connects retinal to Asp-96. The simulated conformational change of the protein involves a 60° bent of the cytoplasmic side of helix F as observed similarly by (Subramanian et. al., EMBO J., 12:1, 1993). The bent is due to a break of hydrogen bonding between Tyr-185 and Asp-212. The helix bent is reversed already during M stage.

W-Pos462

3-D DIFFERENCE MAP OF THE M-INTERMEDIATE IN THE BACTERIORHODOPSIN PHOTOCYCLE ((Janet Vonck, Bong-Gyoon Han, Robert M. Glaeser)) Life Sciences Division, Lawrence Berkeley Laboratory, University of California, Berkeley, CA 94720.

In the bacteriorhodopsin photocycle, the M-intermediate plays a key role in the proton pumping process. There is much evidence suggesting that a protein conformational change takes place during the lifetime of M, which closes access from the extracellular side to the Schiff base and opens access to the cytoplasmic side, thus ensuring directionality of proton pumping. Distinct changes in the projection structure of the protein between the ground state and the M substates have been shown by several diffraction techniques. We have extended these studies to three dimensions using electron diffraction of glucose-embedded purple membrane in the ground state and the M intermediate, trapped at low temperature. Recent progress in preparing flat specimens for electron microscopy has considerably improved the success rate of the collection of data from tilted specimens. A preliminary M-bR difference map from specimens tilted up to 30° shows that no major tilting or shifting of α-helices occurs, but instead there are small differences all over the protein, not limited to the vicinity of the Schiff base. Due to the low vertical resolution the differences cannot be assigned to specific amino acid residues yet. Work on a higher resolution map is in progress.
Supported by NIH grant GM51487.

W-Pos463

DIVERGENCE OF HALOBACTERIAL RHODOPSINS IS GENERA SPECIFIC ((Y. Mukohata, T. Tamura and K. Ihara)) Department of Biology, School of Science, Nagoya University, Nagoya, Japan 464-01

Bacteriorhodopsin (bR), halorhodopsin (hR), sensory rhodopsin (sR) and phoborhodopsin (pR) are a set of four retinal proteins of the bR family which has been found in *Halobacterium salinarium* (*halobium*).

Research spurred by the second proton pump archaerhodopsin-1 (aR-1)* in a new isolate (now *Halorubra stoeckenii*) brought about more than 20 new amino acid sequences. They are classified into four homolog groups of bR, hR, sR and pR. One each of these four exists (typically) in one species (e.g., cR-3, chR-3, csR-3 and v-pR in *Haloarcula vallismortis*), and forms a (cR-3) family. Members of each homolog group are further grouped into four tribes (aR, bR, cR and *nab*) by homology indices. Those homolog members within a tribe (e.g., aR-1, aR-2 and aR-3; proton pumps in families of the aR tribe) are highly homologous (75-95%) with each other.

Relatedness of rhodopsins was analyzed by the N-J method and a phylogenetic tree was constructed. The tree branched first into four homolog groups, and then each homolog branched into tribes and families. The branching pattern of proton pumps was well corresponded with that of anion pumps, and also with sensors.

The DNA sequences encoding 16SrRNA of these new rhodopsin-carrying strains were also analyzed to construct another phylogenetic tree. Branching of genera and species in this tree of *Halobacteriaceae* was again well corresponded with the branching of tribes and families of each rhodopsin homologs.

Those results suggest that a set of four rhodopsin homologs in primeval forms had existed when ancestry halobacteria diverged into genera, and then species. The rhodopsin tribes/families thus diverged in a manner specific to each genus.

* Mukohata, Y. *et al.*, presented at the 32nd Annual Meeting. *Biophys. J.*, 53, 376a (1988).

FOLDING—ASSEMBLY II

W-Pos464

PHYSICO-CHEMICAL STUDIES OF THE $D(G_3T_4G_3)*D(G_3A_4G_3)*D(C_3T_4C_3)$ TRIPLEX AND ITS STABILIZATION ON DRUG BINDING ((P. V. Scaria[1], Stephen Will[2], Corey Levenson[2] and Richard H. Shafer[1])) [1]Dept. Pharmaceutical Chemistry, Univ. California, San Francisco, CA 94143 and [2]Rosche Molecular Systems, 1145 Atlantic Avenue, Alameda, CA 94501

We have targeted the $d(G_3A_4G_3)*d(C_3T_4C_3)$ duplex for triplex formation with $d(G_3T_4G_3)$ in the presence of $MgCl_2$. The resulting triple helix, $d(G_3T_4G_3)*d(G_3A_4G_3)*d(C_3T_4C_3)$ is considerably weaker than the related triplex, $d(G_3A_4G_3)*d(G_3A_4G_3)*d(C_3T_4C_3)$, and melts in biphasic manner, with the third strand dissociating at temperatures about 20 - 30°C below that of the remaining duplex. This is in distinct contrast to the $d(G_3A_4G_3)*d(G_3A_4G_3)*d(C_3T_4C_3)$ triplex which melts in essentially a single transition. Gel electrophoresis under non-denaturing conditions shows the presence of $d(G_3T_4G_3)*d(G_3A_4G_3)*d(C_3T_4C_3)$ triplex as a band of low mobility compared to the duplex or single strand bands. Binding of the $d(G_3T_4G_3)$ third strand and the purine strand of the duplex can be monitored by imino proton NMR spectra. Differential scanning calorimetric studies show that this triplex is considerably less stable than the triplexes formed by the binding of all purine or all pyrimidine third strand to the duplex, $d(G_3A_4G_3)*d(C_3T_4C_3)$. Fluorescence energy transfer experiments combined with UV melting studies using labeled oligonucleotides suggest that the preferred orientation of the third strand is parallel to the purine strand of the duplex. Intercalating agents like ethidium bromide and daunomycin seems to preferentially stabilize the third strand binding.

W-Pos465

DNA MESOPHASES: CHOLESTERIC - HEXAGONAL TRANSITION. ((R. Podgornik, H.H. Strey, D.C. Rau, K. Gawrisch, A. Rupprecht and V.A. Parsegian)) LSB/DCRT, NIH, Bethesda, MD 20892 and Stockholm University, Physical Chemistry, Sweden.

Osmotic stress has been used to probe the cholesteric - hexagonal transition in long ($\cong \mu m$) oriented wet-spun DNA as well as in unoriented DNA fragments. The transition can be detected through the form of the dependence of the osmotic pressure on the interhelical separation as well as through the behavior of the bond-orientational order parameter in the hexagonal phase, the lineshape of the ^{31}P NMR spectra or the parameters characterising the cholesteric texture between crossed polarizers. We present quantitative data for the behavior of each of these characteristics close to the transition point in 0.5 M NaCl. This is the first systematic measurement of the free energy close to the hexagonal-cholesteric phase transition as the available data from the literature always deal with gravimetrically prepared samples at unknown water and salt activities. It appears that the cholesteric-hexagonal transition is either second-order or weakly first order. In view of this finding we discuss the possibility that the cholesteric-hexagonal transition is accomplished through an intermediate hexatic phase with no long range positional order. We also present data on the dependence of this transition on ionic strength, a dependence that appears to play a role analogous to temperature for thermotropic liquid crystals. We suggest that the osmotic stress technique can be used to the same advantage to investigate the phase diagram of long polyelectrolytes in aqueous solutions as it has been used with lipid or surfactant mesophases.

W-Pos466

CHEMICAL FUNCTIONALITY MODULATES OSMOTIC PRESSURE DEPENDENCE OF THE B-TO-Z TRANSITION IN DNA.
((Y. Choe, S. Kim, B.J. Short, Jr., and R.S. Preisler)) Dept. of Chemistry, Towson State Univ., Towson, MD 21204.

Our laboratory, along with Rau and Chen at NIH, have observed a B-to-Z transition at high osmotic pressures generated by neutral polar solutes. In a series of hydroxylic compounds with one carbon per hydroxyl, the larger solutes drove the transition at lower osmotic pressure, suggesting that they were more highly excluded from the DNA hydration layer. We have now compared the osmotic effects of alcohols and diols with larger C/OH ratios. The larger the ratio, the lower the osmotic pressure required to stabilize the Z-DNA conformer of poly[d(G-m^{5}C)]. The observed trend could imply either that -CH is more strongly excluded than -OH from the DNA hydration layer or that solute hydrophobicity is a factor in addition to osmotic pressure. The latter notion receives support from studies on the ability of various neutral polar compounds to solubilize the somewhat hydrophobic guanosine nucleoside. The higher the C/OH ratio, the greater the solubility of guanosine at constant osmotic pressure. This system models one aspect of the B-to-Z transition, because guanine bases are more exposed to solvent in Z-DNA than in B-DNA. Supported by a Student Research Grant to BJS and an Industrial Academic Partnership Board Research Award to YC (Towson State Univ.).

W-Pos467

STUDIES OF SEQUENCE-DEPENDENT TERTIARY STRUCTURE IN SUPERCOILED DNA BY SITE-SPECIFIC RECOMBINATION. ((H. Tsen and S.D. Levene)) Program in Molecular and Cell Biology, University of Texas at Dallas, P.O. Box 830688, Richardson, TX 75083.

Site synapsis in DNA, the close juxtaposition of DNA sequences required in interactions involving DNA-binding proteins bound to multiple sites, is an essential event in many cellular processes such as DNA replication, transcription, and recombination. The synapsis of protein-binding sites located along the contour of a single DNA molecule requires that the intervening DNA segment form a loop, an unfavorable DNA conformation that is strongly influenced by the molecule's tertiary structure. The required tertiary structure for site synapsis is frequently supplied by DNA supercoiling. In some important cases supercoiling alone is not sufficient, but DNA sequence elements that impart net curvature to the axis of the double helix are also required. An important role of intrinsically bent DNA may be to facilitate site synapsis near the terminal loop of a superhelical DNA molecule.

We have used site-specific recombination carried out by the Integrase (int) system of bacteriophage λ to study the effects of intrinsically bent DNA sequences on the tertiary structure of supercoiled DNA. Substrate DNA molecules bearing the λ attachment sites *att P* and *att B* symmetrically arranged about oligo (dA) - oligo (dT)-containing DNA segments were constructed and the distributions of topological forms generated by intramolecular, site-specific int recombination were analyzed. Distributions of knotted and catenated forms were obtained by using substrates with inversely and directly repeated *att* sites, respectively. The attachment sites divide the contour of a DNA ring into two domains and the topological distribution of recombination products is a function of the number of interdomainal superhelical turns trapped at site synapsis. Localizing of the bent region at superhelix ends reduces the overall complexity of knotted or catenated products obtained with these substrates by biasing the distribution of interdomainal superhelical turns. We studied the distribution of knotted and catenated recombination products as a function of the extent of bending, which was systematically varied over the range from approximately 0° to 180°.

W-Pos468

STRUCTURE CHARACTERIZATION OF MODEL MEMBRANE BOUND AND SOLID SURFACE ADSORBED SELENOMETHIONINE-LABELED BOVINE PANCREATIC PHOSPHOLIPASE A_2 USING X-RAY STANDING WAVES ((J. Ahn, J. Wang, S. Kirchner, Z. Yin, M. Caffrey)) Chemistry Dept., The Ohio State University, Columbus, OH 43210.

X-ray standing waves (XSW) have been used to study the topology of selenomethionine-labeled phospholipase A_2 (Se-Met^8-PLA2) adsorbed on a silver mirror surface and bound to a negatively charged model membrane. The data suggest that the Se-Met^8-PLA2 adopts a non-native conformation on the bare silver mirror since the selenium atom resides directly on the mirror surface (mean position of selenium layer, $\mu = 0.5$ Å, half width at half-height, $\sigma = 0.5$ Å). In sharp contrast, Se-Met^8-PLA2 appears to maintains its native structure at the surface of a self-assembled monolayer (SAM) of ω-thiolundecanoic acid on silver. In this case, the selenium is located 21.5 Å (SAM accounts for 12 Å of this 21.5 Å based on ellipsometry measurements) above the silver mirror surface with an associated spread (σ) of 9 Å. The surface density of selenium in the case of the PLA2/silver sample is 6-times higher than that of the PLA2/SAM/silver sample corroborating the view that the enzyme interacts very differently with the two surfaces.

Supported by NIH DK 45295

Acknowledgements: We thank Dr. M. Gelb (University of Washington, Seattle, WA) for providing the ω-thiolundecanoic acid used in this project.

W-Pos469

CARRAGEENAN CONFORMATION FROM OPTICAL ROTATION AND CIRCULAR DICHROISM. ((S. E. Schafer and E. S. Stevens)) Department of Chemistry, SUNY, Binghamton, Binghamton, NY 13902.

Carrageenan is a family of water soluble galactans extracted from marine red algae. Their ability to form aqueous gels has given them substantial commercial importance. In the case of ι-carrageenan, the strong x-ray diffraction evidence for the existence of right-handed double helices in the solid state has led to a double-helix model for the microstructure of the gel. Earlier analysis, by Rees and coworkers, of the optical rotation changes observed during the gel-sol transition supported the notion of solid-gel conformational equivalence. We have applied a more recent method of analyzing optical rotation, less empirical than the previous one, and confirm the likelihood that the chain conformation found in the solid state also predominates in the gel. In addition, the previously reported CD of carrageenans in the 140-190 nm region is interpreted with the help of a newly proposed saccharide sector rule. The analysis indicates that the CD of dried gels contains a positive CD linkage contribution, as predicted for the helical conformation found by x-ray diffraction.

W-Pos470

BACTERIAL LIPOPOLYSACCHARIDE CONFORMATION: LOCALIZATION OF FLUORESCENT PROBES BY FLUORESCENCE RESONANCE ENERGY TRANSFER. ((C. Aurell Wiström*, G.M. Jones¶, P.S. Tobias§ and L.A. Sklar*¶)). *LS-NFCR, LANL, Los Alamos, NM 87545, §Immunology, TSRI, La Jolla, CA 92037, ¶Cytometry, UNM, Albuquerque, NM 87131, USA.

Bacterial endotoxins or lipopolysaccharides (LPS) a cell wall component of gram negative bacteria are known for their involvement in septic shock. Eventhough the chemical structure of LPS is known for many bacterial strains the supramolecular structure of LPS fragments in the blood stream is still unknown. Fluorescence resonance energy transfer (FRET) was used to study the organization of fluorescein isothiocyanate labeled LPS (FITC-LPS) as donor (D) from different strains in a sulfobetaine palmitate micelle system. Acceptor (A) probes were two amphiphilic molecules 1, 1-dilinoleyl- 3,3,3',3'tetramethyl indocarbocyanine perchlorate, "C18-DiI" and octadecyl B rhodamine chloride (C18-Rhd). The Förster transfer distance, R_0 was calculated from first principles for the D-A pairs, FITC-LPS to C18-DiI, R_0 = 68Å and FITC-LPS to C18-Rhd, R_0 = 58Å solubilized in micelles. Energy transfer efficiency, T , of FITC-LPS from S.minn. Re 595 (MW 2500) in the presence of 1 C18-DiI per micelle as A was 66 % compared to LPS isolated from S.minn. (MW 20K) 13 %. Upon addition of the C18-Rhd as A, the T of D fluorescence was slightly less. Distance of closest approach of different FITC-LPS and A probes indicate that short LPS (S.minn. Re 595) all chain must be in close to micelle surface, for larger LPS some FITC are at distances approaching 1.5 R_0 and farther from micelle surface. Data suggest that LPS with different polysaccharide lengths may have several FITC derivarization sites along the O-antigen chain. Supported by NIH grants to L.S. and P.T. (GM 37696), Los Alamos NFCR (P41-RR01315, LDRD X195) Cancer Research and Treatment center, UNMSOM.

W-Pos471

A MULTI-STATE MODEL FOR THE MAIN PHASE TRANSITION OF PURE LIPID BILAYERS

Morten Nielsen,[1] Ling Miao,[1] John H. Ipsen,[2] Ole G. Mouritsen,[2] and Martin J. Zuckermann,[1]

[1]McGill University, Montreal, PQ, H3A 2T8, Canada; [2]The Technical University of Denmark, Building 206, DK-2800 Lyngby, Denmark

A statistical mechanical multi-state lattice model is used to describe the main phase transition of pure phospholipid bilayers. The states represent *trans-gauche* isomeric conformations of the lipid chains and the paramenters of the model of Tevlin et al. are used for the degeneracy, the length, the cross sectional area, the NMR order parameter and the internal energy of each conformation. The Van der Waals interactions between neighbouring chains in different conformations are calculated using the Pink model and a hydrophobic mismatch interaction between selected neghboring conformations is imposed. Finally an elastic interaction between polar heads is treated via a quadratic term in the cross-sectional area of the lipid chains. The model is investigated by computer-simulation techniques which fully allow for thermal density fluctuations and which operate on a free-energy level and hence permit an accurate identification of the phase transition and the related physical properties such as the lateral compressibility, specific heat and NMR order parameter. The model is initially simulated on a triangular lattice of lipid chains. However as this does not treat the fluid nature of the liquid crystalline phase of a lipid bilayer properly, the use of a two-dimensional dynamically triangulated network in conjuction with this model is discussed.

W-Pos472

SURFACE AREA OF NONIONIC DETERGENTS IN LIPID MEMBRANES ((G. Lantzsch, H. Binder, H. Heerklotz)) Universität Leipzig, EXPI/BIM, Linnéstr. 5, D-04277 Leipzig, Germany

The surface area occupied by nonionic detergents of the type $C_{12}EO_n$ (n = 1-8) in a POPC membrane was studied by time resolved fluorescence resonance energy transfer between the two probe molecules NBD-PE and Rhodamine-PE.
For n = 1-3, the membrane surface was found to expand by 0,25 - 0,30 nm^2 per incorporated $C_{12}EO_n$ molecule. This value corresponds to the cross-section of one hydrocarbon chain in liquid-cristalline phases.
On increasing n from n = 4 to n = 8 the net area per molecule increases from 0,42 nm^2 to 1,16 nm^2. These results can be explained by a compact conformation of the EO-chains hydrated with about two water molecules per EO-unit. Thus a with n increasing conical shape of the detergent molecules is suggested in terms of the Israelachvili concept of packing constraints. Consistently, DPH time resolved anisotropy indicate that the long chain detergents destabilize the alkyl-chain region, whereas the anisotropy of the NBD, localized in the headgroup region, remains constant.
The saturation mole fraction of each detergent within the membrane is deduced on the basis of an „effective" packing parameter .

W-Pos473

THE EFFECTS OF CHOLESTEROL ON GEL PHASE CONTENT IN GEL-FLUID MIXTURES OF DSPC AND POPC. ((M. Dovi, M. Breed, M. Hutchison and C. H. Spink)) Chemistry Department, SUNY-Cortland, Cortland, NY 13045.

Using the fluorescence Excimer/Monomer ratio of 1-palmitoyl-2-pyrenedecanoylphosphatidylcholine (PyrPC) as a probe, the effect of cholesterol on the gel phase content of mixtures of distearoylphosphatidylcholine (DSPC) and 1-palmitoyl-2-oleoylphosphatidylcholine (POPC) has been studied. The E/M ratio of 4% PyrPC in DSPC-POPC mixtures without cholesterol showed that the probe partitioned into the fluid phase by a 4/1 margin, but that there is a significant difference between the E/M ratio in gel-phase and the fluid-phase of the mixtures. Addition of cholesterol to the DSPC-POPC bilayers caused significant decreases in the E/M ratio, which can be interpreted as due to a break up of the gel phase DSPC. A model is presented that allows calculation of the changes in the gel phase content with increasing amounts of cholesterol. The results have significance to the interpretation of the physical effects of cholesterol on cell membrane fluidity.

W-Pos474

MEMBRANE / WATER PARTITION OF NONIONIC DETERGENTS AND ITS RELEVANCE FOR SOLUBILIZATION

((H. Heerklotz, H. Binder, G. Lantzsch, G. Klose)) Universität Leipzig, EXPI/BIM, Linnéstr. 5, D-04277 Leipzig, Germany

Mixed aqueous dispersions containing palmitoyl oleoyl phoshatidylcholine and oligo (ethylene oxide) dodecyl ethers $C_{12}EO_n$ with n=2-8 have been investigated. The aggregates composition has been determined as a function of the aqueous detergent concentration using laurdan fluorescence spectroscopy. The partition of the detergent between the aggregates and the aqueous phase has been evaluated on the basis of the regular solution model. Solubilization has been analyzed in terms of the limiting detergent fraction in the membrane, the minimal detergent fraction in micelles and the critical aqueous detergent concentration using thermodynamical coexistence conditions for the aqueous, bilayer and micellar pseudo-phases. A thermodynamic criterion for solubilization is presented.
The standard chemical potential differences of the transfer of the detergents from water to the bilayer have been found to follow the empirical relation
$\Delta\mu°(n= 2\text{-}8) = -37.6$ kJ/mol + n * 0.9 kJ/mol. Thus, a similar conformation and localization of the oxyethylene units within the membrane are suggested.

W-Pos475

STRUCTURE CHARACTERIZATION OF MEMBRANE BOUND AND SURFACE ADSORBED CYTOCHROME c

((Z. Yin[a], J. Wang[a], S. Kirchner[a], M. Caffrey[a], C.J.A. Wallace[b] and I. Clark-Lewis[c])) [a]Chemistry, The Ohio State Univ., Columbus, OH 43210, [b]Biochemistry, Dalhousie Univ., Halifax, Nova Scotia, Canada B3H4H7 and [c]Biomedical Research Center, Univ. of British Columbia, Vancouver, B.C., Canada V6T1W5.

Our initial x-ray standing wave (XSW) study of the membrane and solid substrate (silver mirror) bound topology of horse heart cytochrome c made use of a singly selenomethionine (Se-Met^{80}) labeled form of the protein (Wang *et al., J. Mol. Biol.*, 237:1-4, 1994). This XSW measurement gave a selenium-to-silver mirror surface distance that eliminated many possible orientations for the bound protein. However, with a single distance measurement, several other orientations were possible. To further refine the protein orientation, use was made of a doubly labeled protein incorporating Se-Met at position 80 and bromotyrosine (Br-Tyr) at position 97 (Se-Br-cytochrome c). On a bare silver mirror, the Br- and Se- to- mirror surface distances are 4 Å and 11 Å, respectively. On an ω-thiolundecanoic acid (ωTUA) coated mirror, the corresponding distances are 26.5 Å and 18.5 Å. Assuming that the protein adopts the same 3-D structure in the surface bound state as it does in the crystal form, these distances are consistent with cytochrome c binding to the bare silver mirror via a docking plane formed by four lysine side chains corresponding to residue numbers 7, 8, 25, and 27. A distinctly different orientation is assumed by the protein on the ωTUA coated surface.

Supported by NIH DK 45295

W-Pos476

THE ROLE OF SOLVATION IN PROTEIN ASSEMBLY: THE EFFECT OF SUCROSE ON DIMER-TETRAMER HB EQUILIBRIUM.

((M.F. Colombo and G.O. Bonilla)). Depto.Fisica - IBILCE - UNESP, S.J.Rio Preto, 15054-000 - Sao Paulo - BRAZIL.

Cooperativity and self-assembly of proteins is accompanied by changes in protein-protein interactions and, consequently, changes in protein hydration. We have recently shown that cooperative O_2-binding to Hb is sensitive to changes in water activity (a_w) (Colombo et al., 1992, *Science* **256**, 655). In the present study, we measure the effect of sucrose on the dimer to tetramer equilibrium constant, using molecular sieve gel chromatography, and confirmed that increasing sucrose concentration favors dimer formation. To analyze these data we formulate a relation to describe the contribution of the chemical potential of water (μ_w) to the chemical potential of a protein (μ_p). In this model we assume that n_w water molecules bind to identical and independent water binding sites on the protein, with a strength k, and find that the chemical potential of a protein is proportional to n_w and μ_w. We also use this formula to calculate the effect of water on the free energy change of dimer-tetramer assembly. We find compelling evidence showing that the splitting of a tetramer due to sucrose is an indirect effect of sucrose through its change in the bulk water activity, according to Le Chateliers principle. As in allosteric control of oligomeric proteins, water appears to be highly important in the regulation of protein assembly. Supported by: FAPESP, CNPq

W-Pos477

SIMULATIONS OF SOLVENT EFFECTS ON FLUORESCENCE SPECTRA AND DYNAMICS OF TRYPTOPHAN ROTAMERS.

((Pedro L. Muiño and Patrik R. Callis)) Department of Chemistry and Biochemistry, Montana State University, Bozeman, MT 59717.

The effect of solvent on the ^1L_a and ^1L_b excited states of tryptophan zwitterion in water has been studied using a hybrid theoretical method that couples molecular dynamics and a semiempirical molecular orbital procedure. The method was developed using indole and 3-methylindole [P. L. Muiño and P. R. Callis, J. Chem. Phys. **100**, 4093 (1994)]. This method yields information about the mechanism and the time scales involved in local and bulk solvent reorganization after excitation of the indole chromophore to the ^1L_a (or ^1L_b) state, as well as the solvent induced inhomogeneous broadening. Results to date predict large differences (~5000 cm^{-1}) in the degree of fluorescence Stokes shift and also predict significant differences in absorption wavelengths for different rotamers. The large effect appears to be due to reinforcement/cancellation effects of the indole ring dipole and zwitterion dipole on the solvent reaction field.

W-Pos478

EFFECTS OF SUCROSE ON THE INTERNAL DYNAMICS OF RIBONUCLEASE A

((Aijun Wang, Andrew Robertson‡, and D. W. Bolen)) HBC&G, Univ. of Texas Medical Branch, Galveston, TX. ‡Dept. of Biochem. Univ. of Iowa, Iowa City, IO

Osmolytes are naturally occurring small organic solutes that can stabilize proteins substantially. Based on their effects on protein functions, osmolytes are classified either as compatible solutes, which have little effect on protein functional properties, or as counteracting solutes, which offset urea destabilizing effects. Both kinds of osmolytes are known to be preferentially excluded from vicinity of proteins, but the stabilization mechanisms are not well understood. The different effects compatible and counteracting osmolytes have on proteins are also unknown. Since protein stability is intrinsically related to the protein structural fluctuations, we are interested in the effects of osmolytes on protein internal dynamics. In this study, we report the effects of sucrose, a typical compatible osmolyte, on structural fluctuations of ribonuclease A(RNaseA). The internal dynamics of RNaseA at specific amide proton sites was studied with and without sucrose by hydrogen exchange (HX) kinetics using 2D NMR. We found that the intermediate HX rates of amide protons are not affected by the presence of 1M sucrose, but the slowest exchanging amide protons become slower in 1M sucrose. The protection factors of the slowest exchanging protons are quite similar to one another while those for intermediate exchanging protons vary widely. Since sucrose increases surface tension and opposes an increase in surface area, the exchange data suggest that amide protons of intermediate exchange rate exchange from the native state by mechanisms with modest to no surface area changes, while exchange of slow amide protons occurs by mechanisms involving large (unfolding) surface area changes.

W-Pos479

SURFACE ADSORPTION PROMOTES ORDERING AND/OR CLUSTERING OF BIOPOLYMERS AND VICE-VERSA.

((A.P. Minton)) NIDDK, NIH, Bethesda, MD 20892

The cytoplasm of most eukaryotic cells contains significant amounts of membranous and fibrous structural elements that collectively present a very large surface area to soluble proteins in the fluid phase. The effect of weak nonspecific attraction between the soluble proteins and the structural elements upon the physical state of the proteins was investigated via simple statistical-thermodynamic models. Proteins are represented by compact particles that interact with the surfaces of "pores" of various geometries through a square-well potential of average force. Model calculations predict that small attractive protein-surface potentials (of the order of a few kT per protein monomer) enhance the effective equilibrium constant for self-association of proteins within a restricted volume by up to several orders of magnitude. Partition of total protein within the pore into "free" (non-surface-interacting) and "adsorbed" (surface-interacting) species reveals that due to purely entropic effects, self-association of adsorbed protein is highly favored over the self-association of free protein, and that adsorption of protein *n*-mers is highly favored over the adsorption of *n* monomers. The possible significance of this result with respect to the organization of proteins in eukaryotic cytoplasm is discussed.

W-Pos480

COMBINED RAMAN AND X-RAY STUDY OF COLLAGEN HYDRATION AND INTERMOLECULAR FORCES.
((S.Leikin*, W.-H.Yang†, G.E.Walrafen†, D.C.Rau*, and V.A.Parsegian*))
*LSB/DCRT and DIR/NIDDK, NIH, Bethesda, MD 20982; and
†Chemistry Dept., Howard Univ., Washington, DC 20059.

Earlier measurements of forces between collagen triple helices suggested that intermolecular interactions might be dominated by hydration forces. These forces, now thought to originate from restructuring of water near molecular surfaces, have been reported in such diverse biomolecular systems as lipid bilayers, DNA, polysaccharide assemblies and protein fibers. In the present work we have combined Osmotic Stress measurements of forces between collagen helices with Raman spectroscopy of interstitial water so that both Raman and x-ray measurements were done on the *same* samples. Raman spectra in the range from 3100 to 3700 wave numbers show a strong water signal, which, in contrast to infrared spectra, is not obscured by amide bands. The amount of water in collagen fibers determined from integrated Raman intensities is in good agreement with that measured from x-ray spacings over a wide range of osmotic pressures from fully hydrated collagen (equilibrated in excess water solution) to very dry fibers (at 15% relative humidity). The shape of water Raman spectra in collagen changes with variation of the osmotic stress and concomitant changes in water concentration. Even at full hydration it is significantly different from the shape observed in bulk water indicating rearrangement in the interstitial water hydrogen bond network.

W-Pos481

DNA Phase Diagram (crystalline - cholesteric - blue phase - isotropic): An osmotic pressure study ((H.H. Strey, R. Podgornik, D.C. Rau and V.A. Parsegian)) LSB/DCRT, OD/NIDDK, NIH, Bethesda, MD 20892

The pressure-density phase diagram of long ($\geq 10kbp$) and short fragment DNA (146bp = 50nm = persistence length) was explored by the osmotic stress method. For the high density phases (hexagonal - cholesteric) small angle x-ray scattering was used to probe the interaxial spacings as well as its packing order. For low pressures (low densities) we measured the density directly by weighing. By variing the salt concentration (2M - 10mM) one can tune the electrostatic repulsion (Debye length) between the DNA molecules. For long DNA at high ionic strength (0.5M NaCl) all phase transitions (hexagonal-cholesteric-precholesteric (blue phase?)) seem to be weak first order or second order, since we never observed any discontinuities in density with respect to pressure. One idea is that the precholesteric region between the cholesteric and isotropic phase shows several phase transitions (blue phases) each with a small heat of transition. When we lower the salt concentration below 100mM NaCl the phase transitions change qualitativly. With decreasing salt concentration we observe strong first order transitions at decreasing osmotic pressures to an expanded non birefringent phase. This phase seems to be dominated by electrostatic repulsion and has presumably cubic order. For short fragment DNA (SFD) the phase diagram looks qualitativly the same as for long DNA, exept that SFD generally packs better. This indicates that SFD shows no entanglement and therefore has less defects than long DNA.

W-Pos482

OSMOTIC STRESS MEASUREMENT OF FORCES BETWEEN UNCHARGED POLYSACCHARIDES.
((C.Bonnet-Gonnet, S.Leikin, D.C.Rau and V.A.Parsegian))
LSB/DCRT and DIR/NIDDK, NIH, Bethesda, MD20892

Direct measurements of forces between biological macromolecules at close separation have revealed unusually strong exponentially decaying repulsion which is now thought to be associated with the energetic cost of the removal of water organized around molecular surfaces. These "hydration forces" have been observed in a wide variety of biological systems including lipid bilayers, DNA, polysaccharides and proteins. In this work we undertake a systematic study of the forces between uncharged carbohydrates such as galactomannans and uncharged substituted carbohydrates such as hydroxypropylcellulose. We concentrate on the effect of solution conditions on the interaction, including pH, temperature, and concentration of salt and small neutral solutes. For example, the measured repulsion between hydroxypropylcellulose molecules is strongly reduced when temperature is increased from 5 to 45 °C so that previously highly soluble molecules self-assemble. Addition of salt promotes assembly and weakens the temperature sensitivity of the measured forces. The temperature dependence and the effect of solution conditions on it are of considerable interest since temperature-favored assembly is a feature common for many biologically important reactions.

W-Pos483

SPATIALLY LONG-RANGED INTERACTIONS ARE ESSENTIAL FOR RAPID HELIX FOLDING AND COOPERATIVITY. ((Shen-Shu Sung))
Research Institute, Cleveland Clinic Foundation, Cleveland OH 44195.

Constant temperature (300 K) Monte Carlo simulations have been carried out on a 16-residue peptide model with alanine side chains. Each backbone peptide unit is treated as a rigid element to reduce the number of degrees of freedom. Non-dihedral variables are used with flexible connections between the rigid elements to facilitate independent local motion. Atom-based potential functions are tested separately with short-range interactions only and with long-range interactions, with respect to the three dimensional spatial distance, and not to the separation in the amino acid sequence. With short-range interactions only, the folding is nearly random and takes 100 to 200 million steps to form a helix. Two major energy changes, separated by 50 to 100 million steps, are observed. With the long-range electrostatic interaction, the folding is guided by electric field and a helix formed within 10 million steps. The transition to helix is cooperative (all-or-none). This observation indicates that the long-range interaction is essential for rapid folding and for the cooperativity. With long-range interactions smaller stabilization energy is needed for helix folding than with short-range interactions only. The small energy change can prevent the multiple minima problem in helix folding. Under the same simulation conditions polyglycine does not fold into stable helices. The folding is sequence dependent, and the method does not indiscriminately force the backbone into helix. These simulations provide insight into the helix folding mechanism.

W-Pos484

ANALYSIS OF LEFT-HANDED POLY(L-PRO)II HELICES IN GLOBULAR PROTEINS. ((N. Sreerama and R.W. Woody))
Department of Biochemistry and Molecular Biology, Colorado State University, Fort Collins, CO 80523. (Spon. by R.W. Woody)

An algorithm to identify the left-handed poly(L-Pro)II type (P_{II}) structure from the x-ray structures of proteins is described. Our algorithm utilizes a virtual bond angle C_{i-1}^{α}-C_i^{α}-C_{i+1}^{α} (τ_i) and a virtual dihedral angle O_{i-1}=C_{i-1}-C_i=O_i (ξ_i), and identifies P_{II} structure among residues not assigned to α-helix or β-sheet by the Kabsch & Sander method. Short segments of P_{II} conformations were identified, and these form a significant fraction (~40%) of unassigned residues. A majority of the P_{II} helices identified were on the surface of the protein, and are likely to be stabilized by solvent. An analysis of protein crystal structures indicates a network of crystallographic water molecules hydrogen-bonded to the exposed C=O and N-H groups. Molecular dynamics (MD) simulations of $(Ala)_n$ (n=6,8 and 12) in the P_{II} conformation were performed for 120 ps in water, and analysis of the MD trajectories also indicates a bridge of water molecules connecting various C=O and N-H groups. Details of the algorithm and analysis will be presented.
(Supported by GM 22994)

W-Pos485

Determination of the Heat Capacities of Polar and Apolar Aqueous Solutions Using the Random Network Model(RNM). (Bhupinder Madan and Kim Sharp)
Department of Biochemistry and Biophysics, Johnson Research Foundation, University of Pennsylvania, Philadelphia, PA -19104.

The random network model (RNM) parameters such as average O-O distance, fluctuations in O-O distance and fluctuations in hydrogen bond angle have been computed from MC simulations for three systems using the TIP4P water model and OPLS parameters. These systems were: pure water, Ar/water and K^+/water. The fluctuations in H-bond angle are much smaller in Ar/water and K^+/water than in pure water. The heat capacity, Cp, of the three systems have been determined from the energy fluctuations of the system. Various contributions to the energies of the three systems have been determined from the RNM parameters. The heat capacity values can be explained by these parameters.

W-Pos486

PARALLEL α/β-BARRELS: SENSITIVITY ANALYSIS OF STRUCTURAL DEVIATIONS TO PARTIAL ATOMIC CHARGE AND van der WAALS RADII PERTURBATIONS. ((L. Shen, T. Tran, T. Thacher, H. Rabitz, J. Novotny)), Bristol-Myers Squibb Res. Inst., Princeton NJ 08543-4000; Biosym Technologies Inc., San Diego, CA 92121; Dept. Chemistry, Princeton U., Princeton NJ 08544.

Stability of proteins is determined in part by the many intramolecular interactions among their amino acid side chains, however, our understanding of atomic details and relative significance of these interactions remains incomplete. We report the use of sensitivity analysis (H. Rabitz, Science 246 (1989) 221) to obtain insight into principles governing, at an atomic level, structural conservation and stability of β-barrels with widely diverged primary structures. The basic folding motif of triose phosphate isomerase (TIM) and mandelate racemase (MRM) is β-strand-turn-α helix repeated 8 times to form closed, 8-stranded, parallel β-barrels, $(\beta/\alpha)_8$. The two barrels have essentially identical (elliptical) cross-sections and interior volumes, but their sequences show no detectable similarity and are mutually circularly permuted, with the β-strand 1 of MRM corresponding to the β-strand 7 of TIM. The TIM and MRM β-barrels were energy-minimized, least-squares superimposed and the root-mean-square function of β-strand backbone atoms, σ, was calculated from the atomic coordinates. Three different sets of parametric sensitivities, $\frac{\delta\sigma}{\delta p_i}$, were then calculated with p_i being either (i) partial atomic charges, (ii) van der Waals radii, or (iii) minimum van der Waals energies of all the atoms forming the core of the β-barrels. Amino acid residue sensitivities, i.e. sums of the atomic sensitivities, were overlayed onto the β-strands in color-coded displays and are currently being interpreted in structural terms. Preliminary results indicate that both positive and negative sensitivites occur, and tend to be spacially segregated. A complete structural interpretation of the sensitivities will be presented.

W-Pos487

ANALYSIS OF LOCAL MINIMUM ENERGY STATES OF MODEL DENATURED PROTEINS ((R.N.Cole and P.G.Wolynes)) University of Illinois, Champaign-Urbana, IL, 61820

We discuss a statistical study on an ensemble of model denatured proteins constructed using the Charm energy force fields. Randomized coordinates consistent with varying degrees of secondary structure were generated. These structures were then minimized to the nearest local minimum energy structure. The variance of the distribution of free energy levels, including an estimated solvent contribution for the denatured states, is compared to the gap in energy between the native state and the average denatured states. We use this to estimate the ratio of the folding transition temperature (Tf) to the glass transition temperature (Tg) for realistic protein models. (Supported in part by an NIH Molecular Biophysics Training Grant.)

W-Pos488

EXHAUSTIVE ENUMERATION OF PROTEIN CONFORMATIONS USING EXPERIMENTAL RESTRAINTS GENERATES FEW CONFORMATIONS FOR ANY CHAIN LENGTH. ((R.S. DeWitte and E.I. Shakhnovich)) Chemistry Department, Harvard University, Cambridge MA. 02138.

An efficient new algorithm which enumerates *all* possible conformations of a protein which satisfy a given set of distance restraints is shown to produce few conformations, regardless of chain length. By rapid growth of all possible self-avoiding conformations on the diamond lattice, this algorithm provides construction of α-carbon representations of a protein fold which manifest a specified set of distance restraints. Earlier work suggested that the number of restraints could be chosen such that only about one thousand conformations were generated, for different chain lengths. By considering conformations as random walks on a lattice, and incorporating the restraints by demanding that the steps taken between residues *i*, and *j*, give no net drift in any direction, we have overestimated the number of conformations that result on average from a set of *n* restraints, for a chain length *N*. It is shown that the number of conformations can be independent of chain length, if *n* is chosen appropriately. As in the previous work, the resulting conformations differ only slightly from one another, and can therefore be grouped into structural families, of which there are typically about 25. Therefore, one can generate very few representative protein global folds that satisfy a given set of distance restraints, for any chain length.

W-Pos489

EXTENSION OF THE LIFSON-ROIG HELIX/COIL MODEL TO INCLUDE HELIX STABILIZING INTERACTIONS. ((William Shalongo and Earle Stellwagen)) Department of Biochemistry, University of Iowa, Iowa City, IA 52242.

The stability of monomeric peptide helices in aqueous solution is modulated by non-covalent interactions not considered by the Lifson-Roig model. Recently, Doig et al. (Biochemistry 33, 3396 (1994)) reweighted selected residue coil states to extend the Lifson-Roig model to include non-covalent helix capping interactions at the termini of helical peptide states. However, this extended model does not account for non-covalent interactions between sidechain pairs which may occur anywhere within helical peptide states. We have extended the Lifson-Roig model to include both helix capping and sidechain pair interactions. Helix capping interactions are included by reweighting selected residue helical states, while sidechain pair interactions are included by applying an apparent ΔG to each peptide helical state if the residues spanned by the interaction are all helical. We have determined statistical weights for both extended Lifson-Roig models by predicting the mean helical contents of 57 alanine-rich peptides from Chakrabartty et al. (Protein Science 3, 843 (1994)) which contain no significant sidechain pair interactions. We have also determined apparent ΔG values for representative sidechain pair interactions in other alanine-rich peptides. The apparent ΔG values were found to be dependent on the location and orientation of the interaction in the peptide sequence and the number of residues spanned by the sidechain pair.

W-Pos490

KINETICS OF OLIGONUCLEOTIDES LIGATION COUPLED WITH CYCLIZATION OF LIGAMERS: A THEORETICAL STUDY. ((M.A. Livshits[1] and Y.L. Lyubchenko[2])) [1]The Engelhardt Institute of Molecular Biology, RAN, Moscow, Russia, [2]Dept. of Microbiology, Arizona State University, Tempe, AZ 85287-2701.

The kinetics of ligation of oligonucleotides allowing the formation of circular molecules was treated theoretically. An analytical solution for the multimerization process has been found. An analysis of the cyclization rate as a function of the multimers sizes for a number of cases has been performed. An application of this theory to the oligonucleotide ligation-cyclization method was analyzed. It was shown that estimates of structural mechanical characteristics of monomers can be obtained from the experimental data on the distribution of circles on their sizes. The recommendations to conditions of the oligonucleotide ligation-cyclization experimets are suggested.

W-Pos491

THE STRUCTURE OF HYDROPHOBIC ION PAIRED PEPTIDES AND PROTEINS IN ORGANIC SOLVENTS.

((James E. Matsuura, Brent S. Kendrick, Jeff Meyer, and Mark C. Manning)) School of Pharmacy, University of Colorado HSC, Box C-238, Denver, CO. 80262.

The dissolution of peptides and proteins in a variety of organic solvents can be realized by using hydrophobic ion pairing, whereby anions are replaced by detergent molecules. These ion paired proteins demonstrate diminished aqueous solubility and enhanced solubility in organic solvents. Secondary and tertiary peptide and protein structure was followed by circular dichroism and FTIR. Thermal stability for insulin and chymotrypsin has been shown to be greatly increased in organic solvents to over 100 °C. Ribonuclease and chymotrypsin have been studied for activity and structure in organic solvents. Ribonuclease in methanol shows a decrease in tertiary structure and an increase in secondary structure, which would normally indicate a loss of function. However, ribonuclease demonstrates activity in 90% methanol. Chymotrypsin ion paired into isooctane has native like structure based on circular dichroism, and has been shown also to be enzymatically active when reextracted into an aqueous media. Small peptides can be ion paired and dissolved into organic solvents, resulting in an increase in secondary structure as compared to water.

W-Pos492

ENERGETICS OF TRANS-MEMBRANE α-HELICES IN MEMBRANE. ((N. Ben-Tal, R. Bharadwaj, A. Nicholls A. Windemuth and B. Honig)) Dept. of Biochemistry, Columbia University, New York, NY 10032.

The energetics of inserting α-helices into lipid bilayers, and the interactions of helices in water, in a lipid environment, and in membranes are studied. An estimation of the nonpolar (cavity/van der Waals) contributions to the free energy, obtained by multiplying the calculated helix accessible area by a solvation parameter, is added to the electrostatic energy, obtained by solving the Poisson equation, to give the total free energy of the system.

It is found that the electrostatic cost of vertically inserting a 25aa polyalanine helix into a 30Å thick membrane is about 10 kcal/mole less than the energetic gain due to hydrophobicity (i.e. the insertion process is energetically favorable). Concerning the insertion process itself, our calculations show a saddle shaped energy curve for vertical insertion, with an energy barrier which is caused by the unsatisfied hydrogen bonding groups at the helix termini. A state of minimum energy is found for helices which are horizontally adsorbed on the interface between lipid bilayers and water. This state supports a mechanism of insertion in two stages: (a) adsorption on the membrane surface followed by (b) the insertion itself.

Concerning helix-helix interactions, an anti-parallel orientation can be up to 20 Kcal/mole more stable than a parallel orientation in membranes. However, it is sufficient for the helix termini to stick out few angstroms from the bilayer surface for their dipole-dipole interaction to be quite small.

W-Pos493

SOLUTION STRUCTURES OF PEPTIDES CONTAINING ß- AND γ-TURNS IN SOLVENTS OF DIFFERENT POLARITY ((P.Xie and M.Diem)) City Univ New York, Hunter College, New York, NY 10021. (Spon. by M.Diem)

Vibrational Circular Dichroism (VCD) spectroscopy has been used to study the solution conformation of a number of small peptides which model ß- and γ-turns. Linear and cyclic (Cys-Pro-Xxx-Cys) (l-CPXC and c-CPXC, X = Gly, D-Ala, L-Ala, D-Phe, L-Phe) were used as model compounds for ß-turns, while *cyclo*-(Pro-Gly)$_3$ (c-PG3) and *cyclo*-(Cys-Ala-Cys), c-CAC, were used as models for γ-turns.

Enormous changes in the VCD spectra were observed for all the above model systems when the solvent polarity was increased from no or low polarity (dioxane or bromoform), medium polarity (DMSO/bromoform or pure DMSO) to high polarity (DMSO/deuterium oxide or trifluoro ethanol). The corresponding infrared absorption spectra barely revealed any differences. The structural changes giving rise to the differences in VCD features were very pronounced even in conformationally restricted peptides such as *cyclo*-(Cys-Pro-Gly-Cys), c-CPGC.

The VCD spectra were reproduced computationally using the Non-Degenerate Extended Coupled Oscillator (NECO) approach, an extension of the exciton formalism to non-identical amide I infrared transitions. These calculations indicate that small changes in the dihedral angles between the peptide linkages may cause enormous changes in the VCD features. Consequently, we interpret the observed VCD spectral changes in terms of structural changes of the turns caused by various degrees of solvent exposure of the carbonyl groups.

W-Pos494

pH INDUCED VARIATION IN LIPID PACKING STRESS MAY CORRELATE WITH RELATIVE PROBABILITIES OF ALAMETHICIN CONDUCTANCE STATES. **((S.M. Bezrukov[1], I. Vodyanoy[1,2], P. Rand[3], V.A. Parsegian[1])) [1]DCRT & NIDDK, NIH, Bethesda, MD 20892, USA; [2]ONR, Europe, London, NW1 5TH, UK; [3]Brock Univ., St.Catharines, L2S 3A1, Canada.**

To examine the influence of lipid packing energetics on ion channel expression, we measure the relative probabilities of alamethicin channels in L-α-Phosphatidylserine (PS) bilayers as a function of pH. The rationale for this strategy is the finding that higher-conductance states are more likely to occur in the presence of lipids prone to hexagonal H_{II}-phase formation (specifically DOPE), than in lamellar L_α-forming lipids (DOPC) (Keller et al. Biophys.J. 65:23-27, 1993). In 50 mM CsCl solutions at neutral pH, the open channel in PS membranes spends most of its time in states of lower conductance and resembles alamethicin channels in DOPC; at lower pH, where the lipid polar groups are neutralized, channel probability distribution resembles that in DOPE. X-ray diffraction studies on DOPS/DOPE mixtures at neutral pH show a progressive decrease in the intrinsic curvature of the constituent monolayers and decreases probability of formation of H_{II}-phases as the charge fraction is increased. We are now examining how proton titration of DOPS itself affects lipid packing energetics, monolayer curvature and strain energy, and so couples to channel formation.

W-Pos495

A MICROSCOPIC INTERPRETATION OF THE "VAPOR PRESSURE PARADOX". ((Rudi Podgornik & Adrian Parsegian)) DCRT&NIDDK/NIH, Bethesda, MD 20892

Among the greater embarrassments avoided by theorists and discussed *sotto voce* by experimentalists is the "vapor pressure paradox". Why do phospholipid multilayers take up less water from a 100% rh vapor than from liquid water? Why do these same multilayers imbibe less water when they are sedimented on a solid surface rather than suspended in the host liquid? We're not talking about a few layers near a surface; the difference in swelling is enough to be seen well in x-ray diffraction which requires many layers uniformly spaced.

We have postulated that one effect of an interface is to suppress mechanical undulations of bilayers -- either because of surface tension or because from forces adhering the first bilayer to a solid surface. The question then is the persistence of this suppression into neighboring layers. As a first approximation we have written the bilayer energy as a cost of pure steric repulsion (to maintain spacing between bilayers) and a cost of bending (to maintain bilayer flatness). Because both contributions involve the bending modulus and they reach equilibrium in suspension, the balance is vulnerable to added perturbation such that enforced stiffening in one layer can be successively communicated over long (~mm) distances to its neighbors. Thus a vapor or solid surface can suppress undulations and limit water sorption almost on a macroscopic scale.

W-Pos496

SYMPLECTIC NUMERICAL METHODS FOR MOLECULAR DYNAMICS SIMULATION ((D. Janežič)) LSB/DCRT, NIH, Bethesda, MD 20892

There are different types of theoretical methods to investigate dynamical properties of complex molecular systems. One technique is molecular dynamics (MD) simulation in which the classical eauations of motion for all particles of a system are integrated over finite period of time. The efficiency and, thus, the scope of the MD method can be increased by introducing algorithms for the integration of the molecular dynamics equations over larger time steps without loss of stability. The need for improved algorithms has recently received higher attention since it is obvious that the time step problem in MD cannot be overcome solely with faster computers. The problem how to increase the time step can be overcome by the use of symplectic methods for the numerical solution of Hamiltonian equations since Hamiltonian systems posses an important property, in that the flow in the phase space is symplectic. An application of symplectic implicit Runge-Kutta integration schemes, the s-stage Gauss-Legendre Runge-Kutta (GLRK) methods of order $2s$, for the numerical solution of MD equation is described. The two-stage fourth order GLRK method, the implicit-midpoint rule (the one-stage second order GLRK method) and the three-stage diagonally implicit GLRK method of order four are studied. The fixed-point iteration was used for solving the resulting nonlinear system of $s \times d$ equations (where s is the number of stages of the method and d the number of degrees of freedom of the system). The algorithms were applied to a complex system of N particles interacting through a Lennard Jones potential.

W-Pos497

PACKING INTERACTIONS IN MODEL PROTEIN INDUCE SEQUENCE SPECIFICITY AND KINETIC STABILITY ((Peter E. Leopold and Eugene I. Shakhnovich)) Department of Chemistry, Harvard University, 12 Oxford St., Cambridge, MA 02138.

In order to develop a model to evaluate the relative importance of the chemically-specific interactions (electrostatic, covalent) and nonspecific interactions (packing) that stabilize proteins structure, we present a packable model of a protein C_α backbone with spherical side chains tangent to the main chain. The side chains have a variety of sizes and a sequence-independent set of up to 26 rotationally-isomeric states, but all secondary and tertiary contacts have a uniformly stabilizing interaction. We show that sequence specificity arises from steric packing requirements alone. We also show that well-designed sequences and rotamer states are independent of the details of the parameter set. Finally, we show that designed structures are kinetically stable during simulations of the C_α backbone.

PEL holds an NIH NRSA GM 15497. EIS acknowledges support from the Packard Foundation. PEL & EIS thank the Aspen Center for Physics.

W-Pos498

PREDICTION OF PROTEIN TERTIARY STRUCTURE CLASS FROM CIRCULAR DICHROISM SPECTRA. ((S.Yu. Venyaminov[1,2], K.S. Vassilenko [1] and F.G. Prendergast[2]))[1]Institute of Protein Research, Russian Academy of Science, Pushchino, Moscow Region, Russia 142292. [2]Department of Pharmacology, Mayo Foundation, Rochester, MN 55905. (Sponsored by F.G. Prendergast.)

Fifty-three circular dichroism (CD) spectra were investigated in order to examine the correlation between the shape of the CD spectrum and the tertiary structure class of the protein. Five classes were considered - all-α, all-β, α+β, α/β and denatured proteins. Spectra from 190 to 236nm, with interval 2nm were described as points in 24-dimensional hyperspace, where coordinates were values of ellipticities at fixed wavelengths. This allows the spectra to be treated as patterns, and subsequently, analyzed using pattern recognition algorithms. Cluster analysis, which does not need predefined information about protein structure, divides spectra into several compact groups, or "clusters" with good correlation with tertiary structure class. To visualize these results, orthogonalization procedures were imposed on the original data set in 24-dimensional space. The new 3-dimensional coordinate system demonstrated well-separated all-β class and denatured proteins. Regions corresponding to all-α, and especially α+β and α/β proteins were not as well resolved. The following approach was then applied to the original data set to obtain an objective mathematical algorithm for the determination of a protein's tertiary structure class from its CD spectrum. Regions in 24-dimensional hyperspace corresponding to all of tertiary structure classes were found by calculating the decision functions, or equations of hyperplanes, which separate groups of spectral patterns of different classes. The class representing the region which includes the protein spectra, can be interpreted in terms of a tertiary structure class for this protein. The accuracy of the method was checked by removing one of the proteins from the training set, finding all the decision functions and determining the class of the excluded protein. This test gives 100% accuracy for all-α, α/β and denatured proteins; 85% for α+β and 75% for all-β proteins. (Supported by GM34847-10.)

W-Pos499

THE KINETICS OF METAL BINDING TO ZINC FINGERS. ((Jeffrey C. Buchsbaum and Jeremy M. Berg)) Department of Biophysics and Biophysical Chemistry, Johns Hopkins School of Medicine, Baltmore, MD 21205.

Zinc fingers contain an alpha helix and two strands of beta sheet. These peptides bind metal ions (zinc, cobalt) in a tetrahedral fashion and specifically bind to DNA. A twenty six amino acid peptide, called CP, was used to study the kinetics of metal binding to zinc fingers.[1] CP was designed by our lab using a database of 131 zinc finger sequences.[2]

Earlier work containing mixtures of half CP fragments hinted at a dimerization of the cysteine containing fragments. Stopped flow data collection confirms the formation of a colored species that is consistent chemically with a dimer form. A chemical mechanism has been postulated and shows good agreement to the data. Spectral analysis of the data using eigen vector searches supports the number of colored species in the mechanism. Stopped-flow experiments were done at 25.0 °C at pH's 6.80, 7.50, and 8.00 using various initial concentrations of peptide and metal.

---

[1]The amino acid sequence of CP is PYKCPECGKSFSQKSDLVKHQRTHTG.
[2]Krizek, B. A..; Amann, B. T.; Kilfoil, V. J.; Merkle, D. A.; Berg, J. M. *J. American Chemical Society*, 1991,113.

W-Pos500

DISULFIDE BONDS IN A RECOMBINANT REPEAT FROM AN AQUATIC INSECT'S SILK PROTEIN. ((S.V. Smith and S.T. Case)) Dept. of Biochemistry, Univ. of Mississippi Medical Center, Jackson, MS 39216-4505.

The goal of this research is to learn about the structure and properties of a bacterially expressed recombinant protein (rCAS) modelled after core repeats found in silk protein spIa from the larval salivary glands of the insect, Chironomus tentans. rCAS consists of 83 amino acids including four cysteines. Laser desorption ionization mass spectrometry on native (N) and reduced and alkylated (R) rCAS confirmed the correct molecular mass and the presence of the four cysteines. On SDS/polyacrylamide gels, N-rCAS migrates faster than R-rCAS. This suggests that intramolecular disulfide bonds are present in N-rCAS. Quantitative Ellman's assays and amino acid analyses were conducted on both N-rCAS and R-rCAS. From the results of these experiments, we conclude that N-rCAS contains two intramolecular disulfide bonds. The ability of N-rCAS to form intramolecular disulfide bonds may reflect an important step in the assembly pathway of Chironomus tentans silk proteins. Supported by U.S. Army Research Grant No. DAAL03-91-G-0239.

W-Pos501

EXPLORING PRION KINETICS AND REPLICATION WITH A SPIN-LABELED PRION PEPTIDE FRAGMENT.

((Karen M. Lundbergt, Chris J. Stenlandt, Glenn L. Millhausert, and Fred E. Cohen‡)) †University of California, Department of Chemistry and Biochemistry, Santa Cruz, CA 95064; ‡University of California, Departments of Medicine, Pharmaceutical Chemistry, Biochemistry and Biophysics, San Francisco, CA 94143.

An infectious form of the prion protein appears to replicate without a genetic component. The mechanism of infectivity is therefore unique and currently not well understood. Recent evidence suggests that the normal cellular form of the protein contains 42% α-helix and no β-sheet whereas the infectious form contains 30% helix and 43% β-sheet. Interconversion to the infectious form is associated with neurodegeneration. In addition, prion infection is often (but not always) accompanied by the presence of amyloid plaques rich in the prion protein. We have developed an experimental method capable of investigating the kinetics of this transformation on a peptide model. A highly amyloidogenic peptide fragment, derived from the H1 helix sequence in the prion protein, is spin-labeled and the resulting ESR signal is used to follow the kinetics of amyloid formation. Both peptide monomer and peptide aggregate are detectable. Kinetic analysis suggests that the peptide aggregate is responsible for the interconversion of free peptide to amyloid. The observed kinetic events appear to support a recent *in vivo* model for prion replication.

W-Pos502

STRUCTURAL AND ELECTRONIC PARAMETERS FOR Co(II)-SUBSTITUTED ZINC-FINGER PEPTIDES ((Igor A. Topol, José R. Casas-Finet, Stanley K. Burt, and John W. Erickson)) Structural Biochemistry Program, PRI/DynCorp, NCI-FCRDC, Frederick, MD 21702. (Spon. by A. Wallqvist)

Tetracoordinated metal binding models were built for the metal chelation spheres of Co(II) in zinc-finger metal binding clusters of the CCHH, CCHC, and CCCC types. Geometrical parameters were optimized using density functional techniques; two different spin states of the metal ion cluster were considered for each structure investigated. Our results predict that the quartet state of Co(II) induces a quasi-tetrahedral structure, whereas all structures were close to a planar configuration for the doublet state. Tetrahedral (high-spin) structures were found to be more stable than the planar (low-spin) counterparts due to electronic correlation effects. These findings are in agreement with published results for related systems of inorganic Co(II)-chelating molecules, and with emerging experimental data for Co(II)-substituted zinc-finger peptides. Extension of our methodology to binuclear metal clusters of the Co_2Cys_6 type suggests that the high-spin (triplet) state is also favored over the low-spin (singlet) state. Using a simple model of d-d electronic transitions, we show that substitution of histidine by cysteine in zinc-finger metal binding clusters leads to a characteristic blue-shift of their visible/near infrared absorption bands, in accordance with experimental results. Calculated metal binding affinities for our models were ranked relative to those for Zn(II) and Cd(II). In contrast to our previous calculations for Zn(II) and Cd(II) binding which indicated an increase in affinity with the number of thiolate ligands, a decrease was observed for Co(II), in agreement with experiment.

W-Pos503

STRUCTURAL CHARACTERIZATION OF CIRCULINS A AND B, TWO NOVEL HIV-INHIBITORY MACROCYCLIC PEPTIDES ((J. R. Casas-Finet, R. E. Cachau, K. R. Gustafson, R. C. Sowder II, L. E. Henderson, and J. W. Erickson) Structural Biochemistry and AIDS Vaccine Programs, PRI/DynCorp, and Lab. of Drug Discovery R&D, NCI-FCRDC, Frederick, MD 21702. (Spon. by R. F. Steiner).

Circulins A and B have been isolated from the tropical tree *Chassalia parvifolia* by anti-HIV bioasssay-guided fractionation. Their amino acid sequence and cyclic structures were determined by endoproteinase digestion, derivatization, N-terminal Edman degradation and FAB mass spectroscopy. Circulins A and B are the largest naturally occurring peptides (30 and 31 res., resp.) in which the entire primary amide chain is covalently cyclized *via* peptide bonds. Sequence homology to the human antigen CD22 was found. ^{1}H NMR spectra of circulins showed chemical shift dispersion consistent with a folded structure. Fluorescence emission spectra of circulin A peaked at 353 nm, typical of a solvent-exposed environment for its single Trp residue. Significant Tyr-->Trp energy transfer at the singlet level was observed, suggesting their relative proximity. 0.1 M DTT or 6 M GuHCl did not significantly alter its wavelength maximum, lineshape or polarization of Trp emission, unless added together. These results strongly suggest that circulin A adopts a compact structure in the native state, in agreement with dynamic anisotropy measurements. CD spectra of circulins A and B confirmed the occurrence of tight beta turns and the lack of alpha helical structure. Modelling of the disulfide bonding pattern of circulin A was carried out by molecular dynamics (MD) simulations using a feedback restrained procedure [FRMD; Cachau *et al., Prot. Eng. 7*, 831 (1994)]. Following visual inspection of all 12 possible configurations, four disulfide bridging schemes were considered based on separation between S atoms and steric hindrance criteria. FRMD biased the MD trajectory towards a single relaxed conformation that showed compact packaging of side chains, with hydrophobic residues oriented toward the surface and charged residues at the entrance to a molecular channel. The model contains a single, centrally-located, water molecule and exhibits a cavity able to accomodate medium-sized cations. These features are consistent with ion channel structures, which in the linear disulfide-bonded defensins account for their antimicrobial properties and activity against enveloped viruses. Circulin A and B effectively inhibited the cytopathic effects of *in vitro* HIV-1 infection (EC_{50} = 125 nM), but were cytotoxic to host cells at higher concentrations (IC_{50} = 625 nM). In agreement with the highly constrained three-dimensional structure suggested by FRMD, circulins were resistant to proteolytic degradation in the oxidized state, whereas their cytoprotective activity was lost upon reduction of their disulfide bonds.

W-Pos504

SITE-SPECIFIC ATTACHMENT OF FATTY ACIDS ESTERS AND TRANSGLUTAMINASE SUBSTRATE PEPTIDES TO BPTI ((Chadler T. Pool and T. E. Thompson)) Dept. of Biochemistry, University of Virginia, Charlottesville, VA 22908.

In order to produce novel protein probes for examining membrane domain structure, we have modified bovine pancreatic trypsin inhibitor (BPTI) by specifically palmitoylating the N-terminus, and by specifically attaching a small peptide at Lys-15 containing a fluorescent or spin labeled group. The N-terminal palmitoylation site and Lys-15, the site of trypsin binding, are at opposite poles of BPTI. The transamidating enzyme transglutaminase was used to attach the short peptide specifically to Lys-15 of BPTI. To verify that only Lys-15 was modified by the enzyme, it was shown that trypsin, which blocks Lys-15, prevents the reaction from occuring. A digest was also performed on the modified BPTI using ArgC endoproteinase. Both experiments indicate that only Lys-15 served as a substrate for transglutaminase leaving the N-terminus and three remaining lysine residues unmodified. All lysine residues were guanidinated to homoarginine. The N-hydroxysuccinimide ester of palmitate was then reacted with the N-terminus using a tetrahydrofuran, phosphate buffered solvent system, thus eliminating the need for detergents normally employed with such esters. Palmitoylation alone did not affect the inhibitory properties of BPTI but did cause dimer formation in aqueous solution. (supported by NIH grant GM-14628)

W-Pos505

METAL-LIGAND COMPLEXES AS A NEW CLASS OF LONG-LIVED FLUOROPHORES FOR PROTEIN HYDRODYNAMICS. ((E.A. Terpetschnig, H. Szmacinski and J.R. Lakowicz)) Center for Fluorescence Spectroscopy, Dept. Biol. Chem., Univ. MD Sch. Med., 108 N. Greene St., Baltimore, MD 21201. (Spon. by E. Akkaya)

We describe the use of an asymmetric Ruthenium-ligand complex as the prototype for a new class of luminescent probes which enable the measurement of rotational motions of proteins on the 10 ns to 1.5 μs timescale. As compared to a symmetric complex $Ru(bpy)_3Cl_2$, the unsymmetric complex $Ru(bpy)_2(dcbpy)(PF_6)_2$ displays higher anisotropies (-55°C) when excited at the long wavelength absorption band (see Figure) (bpy, bipyridyl; dcbpy, dicarboxy bipyridyl). For covalent attachment to proteins, we synthesized a reactive NHS-ester derivative of the complex. To demonstrate the usefulness of the probe, the time dependent intensity and anisotropy decays of protein conjugates like human serum albumin, concanavalin A, human immunoglobulin G (IgG), and Ferritin were measured in solutions of increased viscosity. The data reveals that the probe is sensitive to changes in rotational motions to 1 μs, a timescale which has been inaccessible using luminescence methods.

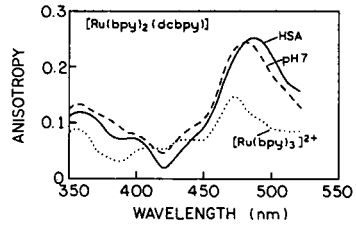

W-Pos506

MODULATION OF SOLVENT INDUCED FORCES BY COSOLUTES: EFFECTS ON DEMIXING OF A BIOPOLYMERIC SOL

((P.L. San Biagio*^, D. Bulone ^, A. Emanuele*, M.B. Palma Vittorelli*^ and M.U. Palma*^))
^ CNR Institute for Interdisciplinary Applications of Physics and * Dept. of Physics, University of Palermo, Via Archirafi 36, I-90123 Palermo, Italy

Gelation is a topological phase transition implying a break of symmetry. Previous work has shown that at intermediate to low concentration (below the random link percolation threshold) the determinative symmetry-break event does not consist in the gelation step, but in a different and preceding step: either the thermodynamic phase transition which corresponds to demixing [1-4] or the (critical) divergence of concentration fluctuations occurring when the system is brought close to its spinodal line. The role of solvent induced forces (SIFs) [5-6] in these steps preceding gelation has been evidenced quantitatively [4,6-7]. Also, it is now clear that SIFs can be modulated by compatible cosolutes [6]. Here we present and discuss the effects of two geometrically very similar molecules (trimethyl amine N-oxide (TMAO) and tert-Butyl alcohol (TBOH)) on the initial symmetry-break (spinodal demixing) which precedes and allows gelation of Agarose aqueous sols at concentrations largely below the random link percolation threshold. Despite the close geometric similarity, the two solutes modulate SIFs in opposite ways, in agreement with expectations drawn from experiments with aqueous solutions of TMAO and TBOH [8], as well as from recent Molecular Dynamics simulations [9]. Reasons for that are briefly discussed.

[1] A. Emanuele et al. *Biopolymers* 31, 859 (1991); [2] P.L. San Biagio et al. *Makromol. Chem.* 40, 33 (1990); [3] A. Emanuele et al. *Phys. Rev. Lett.* 69, 81 (1992); [4] P.L. San Biagio et al. *Phys. Rev. Let.*, submitted (1994); [5] F. Bruge' et al. *J. Chem. Phys.* 101, 2407 (1994); [6] M.U. Palma et al. in "Hydrogen-Bond Networks", M.C. Bellisent-Funel e J.C. Dore Eds., (NATO ASI.C Series, vol. 435, 1994) pp. 457-479; [7] P.L. San Biagio et al. *Biophysical J.* 60, 508 (1991); [8] D. Bulone et al. *to be published*; [9] R. Noto et al. *to be published*

W-Pos507

INVESTIGATION OF MOLECULAR MOTION AND INTERPROTEIN INTERACTIONS IN SOLUTION BY TDDS AND ^{1}H NMR. ((I.V.Ermolina, A.G.Krushelnitsky, I.N.Ivoylov I.V.Nesmelova*, V.D.Fedotov)) Kazan Institute of Biology, POB 30, 430503 Kazan, Russia
*Kazan State University, Kazan, Russia.

The results of the dynamic protein behavior in solution studied by time domain dielectric spectroscopy (TDDS) and non-selective ^{1}H NMR relaxation are presented. The analysis for myoglobin and lysozyme solutions in wide range of concentrations in temperature interval from 5° to 35°C was carried out in terms of correlation functions. It was found that the correlation function of the protein motion can be presented as a sum of three components corresponding to three kinds of protein motion: internal local motion, anisotropy rotational Brownian diffusion and a slow motion with correlation time almost by the order greater than Brownian tumbling time. To explan the origin of slow component the model of the protein motion in solution, which takes into account electrostatic interprotein interactions was suggested. According to this model each dipole moment in solution experiences electrostatic torque from electrical charges and dipoles of the neighboring proteins. The analysis of microdynamical parameters has shown that the electrostatic interactions don't change substantialy the parameters of local motions, but give rise to the anisotropy of the protein Brownian rotation almost not changing the time of this tumbling and to ability of the additional slow motion detection. The fluctuation time of a local electrostatic field, i.e. characteristic time of slow motion is probably connected with translation diffusion. For the analysis of the presented model the translation diffusion coefficients for myoglobin in solution in an appropriate range of concentrations were measured. A correlation time of the translation motion calculated from these coefficients has the value close to the correlation time of slow motion obtained from the experiment. Besides, these times show a synchronous behaviour depending on concentration of a solution. The theoretical estimations of tumbling anisotropy parameter made it possible to explain the essential quantitative difference of this parameter when obtained from TDDS and NMR experiments.

W-Pos508

IN ENZYMIC CATALYSIS FUNCTION OFTEN FOLLOWS FORM -Rufus Lumry, Chemistry, Dept. ,Univ. of Minnesota. Catalysis with small molecules and solids usually depends on the catalyst as a transient donor or acceptor of electrons. Another class of catalysts supplements this with mechanical force to raise reactant free energy toward the transition state. The total Eyring free energy of activation minus the mechanical work still measures the probability of the fluctuation into the TS but with a well designed mechanical catalysis the magnitude of the force can be large and its vector direction can be chosen for maximally efficient application. Then every 1.4 kcal of mechanical work produces a tenfold increase in rate. If the large mechanical devices necessary to generate the force vectors can be constructed, designer catalysts of this kind become possible. But Henry Eyring realized that nature had long since adopted this "rack" mechanism for enzymic catalysis. Now peptide synthesis makes this device available once all the details of mechanism become known. Some details are still obscure but several have become apparent as consequences of the patterns of palindromy ubiquitous in the B factors of gene-duplication enzymes.(e.g.: trypsin, pepsin, phosophlipase A2). The atoms with lowest B factors form the hydrogen bonded skeleton of the knot which is completed by their residues to describe form of matrices and surface although not detailed residue composition. In single-chain enzymes formed initially by gene duplication this construction enforced a very specific structural feature: the two functional domains of each catalytic machine are arranged about an approximate non-crystallographic dyad axis passing through the inter-domain connection point and between the two primary chemically-functional protein groups, one on each knot. Simple vector diagrams show how with this construction slight matrix contraction produces near maximum force along the reaction coordinate. The HIV-1 protease consists of identical units in tail-to-tail association. and so has perfect palindromy. The gene-duplication enzymes synthesized initially in tail to head arrangement have mutated to approximate tail-to-tail residue arrangements. The fact that the only feature necessary to conserve a gene-duplication enzyme family is its palindromic pattern implies that function follows form. (Lumry in *Protein-solvent Interactions*, Ed. Gregory, M. Dekker 1994, chap. 1.).

W-Pos509

KINETICS OF PORE FORMATION INDUCED BY MELITTIN IN LIPID VESICLE MEMBRANES ((S. Rex and G. Schwarz)) Department of Biophysical Chemistry, Biocenter of the University, CH 4056 Basel, Switzerland

The lipid bilayer of unilamellar vesicles is permeabilized upon the addition of the bee venom peptide melittin to the outer aqueous medium. We have studied this phenomenon employing the efflux of an entrapped self-quenching fluorescent dye in the case of liposomes of different sizes prepared with the electrically neutral lipids POPC and DOPC. The physical conditions of the experimental systems were characterized using dynamic light scattering, gel filtration, fluorescent energy transfer and osmometric measurements. In particular, it could be definitely shown that the release of the dye molecules takes place through some kind of pores made up by the membrane associated peptide. The time course of the efflux signal (i.e. the increase of fluorescence emission) and the dequenching of internal dye are analyzed by means of recently developed theoretical approaches. This results in quantitative data of the pore kinetics which are discussed in terms of a basic molecular mechanism.

W-Pos510

SEDIMENTATION EQUILIBRIUM STUDIES OF SOME INVERTEBRATE HEMOGLOBINS. ((D. Zhu, E. Braswell, S. Vinogradov and W. Royer)) U of Conn., Storrs, CT 06269, Wayne State U., Detroit, MI 48201 and U of Mass Med School, Worcester, MA 01605.

Modern sedimentation equilibrium (SE) studies are proving of value in elucidating aspects of the oligomeric nature of various hemoglobins (Hb). In the case of leech (*Macrobella decora*) Hb the molecular weight (MW) of the native molecule and the tetramer were found by SE to be 3490 ± 80 and 61.8 ± 3.6 k Da respectively. The oxy-tetramer was found to partially dissociate into monomers and dimers. The ln of the association constant of the monomer to dimer (ln $K_{1,2}$) and of the dimer to tetramer (ln $K_{2,4}$) in l/g units were found to be 5.9 ± 0.2 and 1.7 ± 0.2 respectively (with little change with temperature from 1° to 20° C). This may be compared with Kellett's (1971, J. Mol Biol 59:401) value of ln $K_{2,4}$ for human oxy-Hb at 20° C of 3.1. Whereas the value of ln $K_{1,2}$ was found by them to be too high to measure by SE. Therefore our results show that the leech tetramer is more loosely associated than human oxy-Hb. In the case of the blood clam (*Scapharca*) the native oxy-dimer was found to dissociate so that ln $K_{1,2}$ (the dimerization of the monomer) had a value of 4.6 ± 0.2 at 25° C and 5.6 ± 0.9 at 1° C, while that of the CO-Hb at 1° C was found to be 6.6 ± 0.4. The deoxy-Hb dimer was too tight to be able to observe any monomer. These results are comparable to Kellett's findings for human deoxy-Hb.

W-Pos511

DISTINGUISHABLE PHASES IN SOLUTIONS OF dA_{20} AND dT_{20} DNA SINGLE STRANDS AND THEIR MIXTURES. ((X. Gao and A.S. Benight)) Department of Chemistry, University of Illinois, Chicago, IL. 60607. (Spon. by K.D. Bishop)

Hydrodynamic behavior of solutions of the individual strands and various stoichiometric mixtures of them were investigated by dynamic light scattering. Single strand solutions at concentrations from ~300 μM to 1 mM (buffered with 10 mM sodium phosphate, 1 mM EDTA, pH=7.0) displayed two distinct hydrodynamic modes. Consistent with individual strands, the faster mode had an apparent diffusion coefficient, D(fast)=(140 x 10^{-8} cm^2/s), and a corresponding hydrodynamic radius, R_H(fast) ~10 Å. For the slower mode D(slow)=(2 x 10^{-8} cm^2/s), R_H(slow) ~1,000 Å, corresponding to a larger hydrodynamic species comprised of many strands. The presence of NaCl from 100 mM to 1.0 M and pH from 4 to 10 affected the ratio of the relative amplitudes A(fast)/A(slow) of the two species but not their diffusion coefficients, suggesting salt and pH alter only the relative amounts of the fast and slow species but not their hydrodynamic structure. When the complementary strand was added D(fast) decreased to (30 x 10^{-8} cm^2/s) and then increased with addition of increasing amounts of the complementary strand. Over the entire titration D(slow) remained unchanged. The A(fast)/A(slow) ratio was also sensitive to addition of the complementary strand. Titratable hydrodynamic behavior of the fast mode provided clear evidence for duplex and triplex formation. (Supported by NSF)

W-Pos512

TOPOLOGICAL MATURATION OF AQUAPORIN CHIP AT THE ENDOPLASMIC RETICULUM. ((W.R. Skach and A.S. Verkman)) University of Pennsylvania and University of California, San Francisco (Intro. S. Shohet)

Aquaporin CHIP (CHIP28) is a 28 kDa integral membrane protein that functions as a mercurial-sensitive water channel in kidney collecting duct, erythrocyte and other tissues. Topological analysis of CHIP has demonstrated four membrane spanning segments in the endoplasmic reticulum membrane (J. Cell Biol. 125:803-815, 1994). In contrast, six membrane spanning segments have been reported for CHIP at the plasma membrane (J. Biol. Chem. 269:1668-1673, 1994). To understand this difference, we performed a detailed analysis of CHIP topological maturation at the ER. Fusion proteins containing a prolactin-derived reporter of translocation at residues A108, T120 and L139 of CHIP were expressed in ^{35}S-methionine pulse-labeled, microinjected Xenopus oocytes. Topology of the P-reporter was determined by protease protection after sequential periods of chase with unlabeled methionine. As we observed previously, immediately after synthesis, the predominant topology of chains (>90%) was consistent with 4 transmembrane (TM) segments. Over a 72 hour chase however, this topology gradually shifted until 50-70% of chains exhibited a topology consistent with 6 TM segments. This process appeared to involve both posttranslational conversion of chains from 4 to 6 spanning topology as well as selected degradation of distinct topologic isoforms. Thus topological maturation, like other aspects of protein folding in the ER, may proceed through posttranslational processing steps involving intermediate folding states, possibly providing a means to regulate the transmembrane topology of some polytopic integral membrane proteins.

W-Pos513

Investigation of Heterogeneity in Macromolecular Solutions

Yujia Xu and David Yphantis, *Department of Molecular and Cell Biology, University of Connecticut, Storrs, Connecticut 06269*

New graphical procedures have been developed to investigate the heterogeneity of protein preparations using equilibrium sedimentation [1, 2]. The heterogeneous systems that can be studied include self-associating systems contaminated by incompetent monomer, self-associating systems contaminated by incompetent oligomer and simple non-interacting monomer-oligomer disperse systems. The new procedures are based on the concentration dependence of the apparent association constants estimated by a nonlinear least square fitting program (NONLIN) and on the assumption of conservation of mass during sedimentation. These procedures can not only detect various types of heterogeneity, but can also discriminate amongst different types of heterogeneity and can estimate the amount of contaminant causing the heterogeneity. The theoretical analysis and some computer simulation results will be presented along with appplication of the procedures to several protein preparations. (Supported by NSF grant #DIR-9218679).

[1] Y. Xu and D. Yphantis *Biophysical Journal, 64:272a, 1993.*
[2] Y. Xu *Biophysical Journal, 66:279a, 1994.*

W-Pos514

A SHORT COLUMN, SHIELDED, TEMPERATURE-CONTROLLED CELL FOR EQUILIBRIUM ELECTROPHORESIS. ((T.M. Ridgeway, A.L. Anderson, P.D. Demaine, and T.M. Laue)) Dept. of Biochemistry and Molecular Biology, University of New Hampshire, Durham, NH 03824.

Cells designed for equilibrium electrophoresis consist of an open ended cuvette sealed with semi-permeable membranes that separate the contents of the cuvette from external buffer chambers. These cells permit the establishment and monitoring of concentration gradients that, in turn, allow the measurement of charge, electrophorectic mobility and diffusion coefficients. Previous work has demonstrated the need for adequate temperature control, as well as for shielding from stray electrical fields, especially in studies of highly-charged polymers. Accordingly, a new cell has been designed, constructed and tested. Cell assembly is straight-forward and provisions have been made for both the driving and voltage sensing electrodes. The sample chamber of the cuvette is 2 x 2 x 2 mm, requiring less that 10 μl to fill. The membranes are laid across the cuvette ends and pressed in place by the buffer chamber O-rings. The cuvette, along with the buffer chambers, are enclosed in an aluminum housing. This housing, in turn, fits snugly inside a thermostatted water jacket, which also serves as a heat sink, light mask and Faraday cage. These improvements noticeably extend the capabilities of equilibrium electrophoresis. Representative findings will be reported here. Funded by NSF DIR 8914571 and BIR 9314040.